Fetal Cardiac Growth & Maturation:

Regulation By Increased Hemodynamic Load

Sonnet Jonker

A dissertation presented to the
Department of Physiology & Pharmacology
and the Oregon Health & Science University
School of Medicine
in partial fulfillment of
the requirements for the degree of
Doctor of Philosophy
January 2006

School of Medicine
Oregon Health & Science University

CERTIFICATE OF APPROVAL

This is certify that the Ph.D. dissertation of
Sonnet Jonker
has been approved

Kent Thornburg

George Giraud

Jonathan Abramson

Virginia Brooks

Daniel Hatton

TABLE OF CONTENTS

FIGURES

TABLES

ABBREVIATIONS

A-A	arterial-to-arterial (refering to an anastomosis)
AngII	angiotensin II
ANOVA	analysis of variance
ANP	atrial natriuretic peptide
ATP	
AT1	angiotensin II receptor 1
AT2	angiotensin II receptor 2
A-V	arterial-to-venous (refering to an anastomosis)
BCA	bicinchoninic acid
bHLH	basic helix-loop-helix
bpm	beats per minute
BrdU	bromodeoxyuridine
CaMK	calmodulin kinase
CDK	cyclin-dependent kinases
DAB	diaminobenzidine
dGA	days of gestational age
DHPR	dihydropyridine receptor
DNA	deoxyribonucleic acid
EDTA	ethylenediaminetetraacetic acid
EM	electron microscope
EPO	erythropoietin
ERK	extracellular-regulated kinase
ET-1	endothelin-1
FGF	fibroblast growth factor
g	gram
GAPDH	glyceraldehyde-3-phosphate dehydrogenase
HIF-1α	hypoxia-inducible factor 1 alpha
HR	heart rate
IGF-1	insulin-like growth factor -1
IHC	immunohistochemistry
KB	kraftbrühe
kb	kilobases
kd	kilodaltons
kg	kilogram
LA	left atrium
LB-AMP	luria broth with ampicillin
LTCC	L-type calcium channel
LV	left ventricle
MAPK	mitogen-activated protein kinase
MEF-2a	myocyte enhancer specific factor 2a
mg	milligram
min	minutes
ml	milliliters
mm	millimeters
mM	millimolar
mmHg	millimeters of mercury
mRNA	messenger RNA
NCX1	sodium-calcium exchanger
ng	nanograms
nM	nanomolar
NS	not significant
PAP	pulmonary artery pressure
PBS	phosphate-buffered saline
PCR	polymerase chain reaction
pg	picograms
PI3K	phosphoinositol-3 kinase
PLN	phospholamban
PMSF	phenylmethylsulphonylfluoride
RA	right atrium
RAP	right atrial pressure
RAS	renin-angiotensin system
rcf	relative centrifigul force (gravities)
RIA	radioimmunoassay
RNA	ribonucleic acid
ROS	reactive oxygen species
RT-PCR	reverse transcription polymerase chain reaction
RV	right ventricle
RyR	ryanodine receptor
SD	standard deviation
SERCA2	SR calcium ATPase 2
SR	sarcoplasmic reticulum
SV	stroke volume
TBST	tris-buffered saline with tween
TTTS	twin-twin transfusion syndrome
t-tubules	transverse-tubules
V	volts
VEGF	vascular endothelial growth factor
V-V	venous-to-venous (refering to an anastomosis)
μg	microgram
μl	microliters

DEFINITIONS

afterload	the impedence against which a ventricle must eject blood during systole
allantois	a vascular fetal membrane, associated with the chorion in the formation of the placenta
amnion	the innermost membrane surrounding the fetus
anastomosis	a communication between blood vessels
angiotensin II	an potent endogenous vasoconstrictor and growth factor
ascites	abnormal accumulation of fluid in the abdominal cavity
ATPase	a protein that hydrolyzes ATP to perform a function
binucleate	*of a myocyte*, containing two nuclei; indicative in the sheep of a terminally differentiated cell
BrdU	an experimental thymidine analogue used to mark cells that have synthesized DNA
chorion	the outermost of the fetal membranes, associated with the allantois in the formation of the placenta
concentric hypertrophy	thickening of the ventricular wall without a change in the mid-wall chamber radius
culture	the *in vitro* growth of cells in a nutrient media
ventricular diastole	relaxation and filling of the left and right ventricles of the heart
ductus arteriosus	a vessel in the fetus that connects the pulmonary artery with the aorta and conducts most of the blood directly from the right ventricle to the aorta
ductus venosus	a vein passing through the liver and connecting the left umbilical vein with the inferior vena cava of the fetus
eccentric hypertrophy	growth of the ventricle such that the mid-wall chamber radius increases
expression	*of a gene*, the detectable presence of mRNA or protein in a tissue
fetofetal transfusion	see twin-twin transfusion
fistula	see anastomosis
foramen ovale	an opening in the atrial septum that is normally present only in the fetus
Frank-Starling mechanism	the increase in stroke volume that results from an increase in end diastolic volume which results from increased ventricular filling pressure or preload
hydrops	abnormal accumulation of fluid in tissues or a body cavity
hyperplasia	proliferative growth
hypertrophy	enlargement of cells or of the heart
in utero	before birth
in vitro	removed from the living organism
in vivo	in the living organism
Ki-67	a nuclear antigen present only during the cell cycle
law of Laplace	a description of the relationship between ventricular wall thickness, the radius of curvature of the ventricle and wall stress. See Appendix B.
mitral valve	the left atrioventricular valve

monochorionic	sharing or developed with a common chorion, therefore sharing a placenta
mononucleate	*of a myocyte*, containing one nuclei; indicative in the sheep of a cell not yet terminally differentiated
myocardium	the muscular wall of the heart
myocyte	a muscle cell
polycythemia	having an excess of blood cells, as measured by hematocrit
postductal	distal to the ductus arteriosis
preload	the degree of end diastolic filling of the ventricle
pressure load	systolic load increased by raising arterial pressure
renin	the enzyme that controls the rate-limiting step of angiotensin II production
sarcolemma	the outer membrane of a myocyte
sarcoplasmic reticulum	the intracellular organelle that acts in the myocyte as a calcium storage and release site
stress	force per area, in the heart the force that causes diastolic distension and opposes systolic contraction
ventricular systole	contraction of the left and right ventricles of the heart
terminal differentiation	a cellular processes after which the myocyte does not proliferate
tricuspid valve	the right atrioventricular valve
twin-twin transfusion	the sharing of blood between monochorionic twins in utero
volume load	increased venous return to the heart leading to increased diastolic distension of the ventricles

ACKNOWLEDGEMENTS

I am grateful for the opportunity to have conducted my graduate training in the OHSU Department of Physiology and Pharmacology, a program that is home to many scientists dedicated to their research and to graduate education. I could not have completed my studies without the support and guidance of many people, more than I can individually thank.

There are two for whom I have especial gratitude:
My mentor Kent Thornburg, thank you for your unreserved support of my potential as a research scientist, and for sharing your enthusiastic and deep knowledge of cardiovascular and fetal physiology. George Giraud, for the immense amount of help you have given me, and for your professional and personal friendship, I thank you.

A few people especially turned me towards physiology: My first physiology teachers, Uintah Shabazz and Stan Swank, showed me the joy of discovering the details. Mark Doyle demonstrated to me that a problem always has a solution if one is sufficiently persistent.

My lab mates have contributed substantially to my research: Donogh McKeogh, Tara Karamlou, Dane Crossley, Natasha Chattergoon, David Barnes, Lian Wang, Piroska Balogh, Elaine Kitano, Nathan Sundgren, Emmeline Hou and Kevin Rogers have aided my studies, provided stimulating conversation or taught me techniques; many of you have been generous friends as well. Special mentions go to Krista Wehrley, Bob Webber and Sam Louey for riding the short bus with me. The administrative staff upstairs have often gone out of their way to help me, especially Andrea Ilg, Evan Bowman and, notably, Lisa Rhuman. My advisory committee has provided expert guidance and valuable critisism.

I could not have done any of this without all of the dedicated people who have shouldered the enormous task of caring for the sheep: Pat Renwick, Lynn Allen, Julie Booth and Loni Socha, as well as Ed and Robert. Roger Hohimer, Lowell Davis and Chuck Roselli have been generous with their sheep hearts, perhaps more times than they knew. I thank, too, Deb Anderson and Job Faber for their generosity and support. Chris Corless and his laboratory, especially Linda Jauron-Mills and Carolyn Gendron, provided expertise for histological techniques. Of course, none of this was possible without the sheep themselves.

I would also like to acknowledge the organizations that have funded my research: the American Heart Association (Predoctoral Fellowship), the Tartar Trust (Fellowship), the U.S. Department of Agriculture (FASEB Summer Conference Award), and the OHSU Graduate Student Organization (Travel Fellowship). I have also been supported, through my mentor, by a grant from the National Institute of Child Health and Development, and through an institutional training grant from the National Institute of Neurological Disorders and Stroke.

Finally- Tim, thank you for being such a great friend. Life is good.

PUBLICATIONS

Jonker S, McKeogh DF, Giraud GD, Karamlou T & Thornburg KL. The calcium transport system of the fetal sheep heart is resistant to regulation by hemodynamic stress. *In preparation.*

Jonker S, Hou EF, Rogers RK, Anderson DF, Faber JJ, Thornburg KL & Giraud GD. Plasma infusion stimulates heart growth via hypertrophy and hyperplasia in the fetal sheep. *In preparation.*

Jonker S, Giraud GD, Louey S, Chattergoon N, Davis L & Thornburg KL. Heart growth induced by chronic anemia in the fetal sheep is not due to myocyte hypertrophy. *In preparation.*

Giraud GD, Louey S, Jonker S, Schultz J & Thornburg KL. Cortisol stimulates cell cycle activity in the cardiomyocyte of the sheep fetus. *In preparation.*

Giraud GD, Faber JJ, Jonker S, Davis L & Anderson DF. Effects of intravascular infusions of plasma on placental and somatic blood flow in fetal sheep. *In preparation.*

Faber JJ, Anderson DF, Jonker SS, Davis LE & Giraud GD. (2005). Fetal Infusions of Plasma Cause an Increase in Umbilical Vascular Resistance in Sheep. *Placenta* **In press.**

Giraud GD, Faber JJ, Jonker S, Davis L & Anderson DF. (2005). Intravascular infusions of plasma into fetal sheep cause arterial and venous hypertension. *Journal of Applied Physiology* **99**, 884-889.

Jonker S, Davis LE, van der Bilt JD, Hadder B, Hohimer AR, Giraud GD & Thornburg KL. (2003). Anaemia stimulates aquaporin 1 expression in the fetal sheep heart. *Experimental Physiology* **88**, 691-698.

Thornburg KL, Jonker S & Reller MD. (2002). Nitric oxide and fetal coronary regulation. *Journal of Cardiac Surgery* **17**, 307-316.

ABSTRACTS

Jonker S, Karamlou T, Faber JJ, Anderson DF, Giraud GD & Thornburg KL. (2005). NCX and SERCA genes are not regulated by hemodynamic stress in the fetal sheep heart. Presented at *3rd International Congress on Developmental Origins of Health & Disease*, Toronto, Canada. *Pediatric Research* **58**, 1082.

Jonker S, Faber JJ, Anderson DF, Thornburg KL, Rogers RK, Hou EF & Giraud GD. (2005). Prenatal hypertension induced by plasma infusion programs cardiac growth and maturation in fetal sheep. Presented at *3rd International Congress on Developmental Origins of Health & Disease*, Toronto, Canada. *Pediatric Research* **58**, 1018.

Jonker S, Thornburg KL, Faber JJ, Anderson DF, Rogers RK, Hou EF & Giraud GD. (2004). Load stimulates proliferation of fetal sheep cardiac myocytes despite low circulating angiotensin II. Presented at *Heart Research Center Scientific Retreat.* OHSU, Portland, Oregon.

Jonker S, Thornburg KL, Faber JJ, Anderson DF, Rogers RK, Hou EF & Giraud GD. (2004). Load stimulates proliferation of fetal sheep cardiac myocytes despite low circulating angiotensin II. Presented at *FASEB Summer Research Conference "Molecular and Cellular Signaling in the Perinatal Cardiovascular System"*. Tucson, Arizona.

Jonker S, Thornburg KL, Faber JJ, Anderson DF, Rogers RK, Hou EF & Giraud GD. (2004). Load stimulates proliferation of fetal sheep cardiomyocytes despite low circulating angiotensin II. Presented at *Student Research Forum*. OHSU, Portland, Oregon.

Jonker S, Davis L, van der Bilt J, Hadder B, Hohimer AR, Giraud GD & Thornburg KL. (2003). Cardiac aquaporin 1 expression is regulated by development and by chronic fetal anemia. Presented at *Student Research Forum*. OHSU, Portland, Oregon.

Jonker S, Davis L, van der Bilt J, Hadder B, Hohimer AR, Giraud GD & Thornburg KL. (2003). Cardiac aquaporin 1 expression is regulated by development and by chronic fetal anemia. Presented at *Society for Gynecological Investigation 50th Annual Scientific Meeting*, Washington, D.C. *Journal of the Society for Gynecological Investigation* **10**, 310A.

Jonker S, Davis L, van der Bilt J, Hadder B, Hohimer AR, Giraud GD & Thornburg KL. (2002). Cardiac aquaporin-1 expression is regulated by development and by chronic fetal anemia. Presented at *Heart Research Center Scientific Retreat*. OHSU, Portland, Oregon.

Jonker S & Thornburg KL. (2001). Developmental regulation of protein tyrosine phosphatase-like A protein in the sheep heart. Presented at *Student Research Forum*. OHSU, Portland, Oregon.

Jonker S & Thornburg KL. (2001). Cardiac expression of protein tyrosine phosphatase-like A protein in the developing sheep heart. Presented at *Heart Research Center Scientific Retreat*. OHSU, Portland, Oregon.

Jonker S, McKeogh DF, Burson MA & Thornburg KL. (2003). NCX and SERCA2a are regulated in the heart during development. Presented at *Heart Research Center Scientific Retreat*. Portland, Oregon.

ABSTRACT

Regulation of growth and control of intracellular calcium concentrations are both critical to the fetal heart for immediate and future health. The heart grows in response to hemodynamic loading conditions and, in the adult, expression of the calcium transport system is also sensitive to hemodynamic load. Myocardial proliferation ceases with terminal differentiation during the perinatal period, at which time the number of myocytes is set for life. In the mature heart, calcium for contraction is obtained primarily from the sarcoplasmic reticulum (SR). In the immature (and failing) heart, calcium transport across the sarcolemma is of greater importance. The mode of fetal myocardial growth, and alterations in the regulation of the calcium transport system, in response to hemodynamic load, is largely unknown and is therefore of scientific and clinical interest. ***Hypothesis***: I hypothesized that chronic plasma infusion, which causes combined venous and arterial hypertension, would increase fetal cardiac mass by inducing myocyte hypertrophy; furthermore, the (endo)plasmic reticulum ATPase (SERCA2) and ryanodine receptor (RyR) (which both control SR calcium) would be down-regulated, and the sodium-calcium exchanger (NCX1) and L-type calcium channel (LTCC) (which both regulate use of extracellular calcium) would be up-regulated. I hypothesized that fetal anemia, which increases venous return but not arterial pressure, would increase cardiac mass by both myocyte hypertrophy and proliferation. I also hypothesized that increased volume and pressure loads would individually down-regulate SERCA2 and up-regulate NCX1 in fetal hearts. ***Methods***: I tested these hypotheses in several groups of surgically instrumented fetal sheep. 1st set: plasma was infused for 4 or 8 days to increase diastolic and systolic loads, and then the hearts were dissociated or frozen. 2nd set: fetuses were phlebotomized daily for 9 days to cause sustained anemia. 3rd set: postductal aortic occluders were inflated for 10 days to increase systolic load, and then the hearts were frozen. Finally, banked hearts of fetuses with surgical arterio-venous fistulas (created to increase volume load) were also examined. ***Results***: Plasma infusion caused venous and arterial hypertension and cardiac enlargement ~30% greater than the hearts of control fetuses. This growth

occurred by both myocyte hypertrophy and proliferation. The degree of terminal differentiation also increased in the hearts of the fetuses infused for 8 days. In these hearts, cardiac NCX1 mRNA and protein decreased slightly. Sustained fetal anemia caused fetal hearts to become ~40% larger than the hearts of control fetuses, but myocyte hypertrophy, proliferation, and terminal differentiation did not occur. Neither increased pressure load imposed by an aortic occluder, nor increased volume load imposed by an A-V fistula, altered expression of NCX1 or SERCA2. ***Conclusions***: The growth of the fetal sheep heart is modified by increased hemodynamic load, but the mode of cardiac myocyte growth depends on the type of load that is imposed. In contrast, the calcium transport system is insensitive to regulation by hemodynamic load in the fetal heart. The sensitivity to regulation of growth by hemodynamic load in the fetal heart may be an important adaptive mechanism, whereas insensitivity to regulation of the calcium transport system may be protective.

CHAPTER 1

Introduction

Fetal cardiac development and growth can go awry and babies can be born with congenital diseases of the heart for many reasons (Rudolph, 2001). Hemodynamic loading conditions are important determinants of fetal heart growth, and can cause such defects. For example, one third of fetal cardiomyopathies unaccompanied by other structural abnormalities occur in recipient twins of fetofetal transfusion (Pedra *et al.*, 2002). When identical twins share a placenta, one fetus can chronically transfuse the other, altering the cardiovascular growth of both fetuses (Wee & Fisk, 2002). This hemodynamic imbalance affects fetal somatic growth, development of the heart and kidneys, and increases the risk of cerebral palsy due to hemodynamic events in the perinatal period. Untreated, mortality due to this condition is 80-100%. Chronic fetofetal transfusion can cause progressive cardiac enlargement and cardiomyopathy (Simpson *et al.*, 1998), but it is not known how fetal myocyte growth contributes to this change or what cellular alterations underlie the functional deterioration.

Normal growth of the fetal heart is coordinated to match the growth of the fetal body by mechanisms that are not well understood. Unique to the fetal heart is the capacity of its myocytes to proliferate in order to build the organ, whereas the adult myocardium is unable to significantly regenerate itself. This period of proliferative growth is concluded near birth by terminal differentiation of the cardiac myocytes, setting the final number of myocytes for life. If the work of the fetal heart is changed by structural abnormalities or increased demand for blood flow, the fetal

heart grows differently. Although the gross morphological features of the congenitally diseased heart may (or may not) be resolved by surgical correction and postnatal growth, the cellular composition of the heart remains abnormal.

Immature myocytes differ from adult cells in their capacity for proliferation, structure, metabolism, and means of calcium use for contraction and relaxation. Adult cardiac myocytes have substantial intracellular calcium stores in their sarcoplasmic reticulum (SR) for excitation-contraction coupling, while fetal cells rely to a greater extent on extracellular calcium for excitation-contraction coupling. The maturational transition from the fetal to adult system of calcium transport occurs as a result of the structural development of the SR and the altered expression of the proteins responsible for transporting and sequestering calcium. The calcium transport system may become dysregulated in diseased mature hearts, but it is unclear if the maturation of this system is altered by intrauterine hemodynamic stress.

My goal is to understand how fetal heart development is modified by hemodynamic stress. I have studied how hemodynamic stresses influence growth patterns of fetal cardiac myocytes by comparing the consequences of increasing cardiovascular load by infusing plasma with the cardiac growth consequent to chronic fetal anemia. I have also investigated how plasma infusion-induced hemodynamic load, arterial pressure load, and volume load alter maturation of the calcium transport system that couples cardiac myocyte excitation and contraction. In order to better interpret any experimentally-induced changes, I also studied the normal maturation of cardiac myocyte growth and expression of the calcium transport system.

I will introduce fetofetal transfusion as a useful clinical framework with which to discuss my data. Next, I will provide a detailed review of our current understanding of fetal cardiac myocyte growth. I will describe what is known about regulation of calcium in the heart and the cardiac excitation-contraction coupling system. Finally, I will explain my guiding hypotheses and I will also share credit with those who contributed ideas, resources, or aid to my thesis.

The Pathophysiology of Twin-Twin Transfusion

If a twin pregnancy is found on the first ultrasound at ~16-17 weeks of gestation to be monochorionic (sharing a placenta), ultrasound examinations are then routinely repeated every 2-3 weeks in order to determine if twin-twin transfusion syndrome (TTTS) has developed. Formerly, a positive diagnosis was based on criteria of a difference in hemoglobin levels and a birthweight discordance between the twins (Weiner & Ludomirski, 1994). TTTS is now diagnosed primarily by the finding of disparate amniotic fluid volumes between monochorionic twins and is staged according to a system that describes the progression of the disease (Quintero *et al.*, 1999). Although staging does not predict outcome based on initial presentation, progression through stages increases the risk of perinatal demise (Taylor *et al.*, 2002).

It is commonly agreed that the majority (80-100%) of twin monochorionic pregnancies contain vascular connections, or anastomoses, in the shared fetal placenta (Bajoria *et al.*, 1995; Machin *et al.*, 1996; Denbow *et al.*, 2000). Fetofetal transfusion, therefore, occurs in almost all twin monochorionic pregnancies. TTTS arises when this sharing of blood is unequal, with net unidirectional transfusion. This occurs in about 10-15% of monochorionic pregnancies (Wee & Fisk, 2002). The placental connections between twins may be arterial-to-arterial (A-A), venous-to-venous (V-V), or the anastomosis may join the arterial system of one fetus with the venous system of its twin (arteriovenous, or A-V). A-A or V-V shunts tend to be superficial, while A-V shunts are usually deep inside the placenta. In fetuses that develop TTTS there is most frequently one or multiple deep A-V anastamoses and a paucity of superficial shunts (Bajoria *et al.*, 1995; Bajoria, 1998; Denbow *et al.*, 2000).

The anastomosed placental vessels are large – measurement of the median minimum external diameter of A-V anastamoses was 1.5mm at ~30-35 weeks of gestation (Bajoria *et al.*, 1995). Superficial anastomoses of monochorionic fetuses without TTTS are larger than anastomoses of fetuses that develop TTTS (which is perhaps protective); superficial shunts are between 0.5 and 8mm in external diameter (Bajoria, 1998). As in any vessel, the pressure gradient and resistance across the

anastomosis determine flow. The flow within an anastomosed vessel and the net rate of transfusion between any given set of twins are unknown. An ultrasound study of placental venous flow before and after intrauterine laser coagulation of anastomoses has attempted to resolve this question (Ishii *et al.*, 2004). It was estimated that the median difference of umbilical venous flow between twins was 40ml/min. After laser coagulation therapy, umbilical venous flow increased in the donor and decreased in the recipient, each by a median amount of 20ml/min. This altered flow cannot represent the net transfusion rate from the donor to the recipient. At a transfusion rate of 20ml/min both fetuses would be expected to rapidly die. Therefore, transfusion rates between fetuses with monochorionic placentas remain unknown.

The health of both fetuses is compromised in TTTS, although each fetus is affected differently (Figure 1). TTTS babies are more often born prematurely than other monochorionic twins, resulting in decreased birth weight, increased risk of chronic lung disease, and decreased survival at 1 year (Lutfi *et al.*, 2004). Premature parturition is a common feature of pregnancies where the fetus experiences hemodynamic stress, and is common in our studies with fetal sheep. Premature delivery of TTTS babies predisposes them to periventricular leucomalacia (white matter damage due to immature vascular development (Blumenthal, 2004)) and ischemic brain injury in the perinatal period (Cincotta *et al.*, 2000). Cerebral palsy and global developmental delay are common outcomes for both donor and recipient fetuses. Brain injury in recipient twins has been found to be exacerbated if the fetus has cardiac hypertrophy or is hydropic (Hyodo *et al.*, 2003). Although the pathophysiological effects of TTTS are different between the recipient and donor fetuses, the risk of initial intrauterine death is equally likely for each fetus (Bajoria *et al.*, 1999b). After the demise of one twin, the other is likely to follow. However, perhaps due to an increased rate of hemorrhage, death of the recipient fetus is more likely to be followed by death of the twin, than is death of the donor.

Today, the best treatment for TTTS is endoscopic laser coagulation therapy to close the anastamoses. This treatment increases survival rates to 76% (Senat *et al.*, 2004). Untreated, perinatal mortality is 80-100% (Wee & Fisk, 2002). Serial amnioreduction, septostomy (puncturing the amniotic

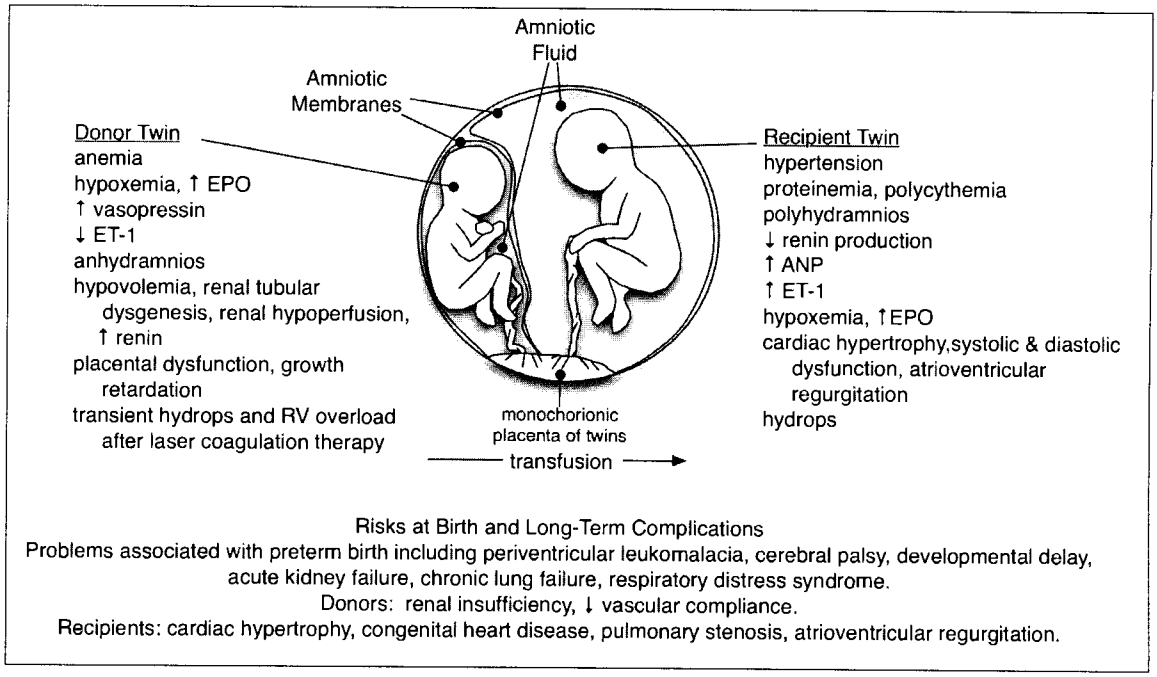

Figure 1. Diagram of possible fetal complications in TTTS.

membranes separating the fetuses) and selective feticide are also treatments warranted in certain circumstances (Fisk & Galea, 2004).

The donor fetus chronically transfuses a small volume of blood to its twin through placental anastomoses, often rendering it anemic relative to its twin (Denbow *et al.*, 1998). Hydrops of the donor twin has been observed, although the etiology is unknown. Hydrops could be due to anemia or acute reversal of transfusion. Indeed, experimentally induced anemia of fetal sheep sometimes causes hydrops. Loss of water and solutes into the extravascular space or to the recipient twin will reduce the blood volume of the donor fetus. Indirect evidence suggests that donor twins are hypovolemic. Anatomic kidney lesions, tubular dysgenesis and increased kidney renin levels suggest renal hypoperfusion in the donor fetus (Mahieu-Caputo *et al.*, 2000; Kilby *et al.*, 2001). The donor's bladder is often invisible on ultrasound examination. Urine production contributes to amniotic fluid (Wlodek *et al.*, 1988), so it is not surprising that lack of amniotic fluid is a diagnostic criterion to identify a donor twin. Prior to keratinization of the skin at about 19-25 weeks of gestation, amniotic fluid is formed through bi-directional diffusion and filtration across the fetal skin and membranes of the

amnion, placenta and umbilical cord. It is likely that this route of amniotic fluid production is also depressed in the donor. Lung and oronasal mucosal secretions are a third source of amniotic fluid. It is not known if these secretions are abnormal in donor twins (Underwood *et al.*, 2005). In contrast, recipient fetuses produce increased amounts of amniotic fluid containing lower protein, sodium and potassium levels than normal (Huber *et al.*, 2004).

Also consistent with hypovolemia of the donor fetus are the high circulating vasopressin levels found in donors (Bajoria *et al.*, 2004). The concentration of essential and non-essential amino acids in donor fetuses is significantly lower than levels in uncomplicated twin pregnancies or recipient fetuses, suggesting that placental dysfunction and nutrient transfer may limit the ability of the fetus to cope with chronic blood loss (Bajoria *et al.*, 2000). Accordingly, many donor twins are growth retarded at birth (Wee & Fisk, 2002). It is interesting that laser coagulation therapy to stop transfusion does not return the *in utero* growth pattern of donor twins to normal, although it rapidly reduces the growth rate of recipient twins (Moreira de Sa *et al.*, 2005). Placental vascular resistance may increase in donor fetuses, indicated by absent or reversed diastolic umbilical artery blood flow (Trudinger & Giles, 1989; Herberg *et al.*, 2005). The increased vascular resistance cannot be explained by the vasoconstrictor endothelin-1 (ET-1) because levels of the ET-1 are low (Bajoria *et al.*, 2003). Persistent postnatal complications may result from altered organ development or physiological function, such as renal insufficiency (Christensen *et al.*, 1999). One known long-term outcome of TTTS is decreased arterial compliance in donor twins studied as children (Cheung *et al.*, 2000; Gardiner, 2001; Gardiner *et al.*, 2003). Increased arterial stiffness might be the result of altered elastin deposition during the perinatal period. Dysregulation of elastin is hypothesized to account for some part of the adult hypertension associated with low birth weight (Barker, 2001).

Recipient twins receive small amounts of extra blood via the placental anastomoses. The transfused blood has been hypothesized to carry hormones from the donor fetus into its recipient twin (van den Wijngaard *et al.*, 2005). This is unlikely to be an important source of vasoactive factors in the recipient fetus for two reasons. First, the quantity of transfused blood is small and becomes diluted in

the recipient's blood. Second, the half-lives of vasoactive substances are typically very short, on the order of seconds to minutes (Al-Merani *et al.*, 1978; Botting & Vane, 1989; Shiba *et al.*, 1989), and therefore they are unlikely to accumulate in the recipient's blood. Components of the blood with long half-lives accumulate in recipient fetuses, resulting in high hematocrits and excessive amounts of protein in their plasma (Weiner & Ludomirski, 1994). Increased hematocrit and increased plasma protein may have important consequences in the recipient fetus. Red blood cell density, measured by hematocrit, is the most significant determinant of whole blood viscosity. A high hematocrit will increase shear stress on the vascular endothelium if flow stays relatively constant. Hyperproteinemia from plasma infusion causes hypertension in the fetal sheep (Giraud *et al.*, 2005), and hyperproteinemia may be a larger component of fetal or neonatal disease in TTTS than previously recognized (Drew *et al.*, 1997).

There is a lack of consensus in published studies about whether the pathology of the recipient fetus is due to an increased volume load or an increased arterial load. Cardiovascular pathology in the recipient fetus has been thought to be the result of a volume load caused by chronic transfusion. Evidence put forward to support this hypothesis includes increased aortic blood velocities that are explained as reflective of the Frank-Starling response to increased preload (Karatza *et al.*, 2002). However, fetuses work near the breakpoint of their Frank-Starling relationship (Thornburg & Morton, 1983), so this explanation does not fully explain the finding unless the normal relationship is changed. Increased aortic blood velocities may result from cardiac growth if the heart is able increase stroke volume. Other investigators now think that increased arterial pressure load is a more important component of the disease because recipient fetuses develop cardiac hypertrophy without chamber dilatation (Barrea *et al.*, 2005). This contradicts earlier reports of dilatation (Fesslova *et al.*, 1998; Simpson *et al.*, 1998). Chamber dilatation, or eccentric hypertrophy, is a hallmark of chronic cardiac volume overload. It is not clear if the earlier reports of cardiac dilatation were due to methodological errors or if both types of cardiac remodeling occur with TTTS. Fetal ventricular hypertrophy can occur from pressure overload created by placement of an arterial occluder (Barbera *et al.*, 2000), or from volume overload caused by the surgical creation of an arteriovenous anastamosis (Appendix A). It

is likely that both stresses contribute to the anatomical and functional remodeling of the recipient heart.

Cardiac diastolic dysfunction may be present in many recipient fetuses; signs of this include prolonged ventricular relaxation times and abnormal flows in the fetal veins (Raboisson *et al.*, 2004; Barrea *et al.*, 2005). Although poorly understood, augmented pulsatility of the ductus venosus is thought to reflect deterioration of cardiac performance (Kiserud, 1997). Additionally, systolic pressures in recipient fetuses (estimated by the magnitude of the atrio-ventricular regurgitant flow) are twice normal for gestational age (Barrea *et al.*, 2005). As would be expected with chronically increased arterial pressure, reduced fractional shortening (systolic dysfunction) is also common in these hearts, as is mitral and tricuspid regurgitation (Kiserud, 1997). Cardiac hypertrophy and decline in heart function are progressive, despite amnioreduction (Barrea *et al.*, 2005) or laser coagulation therapy (Herberg *et al.*, 2005). Congenital heart disease, valvular regurgitation and outflow obstruction (primarily of the right ventricle) may persist after birth; more than 10% of recipient twins show abnormal systolic and diastolic function as young children (Herberg *et al.*, 2005).

The kidneys of recipient fetuses are affected as well, with hemorrhagic infarction and structural abnormalities reported (Mahieu-Caputo *et al.*, 2000). These fetuses have severely depressed renin-angiotensin systems (RAS) (Christensen *et al.*, 1999; Kilby *et al.*, 2001), but elevated levels of ET-1 (Bajoria *et al.*, 1999a) and atrial natriuretic peptide (ANP) (Bajoria *et al.*, 2001a). As in other pregnancies, erythropoietin (EPO) in TTTS twins is correlated with fetal hypoxemia (Bajoria *et al.*, 2001b). It is not intuitive that EPO levels would increase in fetuses that are the recipients of transfusion. However, EPO is often increased in one or both TTTS twins.

Unidirectional fetofetal transfusion upsets the balance of developing organ systems in both donor and recipient twins. These disturbances often lead to death of one fetus, putting the twin at increased risk of death or complications. Some aspects of the disease continue to progress *in utero* despite treatment of symptoms or interruption of the anastamoses. Altered fetal development in response to this condition has been shown to have implications for adult heath, but most aspects remain unexplored. No

animal model has been developed to investigate the pathophysiological development of this syndrome, which limits our understanding of clinical findings. It is not known how the fetal myocytes of the heart respond in this condition or how the cardiac calcium transport system is altered.

Although gross alterations in the growth of hearts from fetuses affected by TTTS have been described, these studies do not provide insight into the specific ways that the myocytes are responding to their conditions. The next section provides a background to understand the ways in which the fetal myocardium can grow, and how these growth processes might be affected in conditions of increased hemodynamic load. The dysfunction observed in the hearts of recipient twins may be due to alterations in cardiac excitation-contraction coupling; this system and how it changes during cardiac maturation is covered in the following section.

Growth of the Fetal Heart

The vertebrate embryonic heart begins to pump as a tube, continues as a looped heart, and then septates into a four-chambered heart. The fetal ventricles pump blood into a vascular system with shunts that allow the placenta to function as the nutrient and gas exchange organ in the place of the lungs and gastrointestinal tract (Figure 2). These shunts are the ductus arteriosus (between the pulmonary artery and the aorta), the ductus venosus (between the umbilical vein and the inferior vena cava), and the foramen ovale (within the atrial septum). Before birth, the right ventricle (RV) accounts for about 60% of total cardiac output (Anderson *et al.*, 1981). Because of the fetal shunts, both of the ventricles are filled at, and pump against, essentially the same pressures. However, the RV has a thinner free wall and a larger radius than the left ventricle (LV). The ratio of the mid-ventricular radius to wall thickness in the late-gestation fetal lamb is ~2.6 for the LV and ~4.5 for the RV (Pinson *et al.*, 1987). Application of the Law of Laplace, which describes wall stress as proportional to the ratio of the chamber size to wall thickness, yields a RV wall stress that is approximately two thirds greater than that of the LV (see Appendix B). After birth the fetal shunts close and the RV perfuses the low pressure circuit of the pulmonary vasculature, while the LV pumps to the high

pressure systemic circuit.

Fetal cardiac growth is primarily achieved by myocyte proliferation, but the fetal myocytes can also undergo terminal differentiation and enlarge (Figure 3). The contribution of proliferation to heart growth diminishes as the myocytes terminally differentiate near term. After birth, myocyte hypertrophy is the primary process by which the heart grows. The myocardium is not composed entirely of myocytes. Connective tissue cells in the neonatal human heart number approximately 1 $\bullet 10^9$, while myocyte numbers at the same age are approximately 2 $\bullet 10^9$ (Adler & Costabel, 1975). Myocyte numbers in the near-term fetal sheep heart are in the same range as numbers in the human neonate (Barbera *et al.*, 2000; Burrell *et al.*, 2003). Extracellular tissue accounts for perhaps 10% of cardiac volume (Barbera *et al.*, 2000). Capillary density increases during fetal growth, but is lower in the postnatal heart and does not change much between birth and adulthood (Smolich *et al.*, 1989). The non-myocyte components of the heart are also influenced by stress during fetal life.

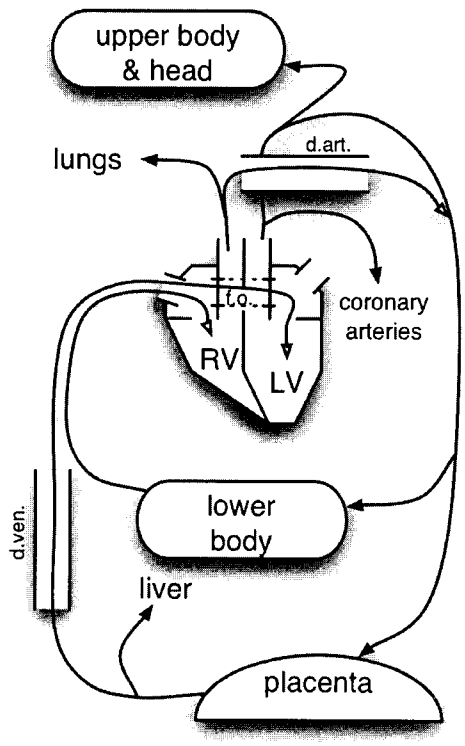

Figure 2. Diagram of the fetal circulation. Blood returns from the placenta via the umbilical veins. Some of this blood is diverted to perfuse the liver. However, most of the richly-oxygenated umbilical venous blood flows through the ductus venosus (d.ven.). The blood flowing from the ductus venosus joins the poorly-oxygenated blood of the inferior vena cava from the systemic circulation to form two streams as they enter the heart. The high-velocity stream from the ductus venosus blood is directed through the foramen ovale (f.o) and into the left atrium and thus the LV, whereas the systemic venous blood stream enters the right atrium and RV (Anderson et al., 1985). Blood from the superior vena cava also preferentially enters the RV (not shown). The RV ejects its blood into the pulmonary artery. Some of this blood continues through the pulmonary arteries to the pulmonary circulation, but most of it enters the ductus arteriosus (d.art.) and is shunted to the descending aorta. The LV ejects its well-oxygenated blood into the ascending aorta, from which rises the coronary arteries that supply the heart, and the arteries that feed the upper body and head. The remainder of the blood ejected from the LV continues past the ductus arteriosus and into the lower body. The umbilical arteries arise near the termination of the aorta.

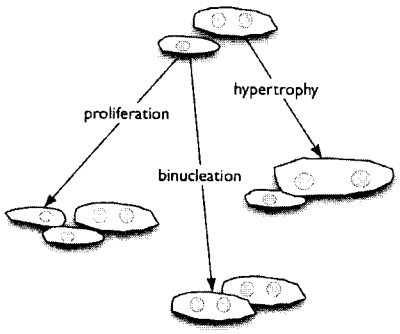

Figure 3. Growth and maturation in the fetal heart. The fetal heart has two populations of myocytes: mononucleated and binucleated. Mononucleated myocytes are known to have proliferative potential, while binucleated myocytes have only been observed to enlarge. Mononucleated cells become binucleated near term and cease to proliferate.

The Role of Proliferation in Fetal Cardiac Growth

The proliferation of immature cardiac myocytes is regulated by a complex milieu of mitogens and anti-mitogens driving intracellular signaling pathways. These pathways integrate the signals and activate transcription factors that initiate production of proteins associated with cell cycle progression and growth. Various methods have been used to study cardiac myocyte proliferation – stereological estimation of myocyte number, counting mitotic figures, immunohistochemistry (IHC) for cell-cycle markers, and incorporation of labeled nucleotides or nucleotide analogs into newly synthesized DNA. Studies have been carried out to describe the normal course of proliferative cardiac growth, but also to discover what interventions alter myocyte proliferation.

Many investigators use Ki-67 IHC to quantify cell cycle activity. Ki-67 is a nuclear antigen that is absent during G0, but present in G1, S, G2 and M phases of the cell cycle (Gerdes *et al.*, 1984). The Ki-67 protein has a short half-life, making it a good marker of proliferating cells (Bruno & Darzynkiewicz, 1992). Studies of cardiac myocyte proliferation that have used both Ki-67 and the thymadine analogue BrdU together have suggested that Ki-67 is a good marker of proliferating cardiac myocytes (Tamamori-Adachi *et al.*, 2003; Wang *et al.*, 2004). Ki-67 IHC is an accepted method of identifying proliferating cells in the fetal myocardium of lambs (Tchirikov *et al.*, 2001), guinea pigs (Saiki *et al.*, 1997) and humans (Huttenbach *et al.*, 2001).

Cell cycle activity as assessed by Ki-67 IHC in the human myocardium has been measured between 12 and 30 weeks of gestation. During this period the levels are high (Huttenbach *et al.*, 2001).

Infants may continue to have low rates until about seven months, but older infants and adults do not show myocardial cell cycle activity. Cardiac myocyte proliferation in the adult heart is a controversial topic (Beltrami *et al.*, 1997), but all investigators agree that it is inadequate to repair pathological myocyte loss. Stereological estimates of myocyte number in the human heart confirm proliferative growth during the last trimester (Austin *et al.*, 1995). High levels of fetal cardiac myocyte proliferation that decrease precipitously after birth are also observed in mice and rats (Soonpaa & Field, 1998). Stereological estimation of myocyte number in the sheep heart also shows a dramatic increase in myocyte numbers during fetal life (Burrell *et al.*, 2003).

It is well established that the mechanical stress imposed by pressure or volume load is a sufficient stimulus to cause cardiac myocyte hypertrophy (Cooper, 1997). Fetal arterial pressure increases throughout gestation (Barcroft, 1946; Reeves *et al.*, 1972). Thus it may influence even normal cardiac myocyte proliferation. Further evidence in the human fetus that hemodynamic stress shapes the growth of the myocardium comes from the congenital heart condition of hypoplastic ventricle. This anomaly may develop very early in development by a restructuring of the ventricle to meet increased impedance to ejection. The resulting myocardial remodeling is characterized by increased wall thickness that diminishes or obliterates the ventricular chamber volume. This condition has been recreated in fetal lambs (Fishman *et al.*, 1978). While mechanical stress is one signal known to regulate cardiac myocyte proliferation (as well as hypertrophy), the specific roles of other growth signals and how these signals are integrated have not been determined.

Two general types of experiments have been designed to study regulation of fetal cardiac growth. In some *in vivo* experiments, hemodynamic conditions are experimentally altered or drugs are administered to the fetus and the growth of the heart is studied in response to the intervention. In the second type of experiment, attempts are made to isolate the agent responsible for the cardiac growth. These experiments may be *in vitro* tests of specific signaling pathways. Sometimes isolation of a specific growth agent is tried *in utero* as well.

The first type of experiment has been most often used to study proliferative growth of the fetal heart.

Proliferation can be induced by a variety of experimental interventions, including aortic banding in guinea pigs (Saiki *et al.*, 1997), maternal exposure to carbon monoxide (Clubb *et al.*, 1986) or hypoxia in rats (Pietschmann & Bartels, 1985), and partial occlusion of the pulmonary artery (Barbera *et al.*, 2000) or partial obstruction of the ductus venosus in fetal sheep (Tchirikov *et al.*, 2001). The mitogens acting directly on the myocyte are not known in these cases, but some possibilities are considered.

Partial aortic and pulmonary artery occlusion both apply a mechanical load on the developing heart by impeding flow. Possible primary mediators of the mechanical load include stretch-activated ion channels, mechanotransduction by integrins and focal adhesion kinases, or cytoskeletal components including calcium-binding proteins and titan (Lammerding *et al.*, 2004). Stretch also directly alters calcium binding to contractile proteins. Altered hemodynamic conditions also change the circulating (or locally-released) levels of growth regulators from other sources, for example angiotensin II (AngII) and ANP.

Experimentally-induced hypoxia also changes fetal hemodynamic conditions by increasing demand for blood flow to support oxygen delivery. Hypoxia has direct effects at the level of the cell. An oxygen-sensitive protein is responsible for constitutive rapid degradation of the transcription factor hypoxia-inducible factor (HIF-1α); low oxygen levels lead to accumulation of HIF-1α (Chi & Karliner, 2004). HIF-1α acts in cardiac myocytes as a growth regulator, possibly by its regulation of the growth inhibitors p53 and p21, and it also activates transcription of the mitogen vascular endothelial growth factor (VEGF) (MacLellan & Schneider, 2000). Low oxygen levels lead to increased generation of reactive oxygen species (ROS) in the myocyte mitochondria, and thus activation of ROS-sensitive proteins (Goldenthal & Marin-Garcia, 2004), as well as ROS damage. Prolonged (~40 day) RV pressure load of the sheep fetus resulted in a marked accumulation of the products of ROS generation in that ventricle (Fouron *et al.*, 2001). Low oxygen levels also lead to decreased ATP levels in myocytes and activation of intracellular cascades sensitive to high-energy phosphate levels. Hypoxia alters release of circulating or local factors, such as ET-1 and insulin-like growth

factor 1 (IGF-1), which then may act on the myocyte. The interconnections between blood pressure, oxygenation and stimulation of circulating or local tissue factors are complex, but each component influences the growth of fetal cardiac myocytes.

The intracellular signaling pathways that regulate proliferation are similarly complex, with extensive cross-talk between the many pathways activated by mitogenic receptors (Figure 4). The intracellular signaling pathways responsible for hypertrophy of mature myocytes have been more thoroughly investigated than the pathways of immature myocytes that control hyperplasia. I refer the interested reader to recent reviews of myocyte growth pathways by MacLellan and Scheider (2000), myocyte mechanotransduction by Lammerding, Kamm and Lee (2004).

Dr. Sundgren has shown, in our laboratory, that IGF-1 induces proliferation of fetal sheep cardiac myocytes both *in utero* and in culture (Sundgren *et al.*, 2003a). He found that AngII also stimulated hyperplasia but not hypertrophy in culture, different from the findings in rats (Sundgren *et al.*, 2003b). Further, he showed that IGF-1 and AngII rely on both the ERK1/2 branch of the mitogen-activated protein kinase (MAPK) signaling cascade and the phosphoinositol-3 kinase (PI3K) signaling pathway for their effects. These pathways are also necessary for hypertrophic growth in binucleated fetal sheep myocytes. In the sheep fetus, the growth response to increased experimental load tends to be a mix of myocyte proliferation, hypertrophy and binucleation. This is true of the pulmonary artery occlusion mentioned earlier (Barbera *et al.*, 2000), as well as a fetal sheep model of volume load (Appendix A). Dr. Segar and his colleagues partially occluded the pulmonary artery of fetal sheep, with or without blockade of either the AngII receptors AT_1 or AT_2 (Segar *et al.*, 1997; Segar *et al.*, 2001). They concluded that AngII was not responsible for the growth response to the pulmonary band because heart weight increased despite receptor blockade. One explanation is that hyperplasia was inhibited and myocyte hypertrophy was exaggerated in these hearts in order to normalize wall tension. Alternately, AngII is not important for mechanical transduction signaling in the fetal sheep heart. These hypotheses, however, have not been tested.

The pathways that regulate cardiac myocyte proliferation are only beginning to be understood. It is

generally believed that the adult heart does not undergo any significant amount of myocyte proliferation. Therefore, the number of myocytes in the heart is primarily determined by the proliferation during the fetal period. Inhibition of proliferation during fetal life could result in a heart with too few myocytes. Conversely, forcing excessive proliferation in the immature heart results in cardiac enlargement and increased myocyte numbers in the mature myocardium (Jackson *et al.*, 1990). The disadvantages of having less proliferation are clear – inhibition of myocyte proliferation results in a ventricle with thin walls and high wall stress (van Tuyl *et al.*, 2004). Furthermore, the aging myocardium with fewer myocytes is more susceptible to progressive apoptosis and heart failure. An excess of myocytes in the adult heart may have disadvantages that are not understood, because newborns with enlarged hearts often have functional problems as well.

Myocyte Hypertrophy During Fetal Cardiac Growth

The term hypertrophy is applied both to cardiac enlargement and growth of individual cardiac myocytes. Hypertrophy of the mature heart has been studied extensively, and it is known that increases in cardiac mass are the result of enlargement of myocytes and the myocardial matrix. Considerably less is known about hypertrophy of the fetal heart. It is tempting to assume that the mechanisms regulating growth are the same in the mature and the immature heart. However, whereas growth signals are hypertrophic in mature cardiac myocytes, these same signals may stimulate either hypertrophy or proliferation in immature myocytes. It is unclear how growth-promoting signals control these two aspects of myocyte growth in the fetal heart.

Dr. Smolich and colleagues described the morphological growth of the sheep heart from four weeks before birth, to adulthood (Smolich *et al.*, 1989). He showed that the cross-sectional areas of cardiac myocytes are small in the fetus and do not change much in the month before birth, but increase rapidly in the perinatal period. The cross-sectional area increases considerably between the neonate and the adult. Cardiac myocytes do not simply grow larger with advancing gestational age, but also increase their myofibrillar content and organization (Brook *et al.*, 1983). Interestingly, banding of

the pulmonary artery of fetal sheep results in a large RV with hypertrophied myocytes, but the myofibrillar content of these myocytes is decreased relative to cell volume (Barbera *et al.*, 2000). Thus the "maturation" induced by fetal cardiovascular load can be abnormal and may be associated with abnormal cellular development.

Experiments by Dr. Sundgren have shown that phenylephrine stimulates hypertrophy of cultured fetal sheep myocytes; however, he found that IGF-1 and AngII do not share this effect (Sundgren *et al.*, 2003a; Sundgren *et al.*, 2003b). He also found that hypertrophy, like proliferation, requires activation of the ERK1/2 and PI3K signaling pathways. In these experiments, hypertrophic responses were confined to binucleated myocytes. The effects of cortisol have also been studied in fetal sheep (Rudolph *et al.*, 1999; Lumbers *et al.*, 2005); they concluded that cortisol leads to myocyte hypertrophy. However, their results are not conclusive because the hypertensive effects of cortisol were not taken into account. Thus far, phenylephrine is the only agent known to cause hypertrophy of cultured fetal sheep cardiac myocytes.

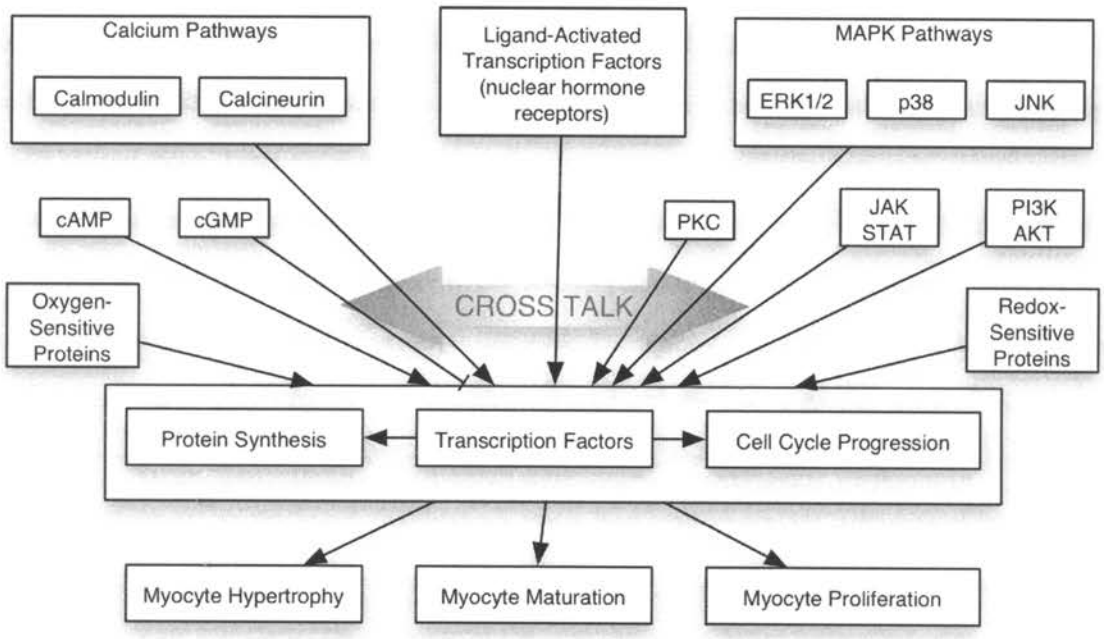

Figure 4. Intracellular signaling pathways that regulate cardiac myocyte growth.

Myocytes can enlarge in either their longitudinal or cross-sectional dimensions. The growth responses of cardiac myocytes are typically generalized as follows: in response to increased load during ventricular systole, myocytes enlarge by cross-sectional growth; in response to increased load during ventricular diastole, the myocytes enlarge by longitudinal growth (Russell *et al.*, 2000). The importance of this is that the ventricles are remodeled according to the timing of the load during the cardiac cycle. Increased myocyte cross-sectional area is associated with thicker ventricular walls, whereas increased myocyte length is associated with an expanding radius of curvature. Thus, according to the law of Laplace, wall stress would be reduced when the ventricular walls thicken, but increased when ventricular chamber enlarges and the radius of curvature becomes greater. In volume load conditions, the ratio of the wall thickness to the radius of the chamber tends to be normal because of wall thickening to match the increased chamber size (Grossman *et al.*, 1975). This might occur because, as explained above, an increase in chamber radius would increase wall stress during systole, which would led to myocardial remodeling.

Experimental data from mature hearts may support these generalizations regarding myocyte growth and ventricular morphology (Schoen *et al.*, 1984; Sawada & Kawamura, 1991). The same may not hold true for the immature myocardium, which can grow by both myocyte hypertrophy and proliferation. Multiple interventions have been evaluated in this laboratory for their cardiac growth effects in fetal sheep: banding of the pulmonary artery (pressure load) (Barbera *et al.*, 2000), surgical creation of an A-V anastomosis (volume load, see Appendix A), IGF-1 infusion (Sundgren *et al.*, 2003a) and infusion of sub-pressor doses of cortisol (unpubulished data). These interventions all fail to stimulate an increase in cardiac myocyte diameter. Pulmonary artery banding and A-V anastamoses in fetal sheep primarily increased hemodynamic load and stimulated cardiac myocyte elongation. Similarly, neither cortisol nor IGF-1 infusion altered cardiac myocyte size. Comparison of these studies leads me to the conclusion that hemodynamic load is an important stimulant of fetal cardiac myocyte hypertrophy. However, after about 1 week of either pressure load by outflow obstruction or volume load by an A-V shunt, the response of the fetal cardiac myocyte is the same: elongation.

Terminal Differentiation of Fetal Cardiac Myocytes

Progressive maturation of cardiac myocytes occurs throughout gestation and is marked by numerous changes as embryonic myocytes acquire the specialized organelles and intracellular organization characteristic of the mature heart. My research has focused on the near-term fetal sheep heart, a period marked by the abrupt cessation of cardiac myocyte proliferation. No conclusive studies have shown why proliferation ceases as cardiac myocytes become mature. In many species the cessation in proliferation is followed by further DNA replication that results in binucleation, as shown in the rat (Clubb & Bishop, 1984), the mouse (Brodsky *et al.*, 1980; Soonpaa *et al.*, 1996), and the sheep (Barbera *et al.*, 2000). Likewise, bi- or poly-ploidy occurs in the nuclei of human cardiac myocytes (Adler & Costabel, 1975). The proportion of myocytes that are binucleated can thus be used as an index of cardiac maturation in the sheep during normal fetal growth (Burrell *et al.*, 2003) and during accelerated cardiac maturation by increased hemodynamic load (Barbera *et al.*, 2000).

The signal for a myocyte to stop dividing and go through terminal differentiation is not known. However, several studies have investigated the expression levels and activities of cyclins, cyclin-dependent kinases (CDK), and CDK inhibitors for their roles in the transition from hyperplasia to hypertrophy in the rat pup (Kang & Koh, 1997; Flink *et al.*, 1998; Poolman & Brooks, 1998). These studies are difficult to interpret because they seek to find an association between expressions or activity levels of cell cycle regulators, and an index of binucleation or proliferation. It appears that there may be a lag period between the time that myocytes stop proliferating and the point at which they become binucleated, and at the same time many myocytes are undergoing hypertrophy (Li *et al.*, 1996). It is thus difficult to pinpoint which cellular processes may be associated with cell cycle regulators. From these studies, however, it appears that the CDKs cdc2, CDK2, CDK4 and CDK6 are upregulated in the transition to terminal differentiation and in hypertrophy. Thus these may regulate withdrawal of the cardiac myocyte from the cell cycle, myocyte binucleation, or myocyte hypertrophy.

It is unknown whether the signal that precipitates terminal differentiation is intrinsic or extrinsic

to the cardiac myocyte. An intrinsic signal could be based on passage of time or number of cellular divisions. One study of cultured cardiac myocytes photographically documented the proliferation of individual lineages (Burton *et al.*, 1999). This study showed that all daughter cells in a given line tended to divide a similar number of times, but when proliferation was slowed (by decreasing the culture temperature) the daughter cells tended to stop dividing after the same amount of time had passed. Thus, these investigators concluded that an intrinsic timer rather than the number of divisions controlled terminal differentiation. However, addition of fibroblast growth factor (FGF) to these cultures stimulated proliferation after the cells initially stopped dividing. Pre-treatment with thyroid hormone "stabilized" withdrawal from the cell cycle and prevented the cells from further divisions stimulated by FGF. A study that may support the hypothesis of a cell cycle "counter" found that transgenic mice over-expressing the proto-oncogene c-myc have increased proliferation in the fetal heart, but then undergo a more rapid decline in myocyte proliferation in the neonatal period (Machida *et al.*, 1997). Likewise, cultured fetal human cardiac myocytes undergo senescence and cease to proliferate by some telomerase-independent mechanism (Ball & Levine, 2005). From these studies it appears that cardiac myocytes have an intrinsic sensor or program that interacts with extrinsic signals to initiate terminal differentiation.

Cardiac Calcium Transport

Cardiac calcium flux couples membrane depolarization with activation of contractile proteins in working cardiac myocytes. The rate and amount of calcium release and removal are essential elements of cardiac function. These features are not fixed processes, rather they are regulated on both a short-term and a long-term basis. This system undergoes maturational changes during fetal gestation, and dysregulation of the system contributes to heart disease in the adult.

The terminology for referring to the system of protein channels, transporters and exchangers that regulate the flux of activator calcium is not standardized. This system is variously referred to as the "calcium-handling system," the "excitation-contraction coupling calcium system," the "calcium-cy-

cling system," and the "calcium transport system." I will use the latter term for clarity and consistency, although I acknowledge that "transport" typically refers to an active process by a particular type of transport proteins. Regeneration and maintenance of the concentration gradient is an energy-dependent process, and so from a broader perspective calcium influx is indeed "transport".

Calcium Transport in Cardiac Myocytes

The myocardial "syncytium" is stimulated to contract in a coordinated fashion by the cell-to-cell propagation of an electrical impulse. This electrical impulse sets into action a cycle of calcium release and uptake within the myocyte (Figure 5). The depolarization of the sarcolemma within the invaginating t-tubule system of the myocyte membrane stimulates the opening of the voltage-sensitive calcium channel, known as the "L-type" calcium channel (LTCC). The opening of a single LTCC can trigger a calcium spark by the calcium-induced-calcium release mechanism of the SR ryanodine receptor (RyR) (Wier & Balke, 1999). The SR can store an enormous amount of calcium because of the calcium-buffering capacity of the acidic glycoprotein calsequestrin. Calcium release from the SR via RyR is normally extremely rapid and is not rate-limiting for contraction; however, the magnitude of the calcium release is directly related to cardiac contractile function. In the cytosol, calcium binds to troponin C, allowing cross-bridge association between actin and myosin and leads to contraction.

Removal of calcium from the cytosol into the SR is driven against a concentration gradient by the SR calcium ATPase 2 (SERCA2). This process is rate limiting for myocardial relaxation (Miller *et al.*, 1990; Lewartowski & Wolska, 1993). Under steady-state conditions the same amount of calcium that enters the cell at excitation is pumped out during relaxation. The cardiac sodium-calcium exchanger (NCX1) is driven by the concentration gradient for sodium, exchanging 1 calcium ion for 3 sodium ions. This process is energy dependent. The sodium-potassium ATPase, which establishes the concentration gradient for sodium, uses 1 ATP for every 3 sodium ions it pumps out, while SERCA2 moves 2 calcium ions for every ATP used and is therefore a more energy efficient method of calcium removal. A sarcolemmal calcium ATPase has a minor role in the removal of calcium dur-

ing active relaxation.

Contractility of the heart is directly related to the magnitude of the calcium transients. This SR transient, in turn, is dependent on SR calcium stores and the amount that is released (Diaz *et al.*, 2005). SERCA2 is a key regulator of SR calcium levels. Inhibition of SERCA2 results in decreased myocardial contractile force and slower relaxation. Under these circumstances, stimulation of RyR may increase calcium transients for a few beats, but unless SERCA2 is also stimulated, the SR content of calcium will fall and the transients will normalize. SERCA2 is constitutively inhibited by the regulatory protein phospholamban. The activities of phospholamban, SERCA2, RyR, LTCC and NCX1 are controlled in the myocyte by phosphorylation and by regulation of expression.

The specific modulators and transcription factors that control gene expression of the cardiac calcium transport system have not been well characterized. Thyroid hormone is an important signal for both NCX1 and SERCA2 expression. Thyroid hormone induces SERCA2 expression in the heart through a thyroid hormone response element (Rohrer *et al.*, 1991; Zarain-Herzberg *et al.*, 1994). Thyroid hormone is necessary to maintain normal levels of SERCA2 expression in the heart (Rohrer & Dillmann, 1988). Normal maternal thyroid levels are required in developing rats in order for the normal postnatal increase in cardiac SERCA2 to occur (van Tuyl *et al.*, 2004). NCX1 levels are negatively regulated by thyroid hormone in the mature and immature heart (Boerth & Artman, 1996; Reed *et al.*, 2000; Shenoy *et al.*, 2001).

There are other myocardial modulators of calcium transport genes. Silencing of SERCA2 in neonatal rat cardiac myocytes causes up-regulation of NCX1 through a calcineurin-dependent mechanism (Seth *et al.*, 2004). Myocyte enhancer specific factor 2a (MEF-2a) regulates SERCA2 expression (Moriscot *et al.*, 1997), and perhaps other calcium transporters as well. Chronic adrenergic stimulation of cardiac myocytes is known to contribute to the progression of disease; blockade of β receptors by propranalol decreases high levels of NCX1 in model of heart failure in the adult mouse (Plank *et al.*, 2003), while only 24 hours of α-adrenergic stimulation in adult rat cardiac myocytes resulted in increased NCX1 and protein levels (Reinecke *et al.*, 1997). Some basic helix-loop-helix

(bHLH) and zinc-finger GATA transcription factors are critical for cardiac development, and DNA consensus binding sites for these are found in the NCX1 promoter region (Nicholas and Philipson, 1999). In the heart, GATA-4 is necessary for NCX1 expression, but the E-box site for bHLH binding is not.

Protein levels are not controlled only by the rate of translation, but also by intracellular turnover and degradation. In cultured neonatal rat cardiac myocytes the half-life of NCX1 protein has been estimated at 33 hours (Slodzinski & Blaustein, 1998). Rapid degradation of calcium transporters by calcium-activated calpain has been described following cardiac insult (Singh *et al.*, 2004b, Singh *et al.*, 2004a), but the mechanisms of constitutive degradation of these proteins have not been well described.

Maturation of the Calcium Transport System

In the late 1970s investigators began studying the calcium transport characteristics of immature hearts. The initial studies confirmed that the fetal cardiac calcium transport differs from the adult, and that the fetal SR is not as effective at concentrating calcium (Nayler & Fassold, 1977). SERCA2 is first detected when the myocytes begin to contract (Jorgensen & Bashir, 1984). However, NCX1 activity is essential for cardiac contractions in the embryo (Linask *et al.*, 2001), as is LTCC

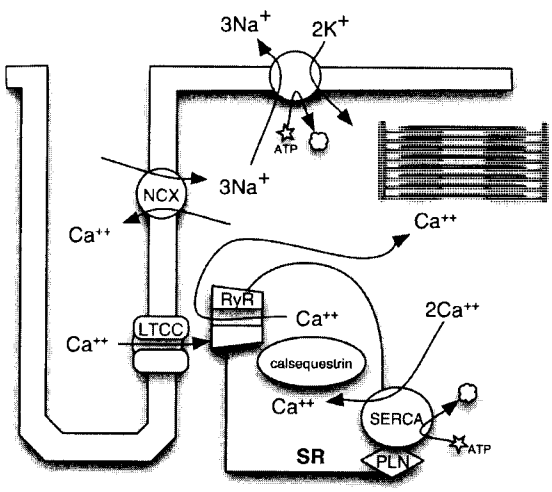

Figure 5. A simplified diagram of the cardiac calcium transport system. LTCC is a voltage sensor that opens to allow a small amount of calcium into the cytosol. This triggers a large release of calcium from the SR by RyR. Calcium binds to troponin C (and other cytosolic calcium buffers) and initiates contraction. To allow relaxation, calcium is removed from the cytosol. At steady state, NCX1 shuttles out as much calcium as LTCC allowed in; this is driven by the sodium gradient established by the sodium-potassium ATPase. The bulk of the cytosolic calcium is restored to the SR by SERCA2, where very high calcium levels can be concentrated due to the abundant binding protein calsequestrin. SERCA2 is an ATPase critical to the regulation of SR calcium levels; its activity is regulated by PLN.

(Rottbauer *et al.*, 2001). Increased SR function may be due to structural maturation of the SR as well as changes in expression of channels and regulatory proteins. The amount of SR protein per gram of rabbit heart tissue more than doubled between the fetus and the neonate, and between the neonate and the adult (Nakanishi & Jarmakani, 1984). These investigators also documented differences in cardiac muscle function among the fetus, neonate and adult, finding a maturation-dependent increase in developed tension, the rate of tension development, and the rate of relaxation at high external calcium concentrations. These early studies sketched a picture in which the fetus has an anatomically and functionally immature SR with a relative inability to concentrate intracellular calcium stores, and an increased reliance on and sensitivity to extracellular calcium levels.

Cardiac myocytes have specialized cellular adaptations to create rapid intracellular calcium fluxes that are essential for contraction (Figure 5). Two specializations are the transverse-tubules (t-tubules) and the SR. The t-tubules are deeply invaginating extensions of the plasma membrane that ensure the rapid and uniform dissemination of depolarization into the interior of the cell and subsequent calcium release. The SR is an extensive intracellular membranous network associated with the myofibrils and t-tubules of the myocyte. Terminal cisternae of the SR are in close approximation to the t-tubules, while longitudinal tubules run between them. This distribution of the SR ensures that calcium can be rapidly delivered, and removed from, the contractile apparatus.

The specializations of the t-tubules and SR gradually develop as the heart matures. As cardiac myocytes grow in size the diffusion distance for calcium between the sarcolemma and the innermost contractile protein becomes greater; the small size of immature cardiac myocytes allows them to function before development of the t-tubule network (Legato, 1979a, b; Sheridan *et al.*, 1979; Forsgren & Thornell, 1981; Maylie, 1982). The very early heart contains little SR. As development proceeds, the organelles develop along with the contractile apparatus. The myofibrillar content of immature cardiac myocyte is less dense and is organized near the plasma membrane (Brook *et al.*, 1983; Smolich *et al.*, 1989). Indeed, in cardiac myocytes of the newborn rabbit, the calcium transient has been found to result in a greater change in concentration near the cell surface (Haddock *et al.*,

1999). The SR of immature hearts is scant and its structure not fully formed, although it is present at birth in all species studied (Smith & Page, 1977; Legato, 1979b; Forsgren & Thornell, 1981; Hoerter *et al.*, 1981; Page & Buecker, 1981; Maylie, 1982; Nakanishi *et al.*, 1987). Throughout fetal maturation the SR content increases and becomes structurally more mature. The lack of these myocyte specializations increases the reliance of immature myocytes on LTCC and NCX1 for contraction. The calcium transient of immature myocytes is dependent on an extracellular source of calcium, but with maturation the role of ryanodine-sensitive stores increases (Agata *et al.*, 1994; Segar *et al.*, 1997; Creazzo *et al.*, 2004).

Inter-species differences occur in the rate at which the cardiac calcium transport system matures. Some of these differences can be attributed to the maturity of the newborn. Precocious species such as sheep tend to have a more mature SR near or at birth (Mahony & Jones, 1986; Michalak, 1987; Pegg & Michalak, 1987) than altricial species such as rabbits (Nakanishi & Jarmakani, 1984). Although sheep are precocious, their cardiac SR is still not fully mature before birth. Two groups published near-simultaneous studies describing the cardiac calcium transport system in the fetal sheep (Mahony & Jones, 1986; Michalak, 1987; Pegg & Michalak, 1987). Both groups found that the fetal lamb cardiac SR was slower to accumulate calcium and could not accumulate as much as the adult. The calcium-ATPase activity of the fetal heart was less than that of the adult heart, and the amount of calcium-ATPase protein (i.e. SERCA2) was less.

Further studies clarified details of mRNA and protein expression of calcium transport genes in various species during development. NCX1 levels are high during the fetal period and decreased in the neonate and adult hearts across many mammalian species, including humans, dogs, rats and mouse (Hanson *et al.*, 1993; Vetter *et al.*, 1995; Qu *et al.*, 2000; Reed *et al.*, 2000). Likewise, there is evidence that the SR protein RyR increases with development (Brillantes *et al.*, 1994). SERCA2 increases antithetically to NCX1 and is high in the mature heart (Wibo *et al.*, 1995; Reed *et al.*, 2000); this change may be due to increased mRNA stability (Ribadeau-Dumas *et al.*, 1999). Interestingly, studies suggest that LTCC expression and current density increases with development

Table 1. Structure and regulation of calcium transport proteins.

Channel / Protein	Composition	Regulation of Activity	Regulation of Expression
L-type calcium channel (LTCC) also known as dihydropyridine receptor (DHPR)	Composed of several subuints, including the pore-forming c1c subunit and accessory c2-d and β subuinits (Striessnig, 1999)	Voltage-gated; activated by PKA-mediated phosphorylation (Striessnig, 1999); auto-inhibition relieved by PKCα.; inhibited by protein phosphatases 1 and 2A-mediated dephosphorylation (Kumar & Joyner, 2003); inhibited by cGMP (NO may activate at low levels) (Striessnig, 1999)	Degraded by calpain (Singh *et al.*, 2004b)
Ryanodine receptor (RyR) or "SR release channel"	Composed of 4 RyR2 polypeptides and 4 FK506-binding proteins (Meissner, 2004).	Opening regulated by calcium ion. RyR is also regulated by CaMK and calcineurin, PKA, thiol oxidation and nitrosylation (associated with NO), and calsequestrin (Meissner, 2004)	Decreased by passive stretch (Cadre *et al.*, 1998); degraded by calpain (Singh *et al.*, 2004a)
Sarco(endo)plasmic reticulum ATPase (SERCA2)	Cardiac SERCA2 (designated "2a") is a large protein with 10 transmembrane domains (Misquitta *et al.*, 1999).	PLN is a key regulator of SERCA2, constitutively inhibiting it. CaMK phosphorylates and activates SERCA2 (Xu & Narayanan, 1999).	Increased by thyroid hormone (Rohrer *et al.*, 1991; Zarain-Herzberg *et al.*, 1994), MEF-2a (Moriscot *et al.*, 1997), β-blockade (Yasumura *et al.*, 2003) and AT1 antagonism (Hashida *et al.*, 1999); degraded by calpain (Singh *et al.*, 2004a)
Phospholamban (PLN)	A small monomer, PLN is thought to be functional in its pentameric form.	PLN is deactivated by phosphorylation by PKA. Dephosphorylated by protein phosphatase 2A (Gergs *et al.*, 2004)	Degraded by calpain (Singh *et al.*, 2004a)
Sodium-calcium exchanger (NCX1)	NCX1 proteins have 9 transmembrane domains, the cardiac form is a splice variant of NCX1 (Philipson *et al.*, 2002).	NCX1 activity is primarily determined by the electrochemical gradients for sodium and calcium.	Increased by retinoic acid (Hudecova *et al.*, 2004), calcineurin (Seth *et al.*, 2004; Katanosaka *et al.*, 2005), adrenergic stimulation (Reinecke *et al.*, 1997; Plank *et al.*, 2003); decreased by thyroid hormone (Boerth & Artman, 1996; Reed *et al.*, 2000; Shenoy *et al.*, 2001)
Calsequestrin	Cardiac calsequestrin is an acid glycoprotein contained within the lumen of the SR.	Calsequestrin is a low-affinity calcium binding protein that increases the calcium storage capacity of the SR.	Degraded by calpain Singh *et al.*, 2004a)

(Brillantes *et al.*, 1994; Kato *et al.*, 1996; Liu *et al.*, 2000), and the channel becomes concentrated in junctional structures during postnatal maturation (Wibo *et al.*, 1998). There is differential regulation of isoforms during development (Haase *et al.*, 2000). One study of channel function suggests that channel inactivation is slower in the neonate than the adult (Katsube *et al.*, 1998), but another study disagrees (Kato *et al.*, 1996). These perinatal transitions may be regulated in part by thyroid hormone (Magyar *et al.*, 1995; Wibo *et al.*, 1995), mechanical stress (Cadre *et al.*, 1998) or other unknown modulators.

Expression of regulatory proteins may also change during development. The sodium-potassium pump, which establishes the sodium gradient to run NCX1, is also up-regulated during development (Hanson *et al.*, 1993), and is regulated by thyroid hormone (Book *et al.*, 1997). Protein phosphatases 1 and 2A, which dephosphorylate LTCC, RyR and phospholamban (PLN), are higher in the immature heart (Kumar & Joyner, 2003).

The SR calcium storage system is relatively undeveloped in the embryo and fetus, but develops to become the primary source of calcium used for excitation-contraction coupling. The differences between the immature heart and mature heart include the amount of SR, the degree of functional association between the SR and the sarcolemma, and the number and function of the calcium channels and pumps in the myocyte, all of which increase with age.

Adult Heart Failure

Heart failure and cardiac hypertrophy have been studied extensively in the adult. It is established that patients with heart disease and animal models of heart failure are heterogeneous because the underlying mechanisms and progression of the disease are complex. In many cases, however, cardiac dysfunction and cardiac hypertrophy are intrinsically linked. This field is too broad to be covered by more than a general overview of the points that are most relevant here. Good recent reviews of the pathophysiological role of excitation-contraction coupling in heart failure are those by Sjaastad *et al.*

(2003) and Yano *et al.* (2005); for reviews of the molecular regulation of growth see MacLellan & Schneider (2000), and Cooper (1997).

One primary cause of hypertrophy is the response of the myocardium to increased wall stress, either systolic or diastolic (Cooper, 1997). The myocardium remodels to normalize wall stress, but this remodeling leads to changes in protein expression and activity that eventually reduce cardiac performance. Mechanical stress can also be directly responsible for altered expression of calcium transport genes. Cyclic stretch of cultured neonatal rat cardiac myocytes causes down-regulation of SERCA2 and RyR, but not NCX1 or PLN (Cadre *et al.*, 1998). Similarly, active tension generation in cultured neonatal rat cardiac myocytes causes down-regulation of SERCA2, but not NCX1 (Bassani *et al.*, 1994). Growth of the myocardium is also responsive to hormonal regulation by agents such as catacholamines, angiotensin II and thyroxine (Cooper, 1997; MacLellan & Schneider, 2000), as is the cardiac calcium transport system (Sjaastad *et al.*, 2003; Yano *et al.*, 2005).

Regulation of calcium flux is at the core of myocyte function (Bers, 2002). If one of the calcium channels or transporters is perturbed by a regulatory factor or altered expression, the entire system will adjust and a new steady state of calcium release with be reached. Reduced magnitude or dyssynchrony of calcium-induced calcium release will reduce and delay the peak force developed by myocytes, decreasing the contractile function of the myocardium. Inability of the SR calcium uptake mechanism to function normally slows removal of calcium from the cytosol and slows myocardial relaxation. Both of these pathologies are found in diseased hearts.

The quantity of calcium available for release is limited by the ability of the myocytes to concentrate calcium in the SR. Hyperphosphorylation of RyR in heart failure increases the calcium leak through these channels during diastole, limiting the amount of calcium that can be stored in the SR. Decreased SERCA2 expression and function also contribute to a relative inability of the SR to concentrate calcium (Yano *et al.*, 2005). NCX1 overexpression, found in some studies, can also contribute to low SR calcium concentrations (for a mathematical model see Shannon *et al.*, 2003). Contrarily, NCX1 activity can be inhibited by PKC and calcineurin (Katanosaka *et al.*, 2005),

which may contribute to elevated diastolic calcium and progression of heart failure. The reduction in the driving force of sodium in the failing heart can also contribute to this process, causing more calcium to enter the cell through NCX1 (Baartscheer *et al.*, 2003).

Hypoxia and ischemia can also affect transcription and activity of the cardiac calcium transport system. Short-term hypoxia or glucose deprivation actually increases expression of SR-associated genes (Temsah *et al.*, 2001). However, increased extracellular lactate levels inhibit cardiac myocyte function and increase diastolic calcium levels, in part by decreasing the activities of SERCA2 and NCX1 (Terracciano & MacLeod, 1997).

Hypotheses

Growth and development of the myocardium occurs concurrently with structural and functional maturation of the cardiac SR. Cardiac growth and regulation of activator calcium in the myocyte are often linked. Abnormal myocyte hypertrophy and dysregulation of cardiac calcium transport also occur together in response to hemodynamic overload in the adult. Fetuses afflicted by TTTS can have both cardiac hypertrophy and dysfunction, but the type of myocardial growth and the mechanisms of dysfunction are unknown. **I hypothesized that hemodynamic overload of the fetal heart would stimulate myocyte growth and altered regulation of the cardiac calcium transport system.** I tested this hypothesis in several different fetal sheep models to learn if there were different responses to pressure and volume components of the hemodynamic stress.

Gradual infusion of plasma into fetal sheep causes changes that are similar to those seen in recipient twins of TTTS. Because AngII is depressed in this model, as in the TTTS recipient twin (Mahieu-Caputo *et al.*, 2000), and because AngII stimulates proliferation in fetal sheep cardiac myocytes in culture (Sundgren *et al.*, 2003b), I predicted that proliferation would not increase in the plasma-infusion model. I hypothesized that 1) **combined venous and arterial hypertension would increase fetal cardiac mass by inducing myocyte hypertrophy and early maturation.** I tested this hypothesis

by infusing plasma into fetal sheep in order to gradually produce arterial and venous hypertension. I dissociated their hearts and measured their myocytes to determine how their hearts grew.

In addition to cardiac hypertrophy, cardiomyopathy with systolic and diastolic dysfunction is often found in recipient fetuses of TTTS (Raboisson *et al.*, 2004). The underlying mechanisms of the dysfunction are unknown, although they are similar to the functional changes in cardiac myocytes when the SR-associated calcium flux is inhibited (Lewartowski & Wolska, 1993). I therefore hypothesized that 2) **cardiac SERCA2, RyR and calsequestrin would be down-regulated and NCX1 and LTCC would be up-regulated in plasma-infused fetuses.** To test this hypothesis I took hearts from plasma-infused fetuses to measure mRNA and protein levels of these genes.

I wanted to understand how afterload and preload might independently regulate the hemodynamic stress-induced changes in fetal gene expression. Active tension development (contraction) down-regulates SERCA2 expression and function in cultured neonatal rat cardiac myocytes (Bassani *et al.*, 1994). In the mature animal, SERCA2, PLN, RyR and calsequestrin levels are reduced as soon as 2 days following induction of pressure load (Matsui *et al.*, 1995). I hypothesized that 3) **fetal pressure overload would down-regulate SERCA2 and up-regulate NCX1.** To test this hypothesis I placed an occluder around the postductal aorta of fetal lambs to impose a pressure overload, and then measured mRNA levels in their cardiac tissue.

Experimental evidence suggests that volume overload can also be a stimulus that regulates expression of the cardiac calcium transport system. Passive tension development (stretch) induces down-regulation of SERCA2 and RyR in cultured cardiac myocytes (Cadre *et al.*, 1998). In the mature animal, chronic volume load induced by an arteriovenous fistula results in decreased expression of SERCA2, RyR and PLN (Hashida *et al.*, 1999). I hypothesized that 4) **fetal volume overload would down-regulate SERCA2 and up-regulate NCX1.** To test this hypothesis I took measured gene expression levels in RNA from hearts of fetal lambs that *in utero* had a chronic surgical arteriovenous fistula.

Donor twins of TTTS are often described as anemic. Anemia in the fetal lamb results in increased

cardiac mass and output (Davis & Hohimer, 1991). Furthermore, the activation of the fetal RAS reported in donor twins (Mahieu-Caputo *et al.*, 2000; Kilby *et al.*, 2001) suggests that proliferation may be stimulated in these hearts. I therefore hypothesized that 5) **fetal anemia would increase cardiac mass by stimulating cardiac myocyte proliferation, hypertrophy and premature terminal differentiation.** I tested this hypothesis by making fetal sheep chronically anemic. I then dissociated their hearts to measure their cardiac myocytes.

Originality and Assignation of Credit

The ideas and hypotheses in this thesis are mine. The work described was primarily carried out by me, but it could not have been done without help. Major contributions to ideas or labor are noted here to avoid any confusion: 1) the plasma-infusion fetal sheep model was developed by, and done in collaboration with, Drs. Faber, Giraud and Anderson. 2) The fetal anemia hypothesis was developed by and done in collaboration with Drs. Thornburg and Giraud. The fetal anemia model was originally developed by Drs. Davis and Hohimer. I instrumented the animals and carried out the daily experiments because I was interested in fetal anemia as a model of the donor twin in TTTS. 3) Using the hearts from the anemia animals, I taught Dr. Chattergoon to make measurements on isolated cardiac myocytes. 4) I was occasionally involved in the surgery or experiments to produce volume loaded fetuses; however, that model was developed by Drs. Thornburg, Karamlou, and Giraud. I used banked heart tissue that had been collected from these fetuses for other purposes.

Other instances of collaboration are noted in the text.

CHAPTER 2

Materials and Methods

Preparation of Animal Models

Humane Treatment of Sheep

All animal protocols used in this thesis were reviewed and approved by the Institutional Animal Care and Use Committee (IACUC). Sheep (*ovis aries*) of mixed western breed were obtained from a commercial breeder. Animals were fed *ad libitum* and had free access to water. Animals were free to stand or lie in a clean pen or stanchion at will. They were observed several times a day by investigators and animal care staff to ensure that they were in good health. Department of Comparative Medicine veterinarians were always available to attend to animals.

Surgical Preparation of Experimental Animals

Anesthesia and Preparation

Time-bred pregnant ewes were allowed to acclimatize to their pens at least three days prior to surgery, and to recover from surgery in the same familiar room. For 24 hours prior to surgery, ewes were fasted (but allowed free access to water) in order to avoid aspiration of stomach contents during surgery. Anesthesia was induced with 400mg ketamine and 10mg diazepam intravenously. The animal was then intubated and anesthesia continued with about 1% isoflurane in a 50/50 volume/volume mixture of oxygen and nitrous oxide. Isoflurane concentrations were adjusted to ensure a surgical level of anesthesia for both ewe and fetus.

Once anesthetized, the ewe was moved to a surgical table. The abdomen and chest were shorn, and then scrubbed and rinsed three times with a betadine soap solution. The ewe was then transported to the surgical suite and connected to a pulse oximeter and end-tidal CO_2 monitor. A final betadine scrub was performed in the surgical suite. The ewe was then draped for surgery, and all items entering the surgical field thereafter were sterile (according to the OHSU IACUC Policy Manual). Surgery then proceeded according to the specific protocol.

Procedure for the Plasma-Protein Infusion Model

The maternal abdomen was opened through a midline incision, exposing the uterus. The uterus was opened and the fetal membranes (amnion, chorion) were sewn to the edge of the incision to protect them for later fluid-tight membrane closure. A purse-string suture was placed around the uterine incision and tightened as the fetus was exposed in order to reduce amniotic fluid loss. The distal hindlimbs of the fetus were exposed and a small (less than 4cm) incision was made in the leg. The pedal artery and vein in each leg was catheterized with a V5 (0.86mm internal diameter) or V8 (1.19mm internal diameter) polyvinyl catheter, and then the incision was sutured. A V8 polyvinyl catheter with multiple side-openings for measurement of amniotic pressure was anchored with the catheters on each leg.

The fetus was then gently returned to the uterus. The uterine incision was closed and then oversewn to prevent leakage of amniotic fluid. The maternal abdominal incision was closed in anatomical layers, and all catheters were tunneled subcutaneously to emerge on the flank of the ewe. Catheters were bundled and stored in a pouch stitched to the flank of the ewe to prevent them from pulling out. One million units of penicillin-G were administered to the amniotic fluid (through a catheter). No other antibiotics are routinely necessary (post-operative cultures have amply demonstrated the adequacy of this regime).

After surgery, animals were returned to a recovery run for 24 hours. Buprenex (0.3-0.6mg subcutaneous) was routinely administered immediately after surgery and for the next two days (2 times per

day) to prevent pain and distress. The ewe was monitored until the she was standing and feeding, which usually occurred within an hour of surgery.

Procedure for the Volume Load Model

Please see Appendix A.

Procedure for Placement of an Inflatable Vascular Occluder

The uterus was exposed as in the plasma-infusion protocol. The head and neck of the fetus were exteriorized and a small (less than 4cm) incision was made in the fetal neck to expose the carotid artery and jugular vein. Occlusive indwelling catheters were placed in these vessels. Two V8 polyvinyl catheters were placed in the jugular vein. One V8 and one V5 polyvinyl catheter was placed in the carotid artery. The fetal incision was closed with suture. Catheters, including a catheter open to the fluid in the amniotic space, were anchored to the fetal skin on the neck and head (to prevent them from pulling out or kinking off).

The fetal chest and forelimbs were then externalized through the uterine incision. The fetal chest was opened through a left thoracotomy and the postductal aorta was isolated. A silicone rubber inflatable vascular occluder (In Vivo Metric, Healdsburg, CA) was placed around this segment of the descending thoracic aorta. The fetal chest was then closed in anatomical layers. The ribs seperated by the incision were gently approximated with 2 ligatures. The muscle layer was then sutured, followed by closure of the fetal skin. The fetus was returned to the uterus and the surgery concluded as in other protocols.

Procedure for the Anemia Model

The fetus was catheterized and neck and amniotic catheters were placed as in other protocols. If it was a twin pregnancy, both fetuses were instrumented through separate uterine incisions. Surgery

was concluded as in other protocols.

Euthanasia and Postmortem

Ewes were humanely killed according to the best laboratory practices recommended by American Veterinary Medical Association (Institute of Laboratory Animal Resources, 1992; AVMA, 2001). A commercially available solution of sodium pentobarbital was injected intravenously (100mg/kg body weight) to kill the ewe. The barbiturate crossed the placenta and anesthetized the fetus as well. The abdomen and uterus of the ewe were then opened and the fetus exteriorized. Blood samples from an umbilical vein and artery were taken. Heparin was injected into a fetal umbilical vein and allowed to circulate briefly, and then a solution of saturated potassium chloride was injected into the umbilical vein ensure that the heart was arrested in diastole. The umbilical cord was tied and cut. The fetus was weighed and its sex was noted.

Organs were then collected from the fetus, beginning with the rapid excision of its heart. The great vessels of the heart were trimmed to a standard length (the aorta was trimmed at the bifurcation of the common brachiocephalic artery, and the pulmonary artery was trimmed at the bifurcation of the pulmonary arteries), the heart was blotted, and then it was weighed. Except for those that were to be dissociated, all hearts were dissected into individual component pieces (left atrium, right atrium, LV, RV and septum) following anatomical markers. The atria were dissected from the ventricles at the level of the annulus of the respective atrioventricular valve and freed from the great vessels. The atria were divided such that half of the intra-atrial septum was allocated to each atria. The ventriclular free walls were dissected free from the septum such that the septum retained a border of endocardium equal to its thickness. The great vessels were then freed from the septum. Tissue to be used for RNA or protein extraction was wrapped in foil and then rapidly frozen in liquid nitrogen. All frozen tissue was stored in a -80°C freezer. If the maternal heart was to be used in a protocol it was then excised and treated.

Sheep plasma was required for fetal protein infusion; consequently, in some cases, the ewe was ex-

sanguinated prior to euthanasia. In accordance with the American Veterinary Medical Association (Institute of Laboratory Animal Resources, 1992; AVMA, 2001) the ewe was deeply sedated and rendered pain-free by the administration of xylazine and ketamine. Exsanguination proceeded only after the euthanasia of the fetus.

Sheep Used for Ontogeny

Control fetuses, lambs and adult sheep were collected for analysis of maturational changes in cardiac myocytes and cardiac gene expression. For the measurement of myocytes, 54 fetuses from 45 ewes, 5 lambs, 4 rams (recently castrated and testosterone-supplemented) and 5 non-pregnant ewes were euthanized. Four fetuses did not have heart or body weights recorded. For measurement of gene expression, 10 fetuses from 10 ewes, 5 lambs, 5 non-pregnant ewes and 5 rams were euthanized. Twelve hearts were taken from pregnant ewes at the conclusion of fetal experiments. Many of these fetuses were obtained as uninstrumented twins from other protocols.

Experimental Models

All fetal sheep experiments had common elements. Ewes were allowed to recover for about 1 week before fetal studies. Towards the end of the recovery period the ewe was moved into a study stanchion where she could eat, drink, stand or lie down at will while continuous pressure recordings were being made. Fetal catheters were typically opened prior to the baseline day in order to monitor recovery from surgery and establish a true baseline.

Daily procedure typically was completed early in the morning before or during the first feeding, when the ewes were laying or standing quietly. The continuous pressure recording was saved and pressure transducers were zeroed to atmospheric pressure and calibrated using a mercury manometer. Catheters were flushed with a small amount of heparinized saline, and a pressure recording of at least 30min was taken. Pressures before and after the saline flush were compared, and the most accurate block of recording was averaged (based on the possible presence of clots in the tip of the cath-

eter, activity of the ewe, and/or the response of the fetus to the saline flush). Pressures were recorded with Abbott Transpac pressure transducers on a calibrated computerized system (ADInstruments, Colorado Springs, CO; Apple, Cupertino, CA). Fetal intravascular pressures were referred to amniotic fluid pressure as zero. Heart rates were calculated from arterial pressure measurements.

Blood samples (3ml) were rapidly withdrawn from the arterial catheter, placed in chilled tubes containing heparin or EDTA, and centrifuged at 4°C for 15min. The plasma was withdrawn and frozen at -20°C. 1.5ml of arterial blood was drawn up into a heparinized syringe, which was immediately capped and placed on ice. This sample was used for determination of arterial blood gases, pH and hematocrit. Blood P_{O_2}, P_{CO_2} and pH were determined using an Instrumentation Laboratories Blood Gas Analyzer (Lexington, MA). Blood hemoglobin and oxygen content was determined on an Instrumentation Laboratories Co-oximeter.

Experimental Method for Plasma Load

The purpose of this experiment was to gradually create arterial and venous hypertension in the fetal sheep by the continuous influsion of plasma. All experiments were begun at an average of 130 ± 2 days of gestational age (dGA).

Plasma for infusion was obtained from ewes as described. The ewe was given 10,000 units of heparin, then phlebotomized into sterile 1 liter bottles containing additional heparin. Whole blood was promptly centrifuged, and the plasma fraction removed and saved. Plasma was passed through a series of filters using vacuum flasks, concluding with a sterile 0.22μm filter-bottle system. Sterile plasma was then stored at room temperature to prevent cold agglutination.

After baseline measurements were taken, intravenous infusion of sterile-filtered sheep plasma was started using a Gilson Minipuls-3 roller pump. The infusion rate was increased by 3.5% per day to correspond to the percent increase in fetal size due to growth. The 8-day infusion group received a total of 121 ± 28g plasma protein in 2159 ± 714ml of plasma over 7-10 days. These experiments were

concluded when the fetuses were 138 ± 1dGA (term is about 145dGA). The 4-day infusion group received at total of 64 ± 19g plasma protein in 1190 ± 240ml of plasma. These experiments were concluded when the fetuses were 134 ± 1dGA. Fourteen control fetuses were included in the 8-day study group from which 8 hearts were dissociated and 6 hearts were frozen in liquid nitrogen. Seven experimental and 8 control fetuses were studied in the 4-day infusion group, the hearts from this group were all dissociated. Control fetuses were age-matched. Seven were instrumented, the remainder were uninstrumented twins of experimental fetuses.

Experimental Method for Volume Load

The purpose of this experiment was to impose a volume load on the fetal heart by the surgical creation of an arterial to venous anastamosis. Please see Appendix A.

Experimental Method for Systolic Pressure Load

The purpose on this experiment was to impose an arterial pressure load on both ventricles of the fetal heart by the inflation of an occluder around the postductal thoracic aorta.

After baseline measurements were taken the inflatable occluder was deflated (except for the inital day, when the occluder was not yet inflated) and the blood pressures allowed to stabilize for 30min

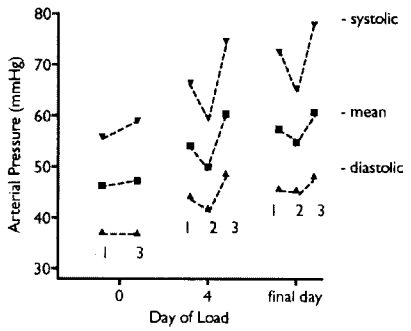

Figure 6. Experimental method for pressure load applied with an inflatable occluder. Arterial pressures are shown for day 0, day 4 and the day prior to the conclusion of an experiment in one fetus. Three periods are shown: 1) baseline measurements, 2) 30min after releasing the inflatable occluder, and 3) 30min after re-inflating the occluder.

(Figure 6). Blood pressure measurements were taken again, and then the occluder was inflated until the waveform of the aortic pressure proximal to the occluder changed (elevated systolic pressure and widening of the pulse pressure) without causing abnormal heart rhythms. The occluder catheter was then clamped and the load maintained until the next day. The hearts of all of these fetuses were frozen in liquid nitrogen.

Experimental Method for Anemia

The purpose of this experiment was to rapidly create and maintain anemia in fetal sheep by daily phlebotomy.

Blood samples collected in EDTA and heparin were taken only on the baseline day and on the last day of the experiment. Baseline hemodynamic measurements were obtained, followed by an arterial sample for determination of fetal blood gases. This concluded the daily experiment if the fetus was a control. If the fetus was experimental, I made a decision of how much blood to remove. My goal was to bring the oxygen content of the fetus down to 2.5g/100ml over several days, and my daily decision was based on health of the fetus, the number of fetuses (singletons typically being larger than twins), previous responses of a particular fetus to bleeding, and the stage of the experiment. For the first several days I typically removed 100ml of blood, then I tapered down to a smaller volume. Blood was rapidly withdrawn from the arterial circulation into a heparinized 60ml syringe, and then the volume was replaced by non-heparinized saline. If more blood was to be withdrawn the procedure was repeated. The fetus was then monitored for at least half an hour (including additional blood gas measurements if justified).

At the conclusion of the experiment, some hearts were dissociated for myocyte analysis; a section of LV was removed prior to dissociation in 3 hearts from each group for wet-to-dry weight analysis. For wet-to-dry weight analysis a section of the LV was excised and weighed fresh. Sections were desiccated in a drying oven for two weeks. Sections weights were checked for three days in a row to ensure that drying was complete. Data are expressed as the weight of the wet section divided by the

weight of the same section desiccated.

Radioimmunoassays

Radioimmnoassay (RIA) technique is based on competition binding principles, where labeled compound competes with sample compound for antibody sites. A standard curve, "total counts" and "non-specific binding" samples were generated for each assay. Robert Webber, in the Thornburg Laboratory, performed all radioimmnoassays. Assays were performed in duplicate.

Angiotensin II

The plasma AngII levels from fetal sheep were measured by RIA using a kit from Peninsula Laboratories (a division of Bachem, Torrance, CA).

EDTA plasma samples were extracted to remove interfering proteins and to concentrate AngII peptide as follows. Plasma samples were thawed on ice and aliquoted. Trifluoroacetic acid was added acidify the sample, and then run through a C18 Sep-column (Varian, Palo Alto, CA). The column was washed, and then the sample was eluted with an acetonitrile buffer. Samples were allowed to dry.

Samples were reconstituted in RIA buffer, as were standards. Primary antibody was added to each tube, except the "total binding" and "non-specific binding" tubes. All samples were incubated overnight at room temperature. I^{125}-labeled AngII was added to each tube, and tubes were again incubated overnight at 4°C. Secondary antibody was then added to each tube with RIA buffer and incubated for 90min. Samples were centrifuged at 1700rcf and 4°C for 20min. Supernatant was aspirated from all tubes except "total counts." Tubes were then counted on a gamma counter.

Maximum binding was calculated from "total binding" minus "non-specific binding" counts. Values were then calculated as percent bound divided by maximum binding. Samples were calculated from

a best-fit line of the standard curve.

Plasma Renin Activity

The renin activity in the plasma of fetal sheep was measured by RIA using a kit from DiaSorin (Stillwater, MN, #CA-1533/53).

The initial step of this assay was generation of angiotensin I. One-half milliliter of each EDTA plasma sample was transferred to a reaction tube on ice and solutions containing PMSF and maleate generation buffer were added. An aliquot of this was transferred for the determination of background and generated angiotensin I. The samples were incubated at 37°C and the background series was kept in the ice bath. Samples were incubated for 60min, and then transferred to the ice bath.

A standard calibration curve was then created. Aliquots from the standard curve, the samples, and the background samples were then pipetted into assay tubes that were coated with an anti-angiotensin I antibody. A tracer-buffer reagent was immediately added and the tubes mixed. All tubes were then incubated for 3 hours at room temperature. Solutions were then aspirated out of the tubes, except for the "total counts" tubes. Tubes were counted in a gamma counter. A best-fit curve was found for the standards, and the angiotensin I concentration of the unknowns was calculated. Renin activity was calculated based on the standard curve and the background samples.

Cortisol

The cortisol concentration in the plasma of fetal sheep was measured by RIA using a kit from Diagnostic Products Corporation (Los Angeles, CA, Coat-a-Count TKC01).

Heparinized samples were used to measure cortisol concentrations in fetal plasma. A standard was created according to the kit protocol. Samples were added to antibody-coated tubes with I^{125}-labeled cortisol and incubated at 37°C for 45min. Samples were then aspirated, and tubes were counted in a gamma counter. Cortisol concentration was calculated based on the standard curve and the back-

ground samples.

Cardiac Dissociation and Assays on Dissociated Myocytes

Cardiac Dissociation

To study characteristics of individual cardiac myocytes such as size and nucleation, hearts were enzymatically dissociated using collagenase and protease as described previously, with some modifications (Barbera *et al.*, 2000). The heart was hung on a dissociation apparatus immediately following euthanasia, making a bubble-free wet seal between the aorta and continuous fluid column in the apparatus. The apparatus consisted of a hub that fit snugly within the aorta (which was then tied on using silk suture) connected to a three-way stopcock to control flow. The stopcock connected to tubing that ran, through a water-jacket to control temperature (39°C), to a series of reservoirs to hold solutions (see Appendix C for solution recipes). The solutions were continuously bubbled with 95% O_2 / 5%CO_2. Anterograde perfusion of the coronaries by retrograde aortic perfusion was initially with a Tyrodes solution until the myocardium had become blanched, then the hearts were perfused with Tyrodes-collagenase solution (160 units/ml collagenase with 0.78 units/ml protease) for approximately 5min. The perfusion solution was changed to 300ml calcium-free Kraftbrühe (KB) buffer to rinse out the collagenase. The ventricles were cut from the heart and each was shaken gently for a few minutes in KB to free myocytes. The myocyte slurry was rested in KB for 30min before fixation with an equal volume of 2% formaldehyde made fresh in phosphate-buffered saline (PBS).

Measurement of Cardiac Myocyte Size

Cardiac myocyte sizes were measured from photomicrographs of methylene blue-stained cardiac myocyte wet mounts taken at 40x on a Zeiss microscope (Zeiss Axiophot, Bartels and Stout, Bellevue, WA). Cardiac myocyte lengths and widths were measured using calibrated Optimas software (Optimas, Seattle, WA). At least 100 cells were measured per ventricle per fetus; no less than 5

myocytes of each type (mononucleated or binucleated) were measured. For all analyses of dissociated cardiac myocytes, fields were selected by a non-repeating, random method (Figure 7). Methylene blue-stained cardiac myocyte wet mounts were also used to count the number of nuclei per cardiac myocyte. At least 300 cells per ventricle per animal were counted, independent of the cells measured for size.

Most near-term fetal cardiac myocytes are torpedo shaped with a length about six to eight times their mid-section diameter. The assumption implicit in the use of cardiac myocyte length and width as surrogates for cell volume is that the mid-section diameter of the cell (or "width") is the same no matter from what direction it bisects the longitudinal axis of the cell. In other words, in cross-section the cell must be round, not ellipsoid. This assumption has been tested by comparing the horizontal width of cells to their vertical width when they are resting on a slide: they were not different (personal communication from Dr. Giraud). The volume of a myocyte calculated by taking the circumferential area times the length (the area of a cylinder) overestimates the myocyte volume as determined by confocal slicing by about 15% (Simpson's rule).

Ki-67 Immuno-Assay for Non-Quiescent Cardiac Myocytes

Cell cycle activity in cardiac myocytes was detected using the Ki-67 antibody MIB-1 (DAKO Cytomation, Glostrup, Denmark). Cardiac myocytes were dried on Superfrost Plus slides, post-fixed in cold acetone for 30min. Antigen retrieval was achieved by boiling the slides in sodium citrate solution (see Appendix C for all solutions) for 6min. Endogenous peroxidase activity was blocked by incubating the slides for 5min with 0.03% hydrogen peroxide. Slides were then incubated at 4°C overnight with 1:200 Ki-67 antibody in blocking buffer. The secondary antibody (biotinylated anti-mouse IgG); Vector Laboratories, Burlingame, CA) was applied to the slides at a concentration of 1:200 in PBS and left at room temperature for 2 hours. Incubation with avidin-biotin complex (Vector Laboratories, Burlingame, California, Vectastain ABC Kit) followed for another hour at room temperature. Positive cells developed dark brown nuclei when the slides were then incubated

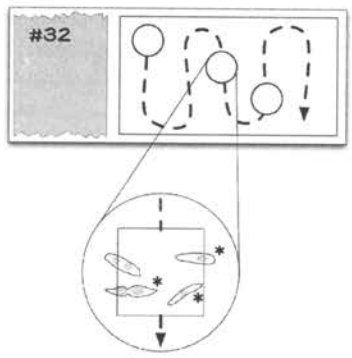

Figure 7. Method for counting and measuring myocytes. Non-repeating microscope fields were selected. Myocytes overlying the left edge of a zone marked in the field were not counted. Myocytes entirely within the field or overlying the right edge were counted (marked with asterisks). Daughter cells of cytokinesis were counted separately.

with diaminobenzidine (DAB). All incubation steps were followed by three washes with PBS. Cells were lightly counter-stained with methylene blue, dehydrated and mounted with coverslips. At least 500 cells were counted per ventricle per fetus for cell cycle analysis. Daughter cells of cytokinesis were counted separately.

Quantification of Protein Expression by Western Blot

Protein Isolation

Total protein was extracted from frozen tissue in order to measure expression and phosphorylation levels. A chunk of frozen tissue (~300mg) was smashed into a fine powder using a chilled hammer, and dropped into ice-cold extraction buffer in a Falcon 2059 tube (for solutions see Appendix C). The tissue was immediately ground using a Brinkman Polytron PT-DA3007/2 generator at 20,000rpm for about 1min. The tube was held in ice while grinding to keep the sample cold. Samples were incubated on ice for 30-45min. Samples were centrifuged at 10,000rcf for 10min to remove whole and fragmented cells and organelles. The supernatant saved as a whole protein fraction at -80°C.

Protein Separation by SDS-PAGE

Denaturing gels were made to separate proteins using a small-format (final blot size 8.5x6cm) BIO-RAD system (Hercules, CA). The soluble proteins were run on 4% polyacrylamide stacking gels

Table 2. Primary antibodies and dilutions used for immunoblots. Antibodies obtained from Abcam (Cambridge, MA)

Protein	abcam #	Antibody Source	Dilution
NCX1	ab6495	mouse monoclonal [300-127]	1:200
SERCA2	ab2817	mouse monoclonal [IID8]	1:2500
Calsequestrin	ab3516	rabbit polyclonal	1:2500
PLN	ab2865	mouse monoclonal [2D12]	1:500

made using a Tris buffer at pH8.8; resolving gels were 10% polyacrylamide and made using a Tris buffer at pH6.8 (see Appendix C for all solutions). Samples to test for soluble proteins were mixed in at least 1x Laemmli buffer with β-mercaptoethanol as a reducing agent, then boiled for 5min in a 100°C heat block immediately before loading on the gel. Membrane-bound proteins were run on 3% polyacylamide stacking gels and 5% resolving gels. These samples were prepared in a 1x Laemmli buffer with dithiothreitol as a reducing agent. Gels were electrophoresed using a reservoir buffer containing glycine at 90-95V until the desired separation was achieved.

Semi-Dry Protein Transfer

Proteins were transferred to a polyvinylidene fluoride (PVDF) membrane (Hybond-P, Amersham, Piscataway, NJ) using a BIO-RAD semi-dry transfer system. The membrane was first cut to fit the gel, then it was soaked in methanol. The membrane was wet for a few minutes in water, then for 15min in a tris-glycine transfer buffer. For some blots (those intended to assay for membrane channels), the transfer buffer contained 25% methanol. Electrophoretic transfer was carried out at 20V for 30min.

Western Protein Blotting

Protein expression and phosphorylation was quantitated using the Western protein blotting method. Membranes were blocked in 5% Milk TBST buffer for one hour, and then rinsed for 20min (all rinses with TBST buffer). Primary antibodies were mixed in 5% Milk TBST buffer as shown in Table 2. The membranes were incubated with the primary antibody overnight at 4°C.

The membranes were then rinsed for 20min, followed by another brief rinse. The membranes were incubated for 1-3 hours with the secondary antibody (Invitrogen anti-rabbit 1:4000, or anti-mouse 1:5000 where appropriate). The membranes were rinsed for 20min, followed by another brief rinse. SuperSignal chemiluminescence system (Pierce) was used to detect antibody binding. A digital detection system was used to create a digital image of the blot, which was then quantitated using NIH ImageJ (Abramoff *et al.*, 2004; Rasband, 2005).

Identification of Immunoblot Bands

Bands on western blots were identified based on gel migration distance, information provided with the antibodies, and previously published reports (Table 2 and Figure 8). Differences from protein sizes in published reports can be due to species and isoform differences, modification or partial degradation of protein, associations with other proteins, and variations in migration speed of proteins and ladder.

The probe to SERCA2 picked up a doublet at about 110kDa (Figure 8a). The antibody used does not distinguish between the 'a" and "b" isoforms. Both isoforms, as well as SERCA3, have been found in the human heart (Santiago-Garcia *et al.*, 1996). Both isoforms "a" and "b" are also found in the mouse heart (Reed *et al.*, 2000), and strong doublet is detected at about 110kDa in rat hearts by an antibody made against canine cardiac SERCA2 (Luss *et al.*, 1999). In some of the adult samples a third band was detected directly below the doublet. This band needs further investigation. The 6

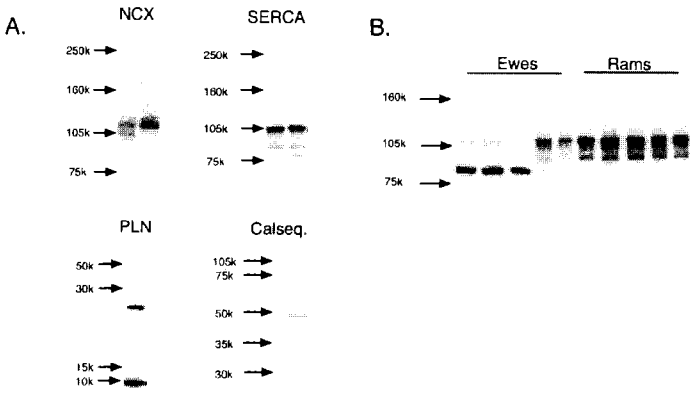

Figure 8. Experimental immunoblot bands. A) Fetal samples with protein standard sizes marked, and B) SERCA2 immuno-blots of adult samples. Calseq. = calsequestrin.

non-pregnant ewes used in the age series were compared to 6 rams (Figure 8b). The third band was present in all adult samples, but it was greatly enhanced in some of the ewes at the expense of the two larger bands. All three bands were included for densitometry.

Functional NCX1 can be detected as a 160, 120, or 70kDa by Western analysis (Philipson et al., 1988; Frank et al., 1992). A band was detected at about 120kDa. A secondary band was detected at about 100kDa (Figure 8a).

Quantification of mRNA Expression by Northern Blot

RNA Isolation

In order to analyze regulation of mRNA expression, total RNA was isolated from frozen tissue using a modified TRIzol method (Invitrogen, Carlsbad, CA).

Tissue was taken from storage in the -80°C freezer and put into liquid nitrogen. The tissue chunk, wrapped in foil, was smashed with a hammer. Frozen fragments (200-500mg) were transferred to a new foil wrapper and re-chilled in the liquid nitrogen. The tissue chunk was returned to storage in the -80°C freezer.

A Falcon 2059 tube was filled with 5ml TRIzol and pre-chilled in a beaker of ice. The frozen tissue fragments were placed in the tube, which was kept in the beaker of ice. The fragments were immediately ground for 1min using a Brinkman Polytron with a 1cm probe. The probe was cleaned between each use with 10% SDS, rinsed with plenty of fresh water, and finally rinsed with 100% ethanol.

Centrifuging the homogenate at 12000rcf for 5min reduced genomic DNA contamination. The supernatant was then transferred to a new Falcon 2059 tube and 1ml chloroform was added. This mixture was shaken vigorously for 15 seconds. The aqueous and organic layers were separated by centrifugation at 12000rcf for 10-20min.

The work area and pipetmen were thoroughly decontaminated using RNAse ZAP (Ambion, Austin, TX). The aqueous (top) phase of the extraction was transferred to four RNAse-free microfuge tubes using RNAse-free barrier tips. Isopropyl alcohol (0.5ml) was added to each sample aliquot and mixed briefly. The samples were then precipitated and collected in a tabletop centrifuge set to 12000rcf for 10min. The supernatant was removed and the pellet washed with 75% RNAse-free ethanol. The pellet was secured to the bottom of the microfuge tube by centrifuging at 7,500rcf for 5min. The wash solution was then completely removed by pipetting and the sample placed in the hood to dry for 10-30min.

A 1:25 solution of RNASecure (Ambion) and RNA Storage Solution (Ambion) was pre-heated to 60°C for 20min to eliminate RNAse contamination. This solution (50µl) was then used to dissolve the RNA sample by pipetting and heating to 60°C for 20min. The samples were then treated to remove genomic DNA contamination using Ambion's DNA-Free DNase kit. Buffer (0.1 volumes) and 3µl Dnase (6 units) were added to the sample and incubated at 37°C for 20-30min. The inactivation slurry was then well mixed and 0.1 volumes were added to the sample. The tube was mixed at room temperature for 2min. The slurry was pelleted and left in the tube, as suggested in the protocol. Samples of RNA were stored in racks in a -80°C freezer.

Quantitation of RNA with Spectrophotometry

A small volume of an RNA sample was diluted (1:50 or 1:100) in 10mM tris buffer (pH 8.5). The spectrophotometer was allowed to warm up, and then it was blanked using the dilution buffer. The absorbance of diluted RNA samples was measured using UV spectrophotometry. The quantity of RNA was calculated according the Beer-Lambert law such that $\text{Concentration}_{RNA} = \text{Absorbance}_{260} \bullet (40\mu g \bullet ml^{-1}) \bullet$ dilution factor. A ratio of Absorbance_{260} / Absorbance_{280} of 1.8 is considered indicative of highly purified RNA.

Agarose Gel Electrophoresis of RNA

RNA samples were checked for quality by gel electrophoresis. Denaturing 1.2% agarose gels containing formaldehyde and a MOPS buffer were prepared fresh. RNA samples were denatured at 60°C for 10-20min in a loading buffer containing blue dye, glycerol, MOPS buffer, formaldehyde, formamide, and ethidium bromide. RNA was then loaded into the gel and electrophoretically separated. Quality of RNA was assessed by the relative densities and crispness of the 18S and 28S ribosomal bands and the absence of a tell-tale low molecular weight smear. Degraded RNA was not used in any experiment.

Northern Probe Template Design

Primer Design

Primers were designed in order to clone a gene fragment to be used as a template for the creation of a probe. Sequences of desired genes from sheep, cow, goat, human, rabbit, dog, *et cetera* (depending on availability), were located in the GenBank database (Benson *et al.*, 2004; Wheeler *et al.*, 2004). The Primer Designer (Sci Ed Software, Durham, NC) program was then used to generate a list of possible PCR primers. The primers were then submitted together in a "short, nearly-exact" BLAST search (Altschul *et al.*, 1990; Wheeler *et al.*, 2004) to detect any unwanted homology with genes other than the one of interest. Primers were then ordered from Invitrogen at a 50nmole scale of synthesis (see Table 3). The primers arrived desiccated; they were resuspended to 150μM in TE (approximately 375μl). The working stock solution was made as 15μM solution of both the forward and reverse primers from the 150μM concentration in dH_2O. The primers for NCX1 and SERCA2 were obtained from Dr. Donogh McKeogh, who designed them while working in the Thornburg laboratory.

RT-PCR and PCR

First-strand cDNA was created by reverse-transcription from sheep RNA using Superscript II (Invitrogen). The following components were mixed and heated to 65°C for 5min in a thermocycler: 1µl oligo(dT) (500µg/ml), 1µl total RNA, 1µl 10mM dNTP mix (10mM each dATP, dGTP, dCTP, dTTP), 9µl H_2O treated with DEPC. The reaction was chilled on ice and the following components added: 4µl First-Strand Buffer, 2µl 0.1M DTT. The reaction was mixed by pipetting, and then incubated in the thermocycler at 42°C for 2min. Finally, 1µl (200 units) of Superscript II was added and the reaction incubated at 42°C for 50min. Heating to 70°C for 15min inactivated the reaction. The cDNA was then used immediately for PCR, or was first stored at 4°C for a maximum of 24 hours.

The cDNA of the gene of interest was amplified using Taq PCR (QIAGEN, Valencia, California). The kit was used to carry out two PCR reactions for each gene: the "Q-Solution" protocol, and the reaction with 3mM Mg^{2+}. Generally, at least one of these reactions was optimal for transcription of the particular gene fragment. For the Q-Solution reaction, these components were mixed in a microcentrifuge tube: 10µl 10x QIAGEN PCR Buffer, 20µl 5x Q-solution, 2µl 10mM (each) dNTP mix, 6.6µl 15mM (each) Primer Working Stock, 0.5µl Taq DNA Polymerase, 1µl cDNA, 59.9µl H_2O treated with DEPC.

For the other reaction, the following components were mixed in a microcentrifuge tube: 10µl 10x QIAGEN PCR buffer, 6µl 25mM $MgCl_2$, 2µl 10mM (each) dNTP mix, 6.6µl 15mM (each) Primer Working Stock, 0.5µl Taq DNA Polymerase, 1µl cDNA, 73.9µl H_2O treated with DEPC. The reactions were then treated to touchdown PCR; the annealing temperatures were as follows: the calculated annealing temperature for the primer pair was averaged and then 4°C was added; this was the initial annealing temperature. The annealing temperature was lowered by 1°C each cycle for 8 cycles, and then the rest of the cycles were completed with that final annealing temperature. The PCR cycle was repeated thirty times.

Table 3. Primer sequences for northern probe creation.

	Forward Primer	Reverse Primer
LTCC α1c-subunit	CGACAGTGCGTGGAATACGCC	ATGAAGGTCCACAGCAGCGTC
RyR	CCCACAACCTGTTGATAC	CCTTGGCTTTCTCTTTGG
Phospholamban	CCTCACTCGCTCWGCTTATWA	CTDGTTRGCAGWGCAGTT
Calsequestrin	AGGCTTTGTGATGGTGGATG	AGAGTGGGTCTTTGGTGTTC
SERCA2	TGAGGCA-AGGGTGTGTATG	GATGACCCGGATGCCTGCC/TT
NCX1	GCCAACGCTGGATCTGATTA	GTGAAGCCACCAAGCTCATT

Subcloning

The cDNA PCR product was separated by electrophoresis on a 1% agarose gel stained with ethidium bromide. The bands were analyzed for size, and appropriately sized, discrete bands were excised from the gel. Using the Bio101 GeneClean kit (Qbiogene) the DNA was purified from the gel. Briefly, the gel was dissolved in sodium iodide, the DNA was bound to a silica matrix, the matrix was washed and dried, and then the DNA was resuspended with buffer. The DNA was then further cleaned using QIAquick PCR Purification kit (QIAGEN). Briefly, the DNA solution was mixed with a binding buffer, and then bound to the column with centrifugation. The column was washed, and then the DNA eluted with buffer. The purified gene fragments produced by PCR were then ligated into the pGEM T-easy vector (Promega). The ligation consisted simply of mixing the purified gene with linearized plasmid and ligation reaction components, then incubating for several hours. Gene-vector constructs were used to transform competent *escherichia coli* bacteria; the cells used were JM109 (Promega), XL1-Blue Subcloning-Grade (Stratagene), and DH5 (Invitrogen). The protocols for all cell types were similar. Briefly, the cells were thawed on ice, a small amount of ligation reaction added, and the mixture incubated on ice. The cells were then heat-shocked at 42°C for 45 seconds (in Falcon 2059 tubes, BD Biosciences). LB media was then added and the cells incubated at 37°C for 30-60min, before being spread on a LB-agar plate containing ampicillin and β-galactosidase. These plates were incubated overnight at 37°C. Cells transfected with pGEM T-Easy were endowed with ampicillin resistance and formed colonies on the plate. White colonies indicated the presence of an insert into the plasmid, which otherwise would give the cells the capacity to metabolize β-galactosidase (which would turn the colony blue).

Identifying Subcloned Genes

Insert-postive, transformed colonies were scraped off the plate, added to 10ml LB, and incubated at 37°C overnight with shaking. A glycerol stock was prepared from 2mls of this culture, combined with 2ml glycerol, and flash-frozen in liquid nitrogen. This stock was stored at -80°C. The remaining culture was pelleted by gentle centrifugation, and then the vector DNA extracted using the Nucleospin miniprep kit (Clontech, Mountain View, California). Briefly, cells were lysed, and then the cellular debris removed by centrifugation. The DNA was alcohol precipitated, washed, and then resuspended in buffer. Yield was determined by spectrophotometery.

Cloned genes were taken to the Vollum Core Sequencing Facility (OHSU). The sample to be sequenced was prepared as follows: 200-500ng plasmid DNA, 3.2pmoles primer (2.11µl T7 primer or 2µl SP6 primer), dH_2O to 12µl. The sequencing core added primers and enzymes. The sequence of the DNA was return in an electronic form, both as a chromatogram file, generated by the sequencer, and as an automatically generated text file. The cloned genes were generally sequenced from either the T7 site or the SP6 site, but not both. Therefore, if the gene fragment was long, a partial sequence was returned. Chromas, a program to visually interpret chromatogram files (Technelysium), was used to manually correct the text file. The corrected sequence was edited to remove sequences corresponding to the vector. The final sequence was the submitted to a BLAST search of GenBank (Altschul *et al.*, 1990; Wheeler *et al.*, 2004) to positively identify the cloned gene as the gene of interest.

Preparing the Template

To prepare the template from which the radioactive probe would be made, a larger bacterial preparation was performed. A small volume (~10ml) of luria broth with ampicillin (LB-AMP) was inoculated from the frozen glycerol stock and incubated with shaking at 37°C for 8 hours. A few microliters of the starter culture was used to inoculate a larger volume of LB-AMP (100-500ml). This culture was left to incubate overnight with shaking at 37°C. The bacteria were then pelleted with gentle

centrifugation and the plasmid was harvested using QIAGEN's maxiprep protocol. Briefly, the pellet was resuspended, then the bacteria were lyzed. A solution was added to precipitate the bacterial DNA; the DNA and the cellular debris were pelleted with centrifugation. An ethanol-salt solution was then added to precipitate the plasmid DNA. After pelleting with centrifugation the DNA was washed, dried, and resuspended in a tris buffer.

In order to isolate the cloned insert from the vector, the maxiprep yield was digested with EcoRI for several hours. The digest was separated on an agarose gel and stained lightly with ethidium bromide. The band containing the insert was excised and the DNA purified as described. The DNA template was stored at -20°C.

RNA Gels and Blots

Ten to 20μg of RNA for northern blot analysis was run on a denaturing agarose gel (0.6-1.2%) as described using very low amounts of ethidium bromide. After separation by electrophoresis, the gel was photographed on a UV lightbox using a digital camera.

Transfer of RNA to a nylon membrane was carried out by an upward alkaline transfer system. A buffer of 10% SSC was used to fill a lower tank. A filter-paper wicking system carried the buffer to the gel. The nylon membrane was placed on top of the gel, covered by several filter papers and a stack of paper towels. The buffer flowed through the gel and carried the RNA up onto the nylon membrane. This was allowed to proceed for approximately 16 hours. The apparatus was then dismantled and the RNA was crosslinked to the membrane using UV light. Membranes were allowed to dry if they were not blocked immediately.

Northern Probe Creation and Hybridization

All standard precautions were observed when working with or disposing of ^{32}P. Radioactive northern probes were created from template DNA using ^{32}P-labelled CTP (New England Nuclear, now

PerkinElmer, Boston, MA). Probes were made either according to Bio-Rad's Magic method or Invitrogen's RadPrime DNA labeling system. Both of these methods involve using the ^{32}P-dCTP to generate a single new DNA strand off each template strand. To purify the probe it was run through a micro Bio-Spin chromatography column to separate free nucleotides from the full-length probe (BioRad).

A small aliquot of the probe (1µl) was added to 20ml of ScintiVerse BD Cocktail (Fisher Scientific) and counted in a scintiallation counter with a wide-open window. The probe was considered good if the result was above 1 million counts.

Membranes were blocked with ExpressHyb buffer (Clontech) for at least one hour at 68°C in a rotating incubator. After blocking, fresh hot buffer was added, as was enough probe to be equal to 1µCi / ml hybridization buffer. The membranes were then hybridized with the probe for at least 1 hour. Membranes were then washed 4 times for 30min each (see Appendix C for buffers) – twice with Wash Buffer 1 at room temperature, and twice with Wash Buffer 2 at 50°C.

The membrane was used to expose either a phosphor-imager screen (Bio-Rad) or film. Phosphor-imager screens were scanned using Molecular Imager (Bio-Rad), while film was scanned and digitized using a flat-bed scanner (HP). When exposing film to the membrane an intensifying screen was used (DuPont Cronex or Kodak Biomax Transcreen-HE). Initially the film I used was Kodak's special-to-the-research community X-OMAT, but due to the dark blue background and long exposure times required I switched to Kodak Biomax MS. Multiple exposures were taken of each membrane in order to obtain one that was dark enough to quantitate but was not saturated.

Table 4. Literature references for mRNA sizes of calcium transport genes.

Gene	Species	mRNA Length
Calsequestrin	rat	2.4kb (Park *et al.*, 1998)
Phospholamban	human	3, 1.7, 0.86kb (McTiernan *et al.*, 1999)
RyR	rat	16kb (Assayag *et al.*, 1998)
LTCC α1C	rat	8.3, 9.7kb (Liu *et al.*, 2000)
NCX1	rat	7.3kb (Assayag *et al.*, 1998)
SERCA2	sheep	4.4kb (Samson *et al.*, 2000)

Quantification of Northern Blots

A RNA standard was run with each northern blot, typical 5 values between 1μg and 40μg (experimental samples between 10-20μg). Densitometry was performed on the standards and an equation fit to them. Three equations were considered, and the best fit was used. The equations were linear, quadratic, or Rodbard fit (four parameter general curve fit function by David Rodbard at the NIH with the form y = (D) + (A - D) / (1 + (x/C)^B)) (Vivino, 2005). Experimental values were calculated from the standard. If experimental blots were darker or lighter than the range of the standard they were not used.

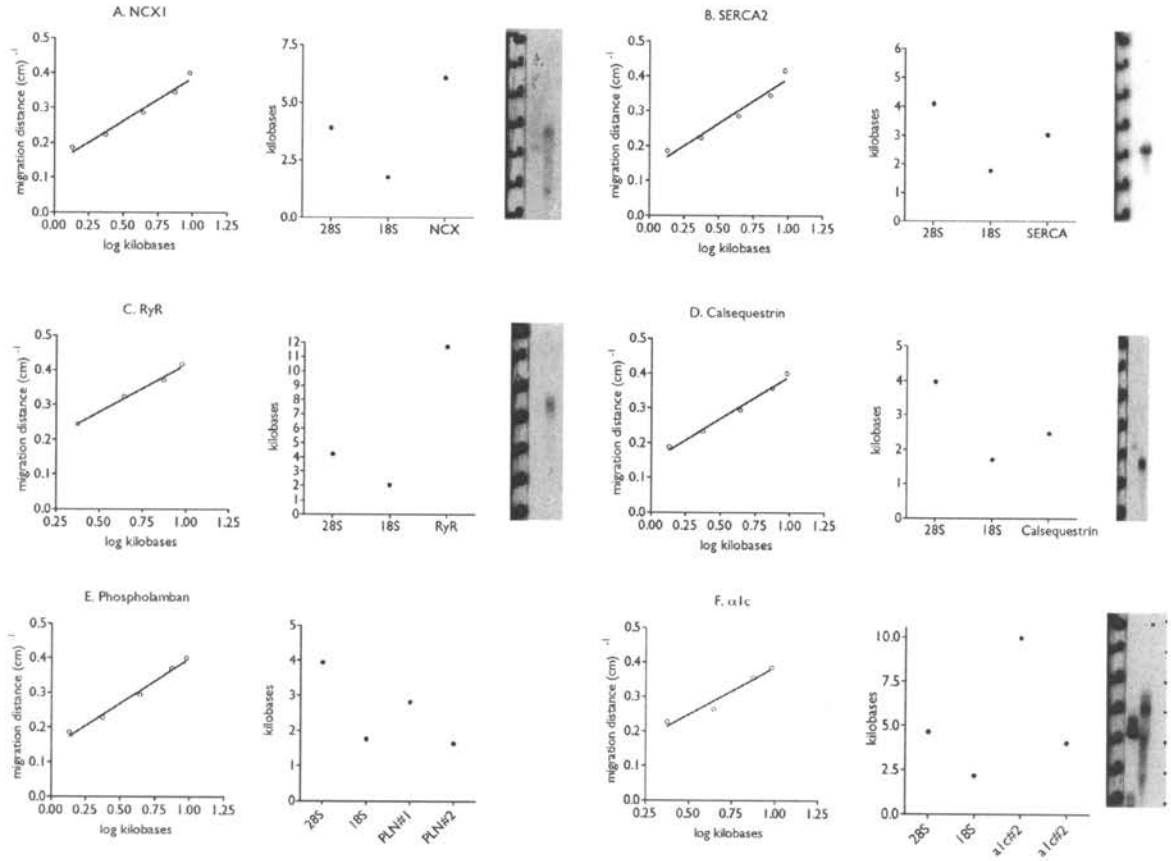

Figure 9. Identifying RNA bands. Lines are fitted for distance-1 against log[kilobases] and the approximate size of the experimental gene calculated. Approximate sizes of the 28S and 18S ribosomal bands calculated for comparison. An image of the northern hybridization is shown. 1) NCX1, B) SERCA2, C) RyR, D) Calsequestrin, E) Phospholamban, and F) LTCC α 1c (the band in the first lane is a hybridization to the molecular marker).

Identification of RNA Hybridization Bands

Hybridization bands from northern blot analysis were characterized for each probe. A single sample of RNA was run on an agarose gel against an RNA molecular weight marker, and photographed with a centimeter ruler. The RNA was then transferred to a membrane and probed as described. Film was exposed to the membrane together with a phospholuminescent ruler, developed, and then scanned. The front wave of the bands of the molecular weight marker were plotted against their migration distance: small molecular weight RNA species run on a gel can be plotted as *migration distance*$^{-1}$ against *log(molecular weight)*. The molecular weight of the strongly hybridized experimental bands was then calculated based on the migration distance of their front wave (Figure 9).

Calculation of the molecular weight of 28S and 18S is shown for comparison: human 28S is 5.0kb and 18S is 1.9kb. Variations in size from reported values (Table 4) could be due to species differences, measurement errors, or variations in RNA migration in a gel. The quantity of ethidium bromide bound to the RNA can change its migration characteristics through a gel, and the mass of RNA can change the resolution of the hybridization bands.

In some cases a second band showed up that corresponded closely in size to a ribosomal band; hybridization to a ribosomal band sometimes occurred in experimental samples. These bands were not included in densitometry analysis.

Other Assays

Protein Concentrations

The concentrations of protein samples were measured using an assay based on bicinchoninic acid (BCA). Protein samples were incubated in an alkaline medium and, by the biuret reaction, the protein in solution reduced Cu^{++} to Cu^{+}. The color reaction is developed by the chelation of two molecules of BCA with one cuprous ion, and the absorbance of the solution at 562nm is read by a

spectrophotometer. The bovine serum albumin standard was made according to directions and 10µl of each was added to duplicate wells in a 96 well plate (Pierce, Rockford, Illinois, #23225). Samples were diluted 1:10 or 1:100 and duplicate 10µl aliquots were added to the plate. BCA reagent was added to each well, and the plate was incubated at 37°C for 30min. The plate was then allowed to cool at room temperature before being read on a plate reader. Sample concentrations were calculated from the standard curve.

Cardiac Myocyte Cell Culture

Some cardiac myocytes were taken from dissociated control hearts to culture. Cells for these experiments were cultured by Dr. Louey or Dr. Chattergoon, simultaneously with their own experiments to test for proliferative or hypertrophic effects of certain agents. I then harvested the myocytes and extracted protein to use for western analysis.

Fetal hearts were dissociated as described. Myocytes concentration in the final KB buffer were counted using a hemocytometer. After the 30min rest period in KB the cells were gently pelleted at 200rcf for 2-5min. The pellet was resuspended in a media containing serum (see Appendix C for all solutions). The myocyte cell fraction was enriched by two consecutive steps in which the cells were preplated in large-volume flasks (Fisher Scientific #13-680-65). When the myocyte-containing media was poured off, fibroblasts and other cell types were left behind. Myocytes were pelleted and resuspended again before plating 1 million myocytes in 35mm culture dishes (density of 1039 / mm^2) pretreated with 3µg/ml lamanin (Sigma #L2020-1MG). Culture dishes were kept in a sterile humidified incubator at 39°C and 5% CO_2, balance room air. After 24 hours the media was changed to serum-free. Forty-eight hours later, the serum-free media was changed for fresh serum-free media. Experiments began 24 hours later with the addition of fresh serum-free media and drugs. Treatments were: no drugs (serum-free), AngII (100nM), ANP (500nM except one experiment 750nM), cortisol (138nM) and phenylephrine (98.2µm) for 48 hours. The doses of these compounds were selected based on their growth effects in culture (Sundgren *et al.*, 2003b and

unpublished data).

Forty-eight hours after drug treatment, myocytes were rinsed once with PBS and 500μl 0.25% trypsin with EDTA (Invitrogen #25200-056) was added to the plates. The cells were loosened from the dish with gentle agitation. After 4min, 500μl of serum-media was added to dilute and inactivate the trypsin, the media was collected, and the cells were pelleted at 6000rcf at 4°C for 4min. The pellet was resuspended in RIPA lysis buffer. This was incubated on ice for at least 30min, the protein yield was measured and the proteins were stored at -80°C.

TUNEL Assay for Apoptotic Nuclei

Some small pieces of fetal ventricular tissue were excised and fixed in zinc-buffered formalin for about 48 hours for the purpose of assessing fetal cardiac apoptosis rates. The tissue was embedded in paraffin and sectioned by Linda Jauron-Mills and Carolyn Gendron in Dr. Corless' histology laboratory.

I then used the protocol and solutions from Serological's ApopTag kit to detect apoptotic myocytes (Chemicon, Temecula, CA, #S7101). The theory behind this technique is that apoptosis induces DNA fragmentation that can be detected by labeling the free 3'-OH termini with digoxigenin-conjugated nucleotides. The labeling is carried out using terminal deoxynucleotidyl transferase (TdT).

Slides were microwaved for 4min, then incubated in an oven at 60°C for 10min. The tissue was deparaffinized in 3 xylene baths for 5min each, then cleared and rehydrated by successive baths of 100% ethanol (10min), 95% ethanol (3min), 70% ethanol (3min) and PBS (5min). Cells were permeabilized with 20μg/ml proteinase K (QIAGEN) for 15min, then rinsed well with water. Endogenous peroxidases were quenched with 0.03% hydrogen peroxide in PBS for 5min, and then rinsed with PBS. After equilibrating the tissue to the incubation buffer, the TdT buffer was added and the slides incubated for 1 hour at 37°C. Soaking slides in stop/wash solution for 10min stopped the reaction. Tissue was rinsed with PBS before incubating with the peroxidase-conjugated anti-

digoxigenin antibody for 30min. Tissue was again rinsed before adding DAB to develop the color reaction. Tissue was counterstained with hematoxylin, dipped in acid ethanol, then incubated briefly in Scott's solution (see Appendix C for solutions). Tissue was then dehydrated with an ethanol series (reverse of above) and ethanol was replaced with xylene before coverslips were mounted.

Apoptotic nuclei were counted on a Zeiss microscope at 400x. The mean number of nuclei of cells that appeared histologically to be cardiac myocytes was found from five fields in each slide. Twenty to 100 fields were then scanned for apoptotic cardiac myocyte nuclei in a non-repeating, random manner. The number of positive nuclei is expressed in relation to the number of fields scanned by the mean number of nuclei per field.

Statistical Analysis

All statistical analysis was performed using Prism (Graphpad Software). The number of groups and type of sample determined the method of analysis used. When two non-paired groups were to be compared an unpaired t-test was used. Comparison of before-and-after between two groups was made by a paired t-test if no samples were missing, otherwise unpaired t-test was used. Linear regression was used to analyze growth during maturation. More than two groups were compared with a 1-way or 2-way analysis of variance (ANOVA). If the data were found to have significant variation overall by ANOVA, the groups were further compared using a post-hoc test. The post-hoc test was based on the type of data and the experimental question; tests included a test for linear trend, Bonferroni's multiple comparisons test of selected groups, Dunnett's test, and Tukey's test. The type of analysis and the result of the analysis are presented in the text with the data. A p value less than or equal to 0.05 was accepted as significant. All data are shown as mean ± standard deviation (SD).

CHAPTER 3

Results

Growth and Maturation of Fetal Sheep Cardiac Myocytes

In order to better understand the normal cardiac myocyte growth during the perinatal period in our mixed western breed strain of sheep, hearts were collected and dissociated from 54 control sheep fetuses and 5 neonates. Heart and body weights were recorded from these animals (Figure 10). Body and heart weights were greater with advancing age, but the ratio of the heart to body was constant during the period studied.

The lengths and widths of mononucleated and binucleated myocytes from the left and right ventricles of these hearts were measured and analyzed (Figure 11 and Figure 12). Myocyte width was greater with advancing gestational age, although the low r^2 value indicates that little of the variation in myocyte width was due to age. Length did not increase over the last third of gestation, with the exception of the mononucleated cells of the LV. I compared myocytes before and after birth, and found that the lengths and widths of cardiac myocytes from the near-term fetus are shorter than those from the neonatal lamb (Table 5).

The fraction of cardiac myocytes that is binucleated is very low prior to 115dGA, but increases rapidly thereafter (Figure 13). Binucleation continues to increase after birth, until it reaches about 75-85%, and is higher yet in the neonate (Table 5). Towards the end of gestation, the proportion of

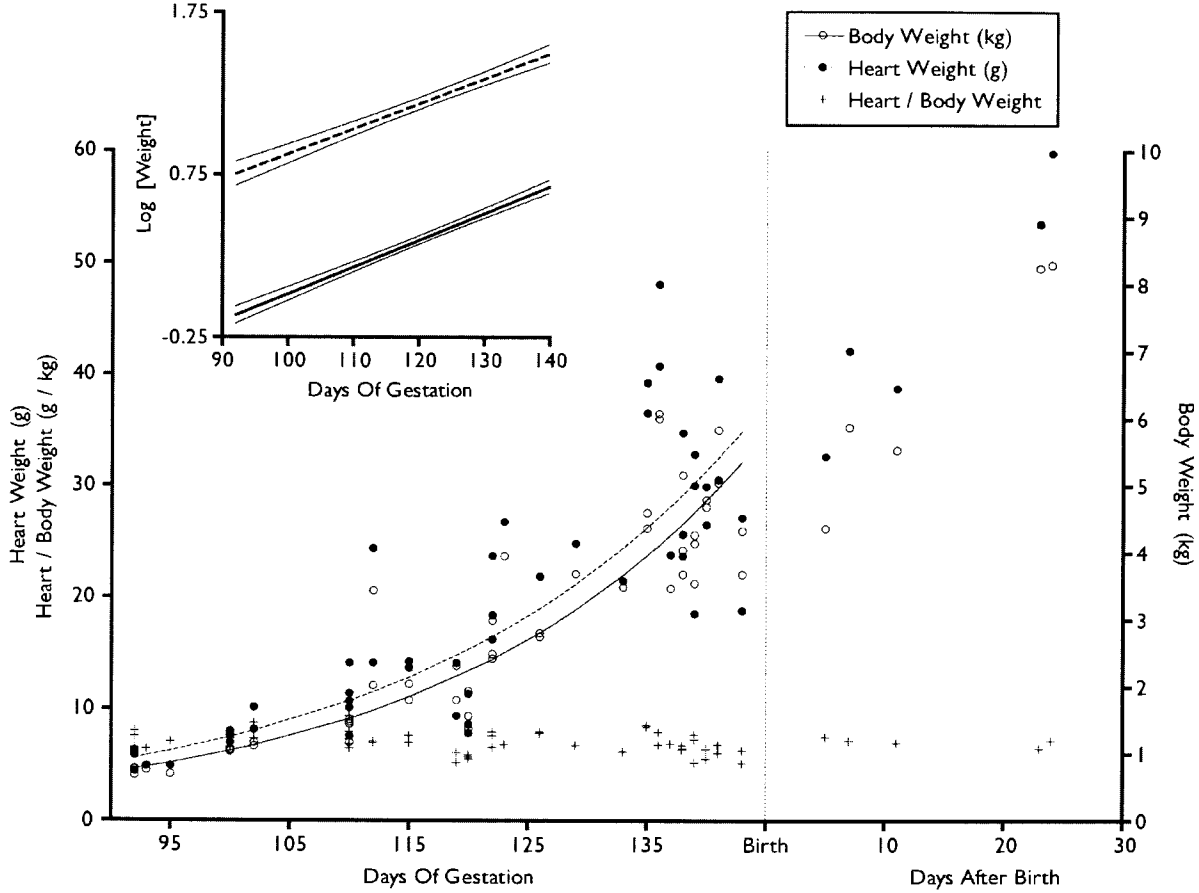

Figure 10. Heart and body weights in perinatal sheep. The best-fit straight line and 95% confidence interval was found for the log transform of fetal weights against gestational age (inset)(log [body weight (kg)] = (-1.638 + 0.017 • age), r^2=0.88; log [heart weight (g)] = (-0.681+0.016 • age), r^2=0.80; n=50). Daily fetal somatic growth was 3.9%, while daily cardiac growth was 3.6%. The ratio of the heart to body weights was constant during the perinatal period (linear regression, r^2=0.05, p=0.0983). 50 fetuses, 5 neonates.

myocytes containing more than two nuclei increases. While myocytes with 4 nuclei can be found in fetal and neonatal hearts, many more myocytes with 4 nuclei are observed in the adult sheep heart (personal observation).

There was no clear trend in the fraction of mononucleated myocytes that are in the cell cycle over the last third of gestation (Figure 14). Little or none of the variation in cell cycle activity in the fetal period is due to maturational age. The fraction of mononucleated myocytes in the cell cycle is higher in the RV of the near-term fetus than the neonate, but this is not the case in the LV (Table 5). No myocytes in the cell cycle were observed in the myocardium of the adult sheep (LV n = 6, RV n = 4).

Cardiac Myocyte Differences Between Genders

In the near-term sheep fetus, gender did not influence body weight (female 4.6 ± 0.7kg; male 4.6 ± 0.1kg) or heart weight (female 30.0 ± 8.5g; male 31.7 ± 9.8g). However, a comparison of four adult male sheep with four non-pregnant adult females of the same breed revealed that the males were heavier (105 ± 2kg vs. 69 ± 8kg, respectively; p=0.0001), and had heavier hearts (444 ± 50g vs. 301 ± 40g; p=0.0044). Heart weight relative to body weight in these adults was the same regardless of gender (males 4.2 ± 0.5g/kg; females 4.4 ± 0.3g/kg).

Cardiac myocyte characteristics were compared between genders in both ventricles by two-way

Table 5. Comparison of cardiac myocytes between the late-gestation fetus and the neonate. Twelve late-gestation fetal sheep, aged 140 ± 2dGA (range 138-143), were compared with 5 neonatal lambs, aged 14 ± 9 days after birth.

	Left Ventricle		Right Ventricle	
	Fetus	Neonate	Fetus	Neonate
Binucleated Myocytes				
Length (μm)	85 ± 5	96 ± 3 ***	93 ± 4	101 ± 4 **
Width (μm)	13 ± 1	18 ± 3 ***	16 ± 1	19 ± 3 ***
Mononucleated Myocytes				
Length (μm)	66 ± 3	72 ± 3 **	69 ± 3	79 ± 3 ***
Width (μm)	12 ± 0	17 ± 4 ***	14 ± 1	16 ± 2 **
Binucleation (%)	57 ± 12	81 ± 7 ***	60 ± 10	74 ± 3 **
Cell Cycle Activity in Mononucleated Myocytes (%)	4.2 ± 3.4	6.4 ± 3.8	6.6 ± 3.8	1.1 ± 1.4 **

***p <0.01, ***p<0.001 different than fetus; Mean ± SD.*

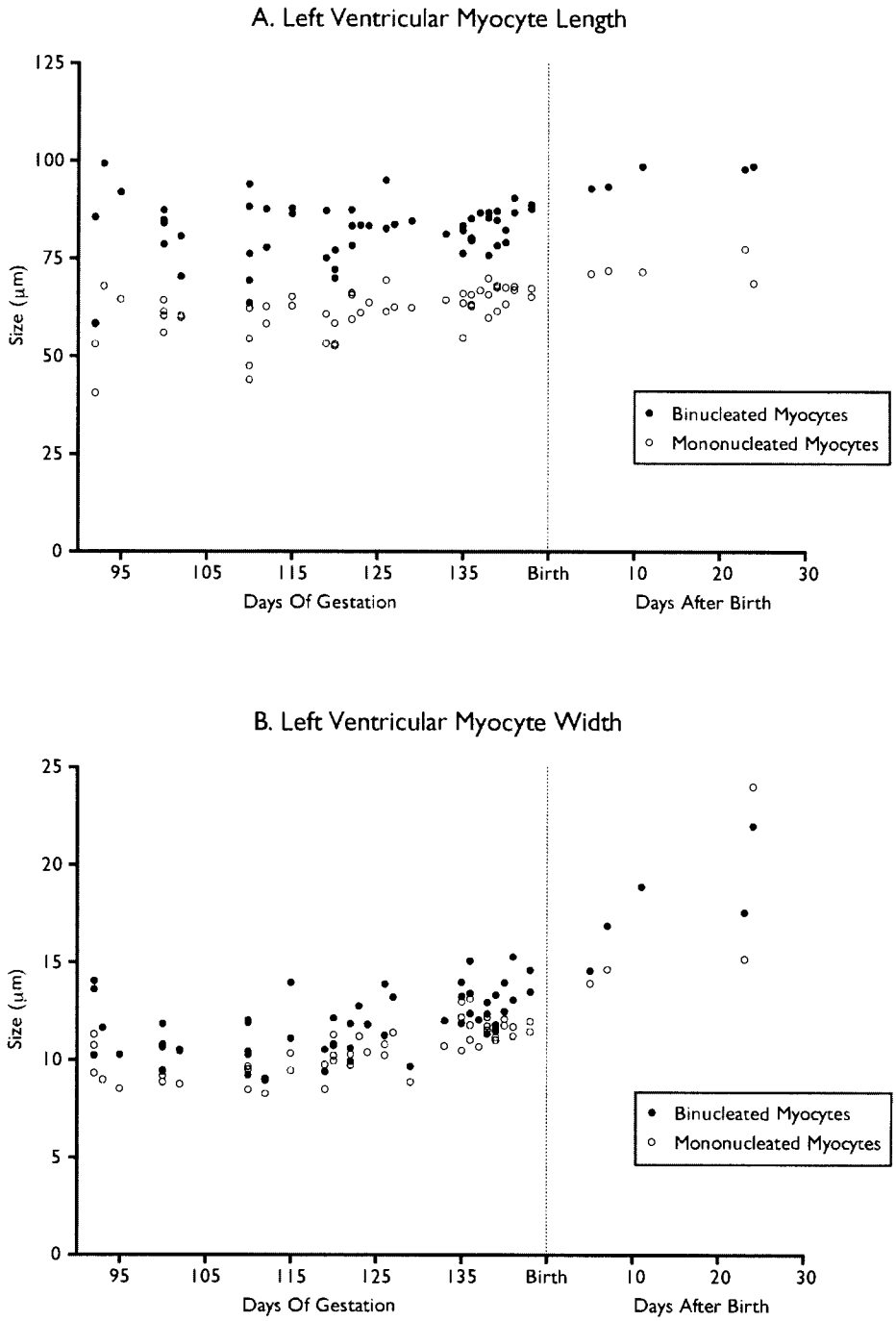

Figure 11. Left ventricular myocyte size during the last third of gestation. The 54 fetal samples (each point an average from one heart) were analyzed by linear regression. The length of binucleated myocytes did not increase significantly during gestation (r^2=0.01, p=0.4185), but the width of binucleated myocytes increased by 0.05μm per day (r^2=0.23, p=0.0003). The length of mononucleated myocytes increased by 0.18μm per day (LV r^2=0.22, p=0.0003), and width of mononucleated myocytes increased by 0.06μm per day (r^2=0.53, p<0.0001).

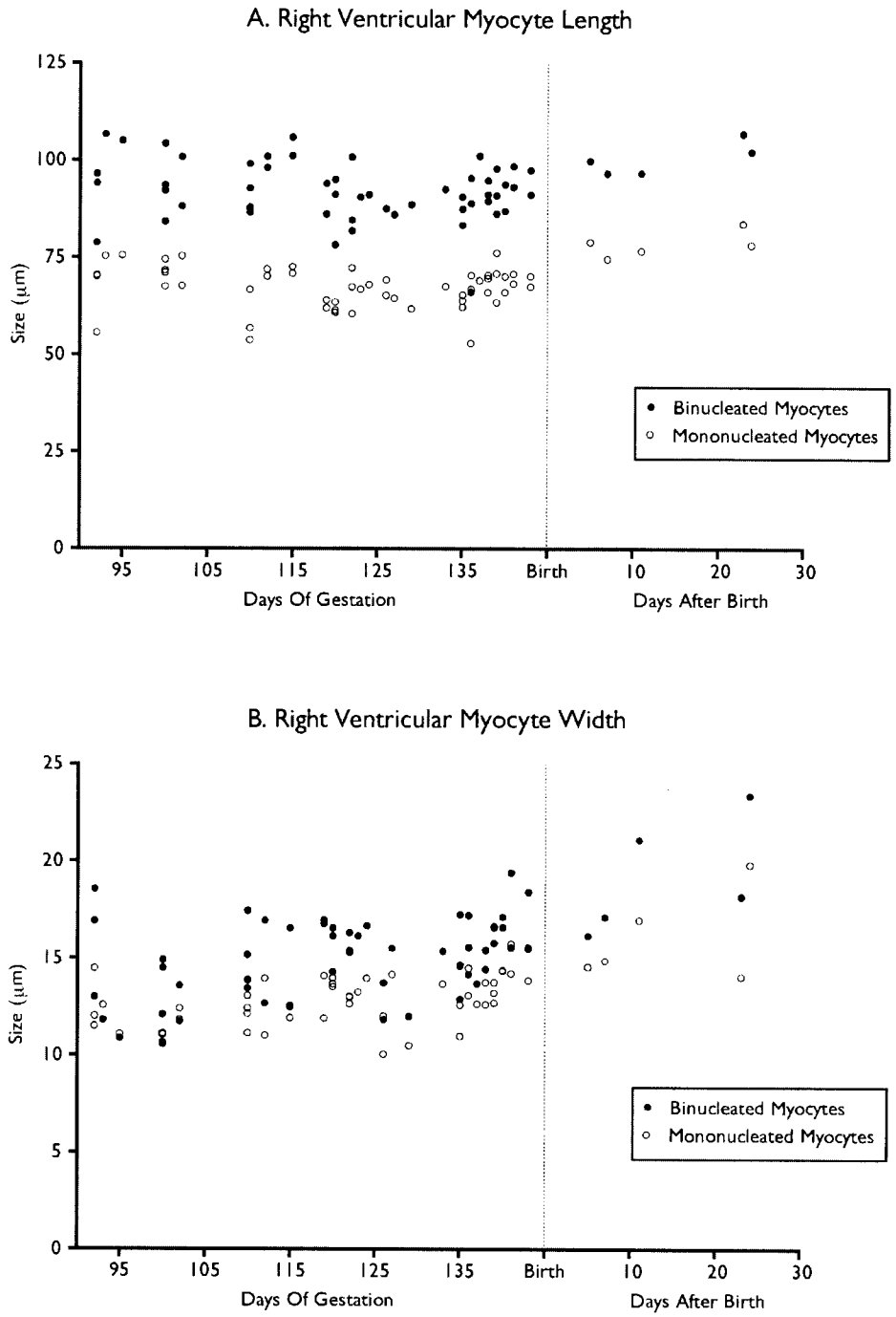

Figure 12. Right ventricular myocyte sizes during gestation and in the neonate. The 54 fetal samples (each point an average from one heart) were analyzed by linear regression. Neither binucleated myocyte length (r^2=0.43, p=0.1313) nor mononucleated myocyte length (r^2=0.01, p=0.4423) increased during the last third of gestation. However, binucleated width increased by 0.05µm per day (r^2=0.15, p=0.0035), and mononucleated width increased by 0.04µm per day (r^2=0.24, p=0.0002) during the last third of gestation.

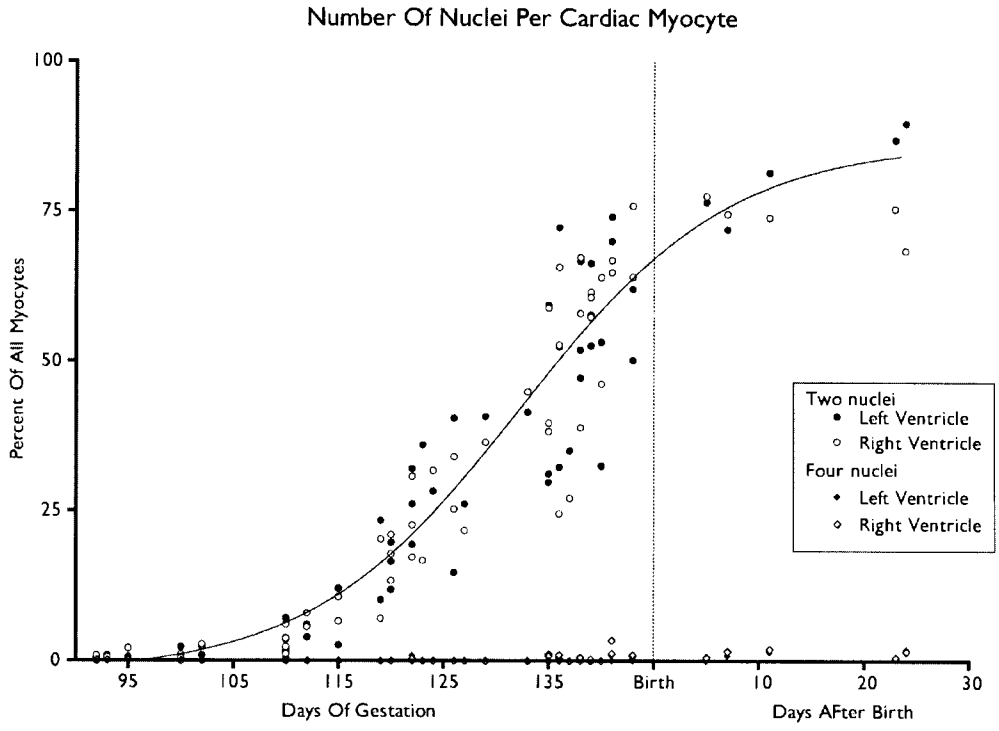

Figure 13. Percent nucleation of myocytes during cardiac growth. Cardiac myocytes in the developing sheep heart undergo binucleation beginning at about 115dGA in mixed western breed sheep (each point represents one heart). No difference in the binucleation rate was found between the right and left ventricles, even though right ventricular myocytes are larger at any given stage of gestation. A line was fit to the data such that binucleation = $-2.309 + 88.939 / (1 + e^{(132.3 - x) / 9.99})$ (r^2=0.90). 54 fetuses, 5 neonates.

ANOVA, followed by Bonferroni's multiple comparison test (Table 6). Myocyte size, binucleated fraction and cell cycle activity were not different between male and female fetuses. The myocytes of the RV were larger than the myocytes of the LV in the fetus, as has been previously reported (Smolich *et al.*, 1989).

In contrast, myocytes of adult sheep varied in size according to gender, but not by ventricle. Adult male sheep had significantly longer myocytes than adult females. The cardiac myocytes of adult sheep are large and may be more sensitive to mechanical shear than the fetal myocytes during the dissociation process. I had difficulty determining if these myocytes were shortened by mechanical damage. This data is therefore preliminary and represent a minimum estimation of cardiac myocyte size of the adult.

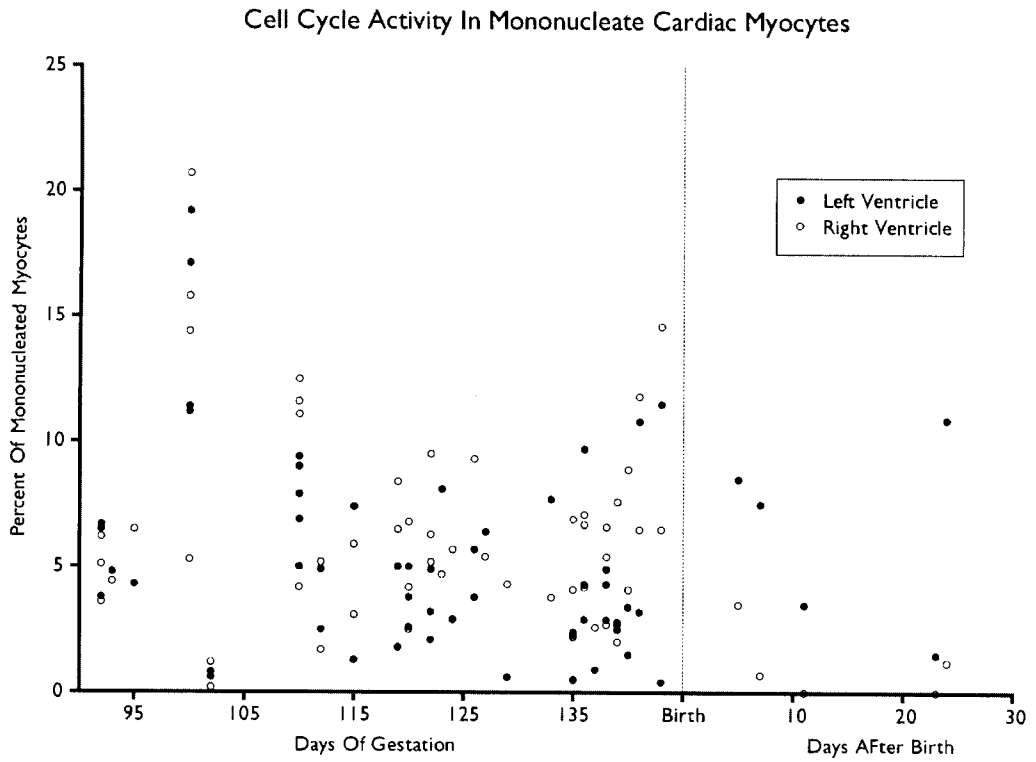

Figure 14. Cell cycle activity in mononucleated cardiac myocytes during gestation and in the neonate as measured by Ki-67 immuno-staining. The fetal data were analyzed by linear regression (LV r^2=0.11, p=0.0133; RV r^2=0.02, not significant). 54 fetuses, 5 neonates.

Normal Maturation of the Cardiac Calcium Transport System

Cardiac mRNA expression levels for NCX1 and SERCA2 were assessed by northern blot analysis. Five animals were analyzed at each age group, except the neonatal group (n=4). The adult group was composed of non-pregnant ewes. Values were expressed in comparison to the "housekeeping" gene GAPDH to normalize for loading; expression of GAPDH did not change with age. Data averaged at each age were compared by one-way ANOVA and Tukey's test for multiple comparisons. The northern blot assay was repeated three times with similar results.

Expression levels of cardiac NCX1 mRNA were highest at 95dGA compared to any later age (Figure 15a and b). Expression levels of SERCA2a mRNA were unchanged across ages except for a peak in

Table 6. Myocytes compared by genders in the ventricles of fetal and adult sheep. Seventeen fetuses between 136 and 140dGA (mean 138 ± 1dGA) were compared by gender (females n=9, males n=8). Four adult male sheep were compared with 5 adult female sheep.

	Left Ventricle		Right Ventricle		Two-Way ANOVA Source of Variation (p value)	
	Female	Male	Female	Male	Ventricles	Genders
Fetuses						
Binucleated Myocytes						
Length (μm)	83 ± 4	84 ± 5	91 ± 4 **	93 ± 5 ***	NS	<0.0001
Width (μm)	12 ± 1	13 ± 1	16 ± 1 ***	15 ± 2 ***	NS	<0.0002
Mononucleated Myocytes						
Length (μm)	66 ± 4	64 ± 4	68 ± 4	69 ± 4 *	NS	0.0061
Width (μm)	11 ± 1	11 ± 1	13 ± 1 ***	14 ± 1 ***	NS	<0.0002
Binucleation (%)	49.7 ± 14.3	41.0 ± 10.6	51.7 ± 13.9	43.6 ± 13.2	NS	NS
Cell Cycle Activity in Mononucleated Myocytes (%)	3.0 ± 1.0	3.9 ± 2.5	5.0 ± 2.3	5.6 ± 3.4	NS	0.0318
Adults						
Length (μm)	171.2 ± 8.7	138.9 ± 6.8 ††	176.1 ± 14.8	142.1 ± 20.2 ††	NS	0.0002
Width (μm)	44.6 ± 3.1	38.2 ± 4.3	37.5 ± 2.9	34.2 ± 4.0	0.0066	0.0152

** p <0.05, **p <0.01, ***p<0.001 different than LV; †† p<0.01 different than female; Mean ± SD.*

the RV of the neonate (Figure 15c and d).

Protein levels from the same hearts were assessed by Western blot analysis (Figure 15). Values were normalized to amount of protein loaded on gel. Equal loading was confirmed by uniform staining of

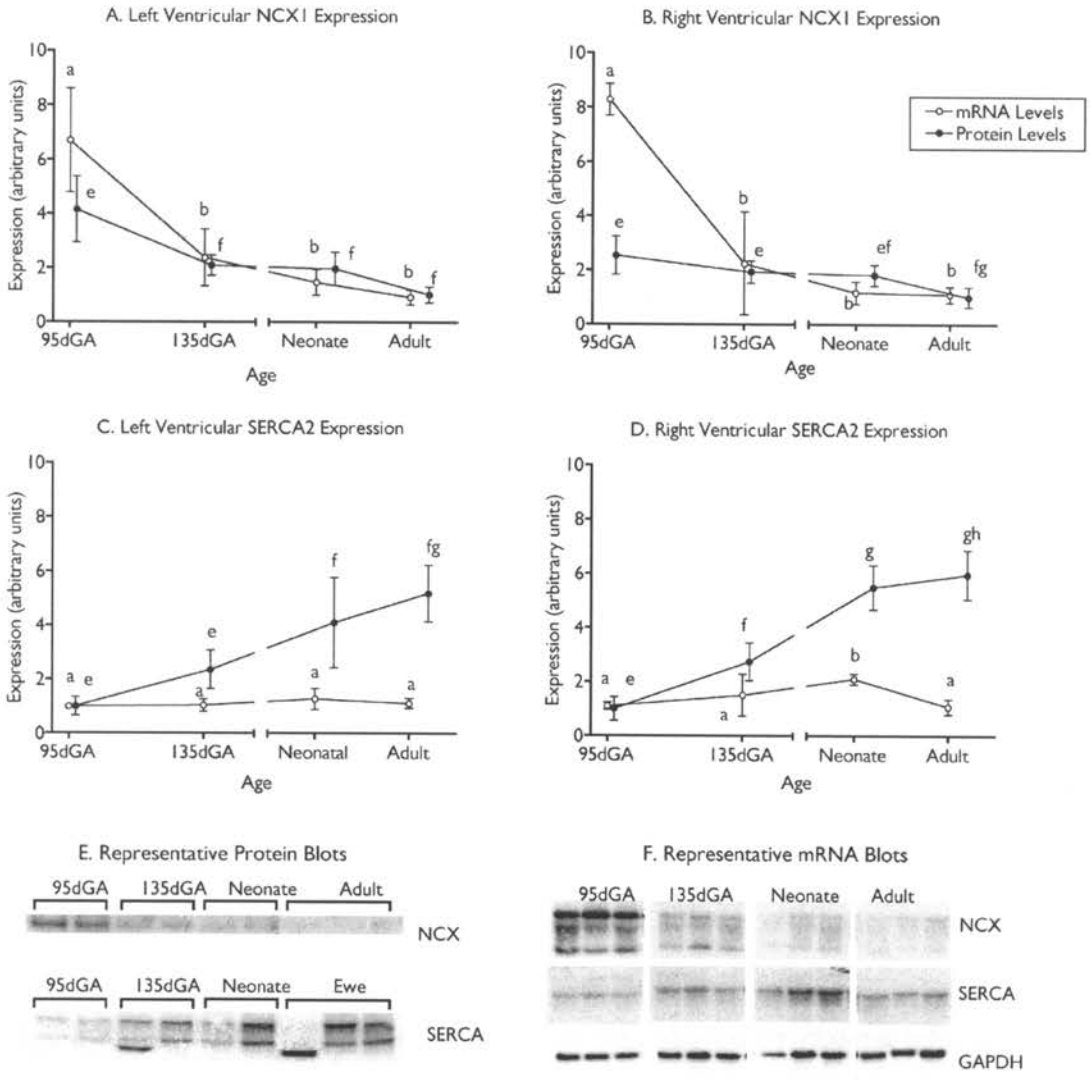

Figure 15. Maturational expression levels of cardiac NCX1 and SERCA2 protein and mRNA. Levels are plotted for A) left ventricular NCX1 (each group n = 5, except western 95dGA and adults n = 4), B) right ventricular NCX1 (each group n = 5, except northern 95dGA and western neonatal groups n = 4), C) left ventricular SERCA2 (each group n = 5, except 135dGA and neonate groups n = 4), and D) right ventricular SERCA2 (each group n = 5, except northern and western 135dGA and western neonatal groups n = 4). Representative LV blots shown for E) protein analysis, and F) mRNA analysis. Groups which are significantly different from each other do not share a letter.

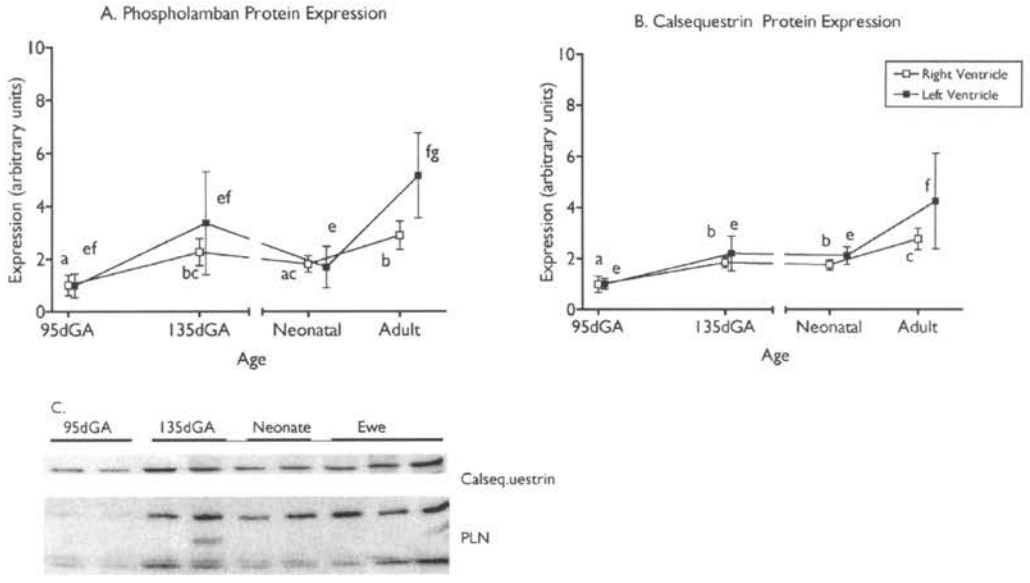

Figure 16. Maturational expression levels of cardiac PLN and calsequestrin. A) PLN (each group n = 5 except RV 95dGA and RV and LV neonatal groups n = 4), and B) calsequestrin (each group n = 5 except RV 95dGA and RV and LV neonatal groups n = 4). C) Representative LV blots . Groups which are significantly different do not share a letter.

the protein bound to the PVDF membrane. Immunoblots were run in duplicate and values were averaged. Data averaged at each age were compared by one-way ANOVA and Tukey's test for multiple comparisons.

NCX1 protein levels were highest in the 95dGA fetal heart and declined with maturation (Figure 15a and b). SERCA2 protein levels were lowest in the 95dGA fetus and increased steadily with age (Figure 15c and d). Phospholamban and calsequestrin protein levels were lower in the immature heart than the mature heart (Figure 16).

Fetal Arterial and Venous Hypertension Induced by Plasma Infusion

Of the 15 fetuses in the 4-day study group, 8 were controls and 7 were infused with plasma. The experimental period for these fetuses concluded at 134 ± 1dGA, and there were no age differences between control and experimental fetuses. Over the course of the 4-day experiment, the plasma-infused fetuses received 64 ± 19g of plasma protein in 1190 ± 240ml of fluid.

Twenty-eight fetuses, evenly divided into control and experimental groups, were allocated to the 8-day study group. The experimental period for these fetuses concluded at 138 ± 1dGA, and there were no age differences between control and experimental fetuses. These animals were further subdivided according to the disposition of the heart; the hearts of 12 fetuses were frozen, the hearts of 16 fetuses were dissociated. Over the course of 8 ± 1 days, the experimental fetuses received 121 ± 28g of plasma protein in 2159 ± 714ml of fluid. As a result of infusion, plasma protein levels increased substantially in experimental fetuses (Table 7).

Cardiovascular hemodynamic measurements from plasma-infused fetuses are displayed in Table 7. Arterial pressure increased from baseline by approximately 50% after both 4 and 8 days of infusion. Venous pressure increased from baseline by more than 50% in both groups, although this was not significant in the 4-day infusion group. Heart rate declined after 8 days of plasma infusion. However, a decrease in heart rate is normal in late gestation. Arterial P_{O_2} and oxygen content decreased after 4 and 8 days of infusion in both groups. Arterial P_{CO_2} increased somewhat, but was only significant in the 4-day group. Hematocrit was unchanged by plasma infusion.

Table 7. Hemodynamics and arterial blood values in plasma-infused fetuses. 4-day group $n = 7$, 8-day group $n = 14$.

	4-Day Infusion Group		8-Day Infusion Group		
	Baseline	Day 4	Baseline	Day 4	Day 8
Mean arterial pressure (mmHg)	43 ± 3	63 ± 4 ***	42 ± 3	57 ± 4 **	63 ± 3 **
Mean venous pressure (mmHg)	3.3 ± 0.6	5.1 ± 1.3	2.8 ± 0.9	4.5 ± 1.6 **	4.9 ± 2.4 **
Heart rate (bpm)	166 ± 10	165 ± 12	175 ± 12	167 ± 15	158 ± 19 *
Arterial pH	7.36 ± 0.02	7.32 ± 0.06 *	7.35 ± 0.04	7.33 ± 0.03	7.32 ± 0.04
Arterial P_{O_2} (mmHg)	20.3 ± 1.4	14.1 ± 2.4 ***	21.3 ± 2.1	18.3 ± 3.1 *	18.1 ± 3.9 *
Arterial P_{CO_2} (mmHg)	53.9 ± 3.7	60.0 ± 2.2 *	53.9 ± 3.4	55.7 ± 2.8	56.4 ± 3.1
Arterial O_2 content (ml/100ml)	7.6 ± 0.8	5.3 ± 1.6 *	7.7 ± 1.2	6.2 ± 1.4 *	5.6 ± 2.1 **
Hematocrit (%)	32.6 ± 3.8	32.3 ± 4.8	33.7 ± 4.8	32.0 ± 3.8	31.9 ± 5.1
Plasma protein (g/l)	33.4 ± 3.4	71.4 ± 7.0 ***	34.0 ± 3.8	66.9 ± 5.9 **	77.8 ± 10.6 **
Plasma AngII (pg/ml)	31 ± 30	6 ± 5	24 ± 20	13 ± 24	9 ± 10 *
Plasma renin activity (ng/ml/hr)	7.8 ± 6.5	1.1 ± 1.8 *	7.0 ± 3.3	2.4 ± 3.2 **	2.1 ± 2.2 **

** $p < 0.05$, ** $p < 0.01$, *** $p < 0.001$ different than baseline; Mean ± SD.*

Table 8. Body and heart weights of plasma-infused fetuses. 4-day control group n = 8, 4-day load group *n* = 7, 8-day group (control and load) *n* = 14 (except component weights *n* = 6).

	4-Day Infusion Group		8-Day Infusion Group	
	Control	Load	Control	Load
Heart weight (g)	24.6 ± 5.4	32.7 ± 5.0 *	29.1 ± 8.2	38.2 ± 5.0 **
Body weight (kg)	4.0 ± 0.8	4.2 ± 0.7	4.5 ± 0.8	4.5 ± 0.5
Heart / body weight (g/kg)	6.2 ± 0.5	7.9 ± 1.6 *	6.5 ± 0.9	8.4 ± 0.7 ***
Heart component weights (g)				
Left ventricle			7.5 ± 2.7	10.5 ± 2.2
Right ventricle			8.0 ± 2.4	11.4 ± 1.7 *
Septum			5.9 ± 2.1	7.2 ± 1.0
Left atrium			1.7 ± 0.8	2.5 ± 1.0
Right atrium			1.8 ± 0.7	2.8 ± 0.7 *

** p <0.05, **p <0.01, ***p<0.001 different than control; Mean ± SD.*

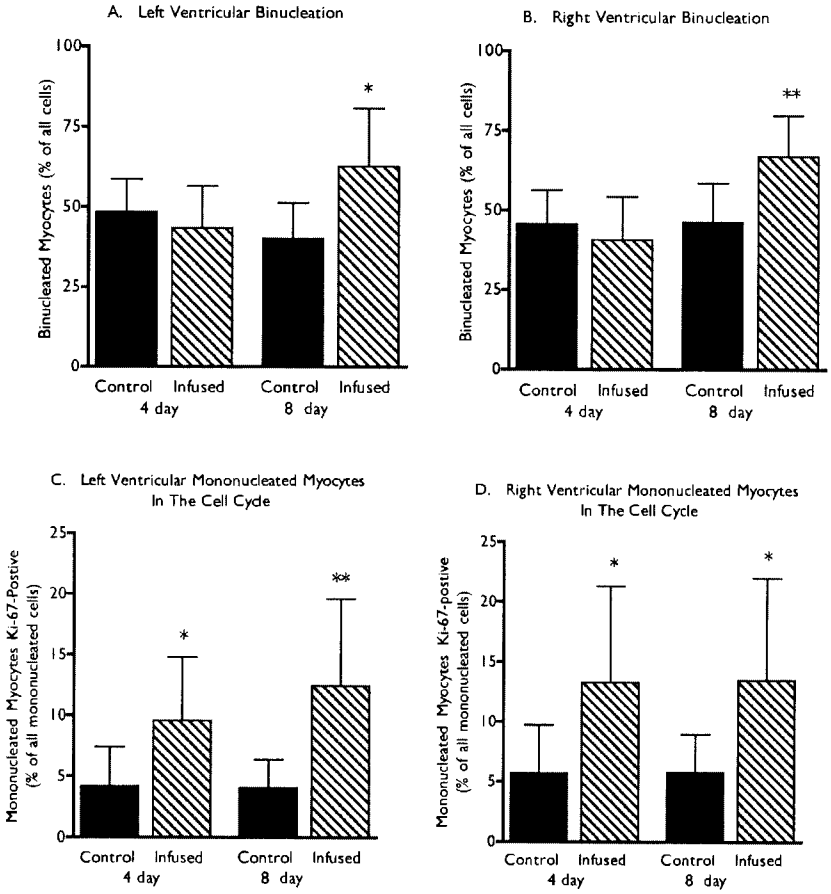

Figure 17. A & B) Fraction binucleated and C & D) cell cycle activity after intravascular plasma infusion. ■ = control; ▨ = experimental. Each group *n* = 8, except 4-day load group *n* = 7. * p <0.05, **p <0.01 than control; Mean ± SD.

The fetal RAS was depressed by chronic plasma infusion (Table 7) as seen by reduced renin activity and low AngII concentrations. Plasma renin activity was very low after 4 days of plasma infusion, and remained low after 8 days. Plasma AngII measurements were variable due to rapid degradation of the peptide (Rosenfeld *et al.*, 1995); decreased levels were evident after 4 days of infusion, but significant only after 8 days.

Myocardial Growth During Plasma Infusion

The weights of hearts from fetuses infused with plasma were about 30% greater than control fetuses, although body weights were not different (Table 8). The weights of the atria, ventricular free walls and septa were collected from fetal hearts that were dissected (n=6 each control and experimental). The chamber walls of experimental fetuses tended to be heavier than the hearts of control fetuses, although the increase only reached significance for the right ventricular free wall and right atrium.

Binucleated cardiac myocytes in both ventricles after 4 and 8 days of plasma infusion were 10% longer than myocytes from control fetuses (Table 9). The widths of these cells were not increased after 4 days of infusion, but after 8 days they were 10% wider than myocytes from control fetuses. Mononucleated myocyte sizes were similarly affected by load (Table 9).

Table 9. Cardiac myocyte sizes of plasma-infused fetuses. Each group n = 8, except 4-day load group n = 7.

	4-day Study		8-day Study	
	Control	Loaded	Control	Loaded
Binucleated myocyte length (μm)				
Left ventricle	81.7 ± 4.0	89.9 ± 6.8 **	82.7 ± 5.0	91.9 ± 7.1 *
Right ventricle	90.7 ± 5.6	100.0 ± 6.7 **	89.8 ± 3.7	101.5 ± 7.0 **
Binucleated myocyte width (μm)				
Left ventricle	12.3 ± 0.8	12.7 ± 0.7	12.5 ± 1.2	14.0 ± 1.2 *
Right ventricle	15.2 ± 1.3	15.6 ± 1.8	15.7 ± 2.1	17.8 ± 1.5 *
Mononucleated myocyte length (μm)				
Left ventricle	62.0 ± 4.0	67.8 ± 6.3 *	63.9 ± 3.5	71.4 ± 7.4
Right ventricle	68.4 ± 4.3	74.7 ± 7.5 *	67.7 ± 4.2	78.3 ± 6.2 *
Mononucleated myocyte width (μm)				
Left ventricle	11.2 ± 0.9	11.6 ± 0.6	11.3 ± 0.9	12.2 ± 1.0
Right ventricle	13.6 ± 0.8	13.4 ± 1.2	13.6 ± 1.0	15.6 ± 1.7 *

** $p < 0.05$, ** $p < 0.01$ different than control; Mean ± SD.*

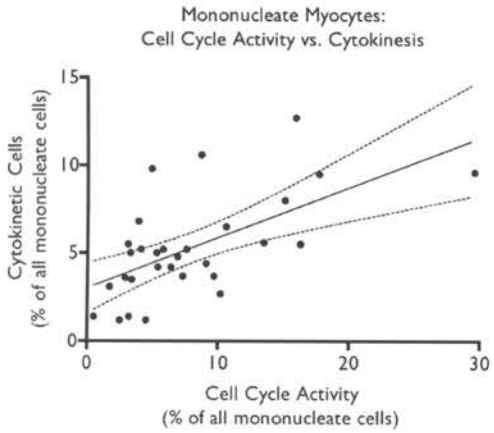

Figure 18. Correlation of cytokinesis and cell cycle activity in mononucleated cardiac myocytes. Myocytes from undergoing cytokineses were identified visually and compared to the fraction of myocytes that stained positive for Ki-67. These values were correlated (Pearson r =0.6109, p=0.0003, n=30). The best-fit line and 95% onfidence intervals of the linear regression are shown (r^2=0.3732, p=0.0003). Myocytes were analyzed from both ventricles of all fetuses (n = 15) in the 4-day study group.

The fraction of binucleated myocytes in the hearts of fetuses infused with plasma for 8 days was 40% greater than the fraction in hearts of control fetuses (Figure 17). However, the binucleation index was not different between infused and control fetuses in the group studied for 4 days. The proportion of myocytes with 4 nuclei was very low in all groups. There was a greater fraction of myocytes containing 4 nuclei in the RV after 8 days of plasma infusion than in control fetuses (0.4% ± 0.4% vs. 1.2% ± 1%, p = 0.0438), but not in the LV (0.1% ± 0.2% vs. 0.6% ± 1%, NS). In fetuses that received plasma for 4 days, there were no changes in the fraction of myocytes with 4 nuclei compared to control fetuses (LV 0% ± 0.1% vs. 0.1% ± 0.2%, respectively, NS; RV 0.4% ± 0.5% vs. 0.3% ± 0.3%, NS).

Cell cycle activity, as measured by the fraction of mononucleated myocytes that stained positive for Ki-67, was increased over control levels after both 4 and 8 days of plasma infusion (Figure 17). Myocytes from the 4-day infusion group were used to measure the fraction of myocytes fixed in the

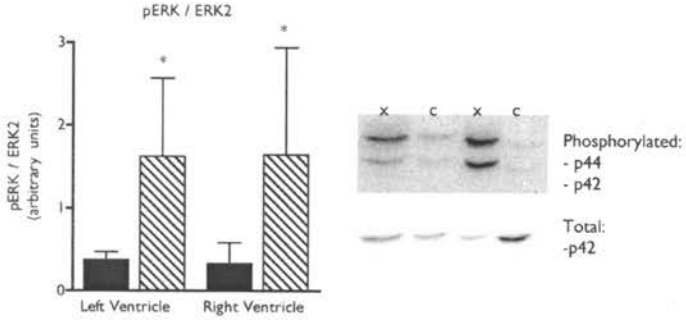

Figure 19. ERK1/2 phosphorylation in plasma-infused fetal hearts. ■ and c = control fetuses (n =); ▨ and x = experimental plasma-infused fetuses (n = 6). A representative LV blot is shown. * p <0.05 different than control; Mean ± SD.

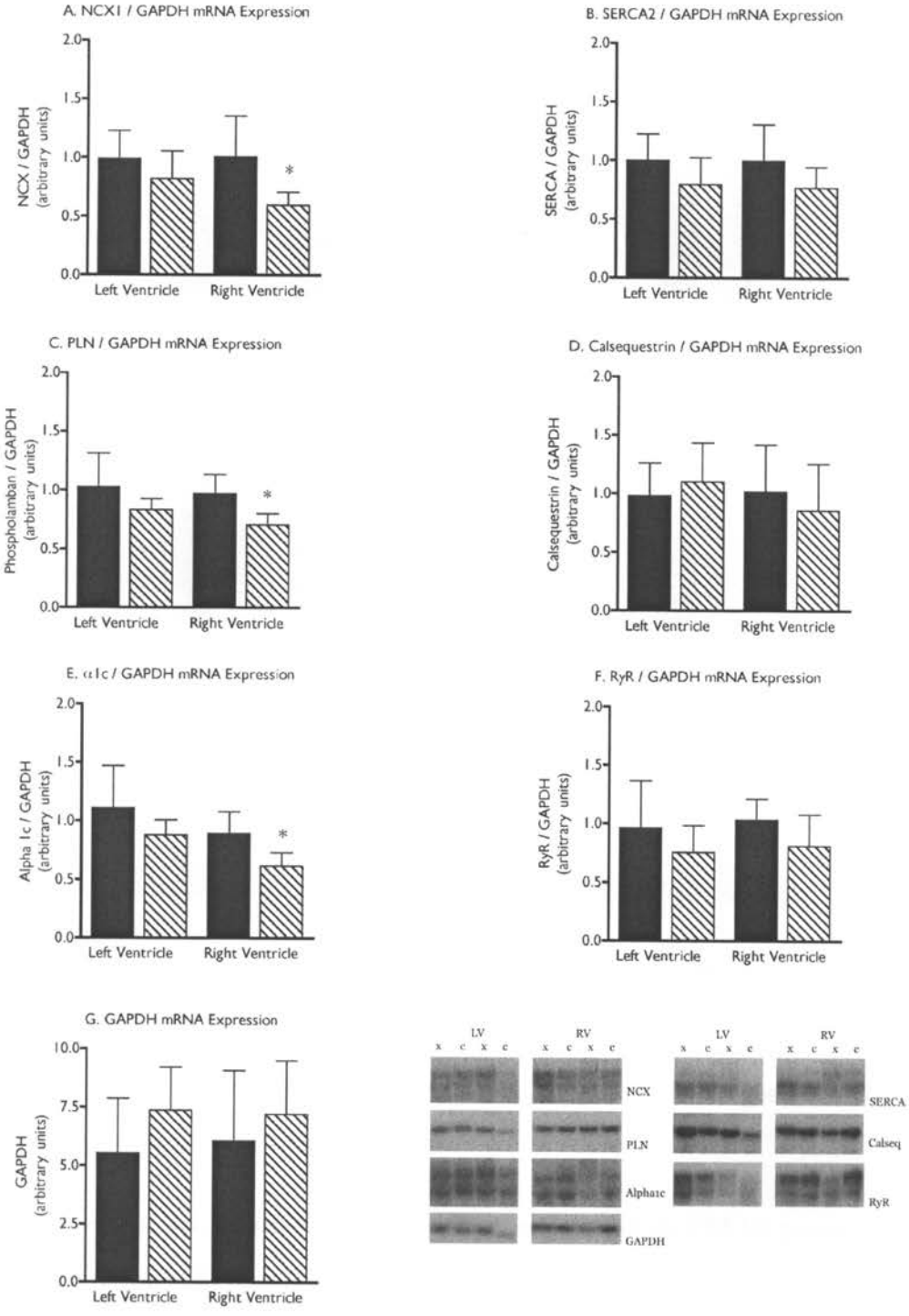

Figure 20. mRNA expression levels in the hearts of plasma-infused fetuses. ■ and c = control (n = 6); ▨ and x = plasma-infused (n = 6). * p <0.05 different than control; Mean ± SD.

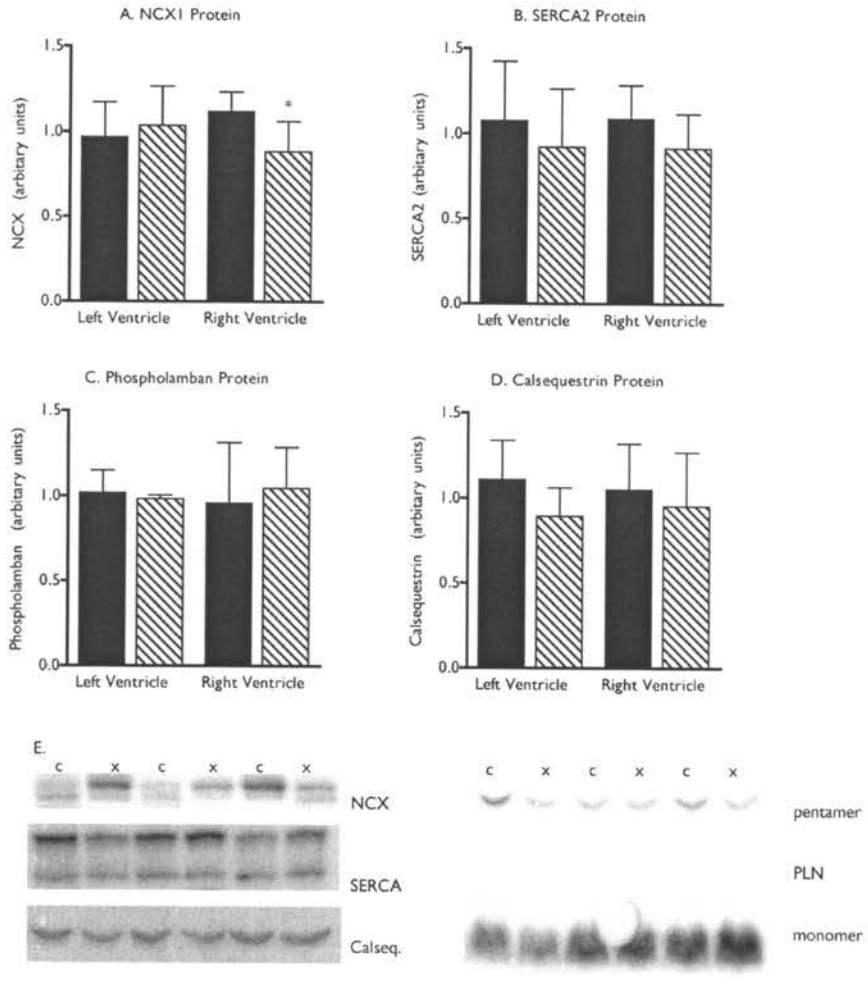

Figure 21. Protein expression levels in hearts of plasma-infused fetuses. A) NCX1, B) SERCA2, C) PLN and D) calsequestrin. E) Representative LV blots. ■ and c = control (n = 6); ▨ and x = plasma-infused (n = 6). * p <0.05 different than control; Mean ± SD.

process of cytokinesis, as determined by visual inspection. The number of daughter cells of cytokinesis was correlated with the Ki-67 rate (Figure 18).

Western blot analysis was carried out to measure phosphorylation of the ERK1/2 proteins p42 and p44. Phosphorylation of ERK1/2 was significantly increased after 8 days of plasma infusion in both ventricles of fetal sheep (Figure 19).

The Fetal Cardiac Calcium Transport System

mRNA expression levels for several calcium transport-related genes were measured by northern blot analysis in cardiac extracts from plasma-loaded and control fetuses (Figure 20). Probes were directed against the channels and transporters NCX1, SERCA2, RyR and LTCC (α1c subunit), the regulatory gene PLN, and the calcium-binding protein calsequestrin. Gene expression was normalized to the housekeeping gene GAPDH and assays were done in duplicate. GAPDH expression did not change in plasma-loaded fetal hearts (Figure 20g). Experimental fetuses were compared to control fetuses. After sustained hemodynamic load induced by plasma infusion, there was a trend for most of the studied genes to be down-regulated; however, this may be attributed to the non-significant increase in GAPDH levels in experimental hearts. Significant differences were found in the RV in NCX1, phospholamban and LTCC α1c expression.

Protein expression levels in the hearts of experimental and control fetuses were measured by Western blot analysis (Figure 21). Blots were carried out in duplicate and averaged. Experimental fetuses were compared to control fetuses using unpaired t-test. SERCA2, PLN and calsequestrin protein levels were not significantly different between experimental and control animals. NCX1 protein levels were somewhat lower in the experimental compared to control RV ($p<0.05$).

Partial Aortic Occlusion and the Cardiac Calcium Transport System

An inflatable occluder cuff was installed around the postductal thoracic aorta of 14 fetuses. The occluder was inflated in order to increase pressure in the proximal aorta and pulmonary artery. I obtained a complete data set and tissue from 6 fetuses. The reasons for the failure of a preparation were varied- one ewe aborted, surgical error accounted for one loss, and one fetus died due to cardiac tamponade after the catheters eroded the aorta. I placed a high-fidelity pressure recording transducer directly into the LV of two fetuses in order to be able to measure the maximum rate of relaxation (a important feature of diastolic function controlled by calcium uptake). These fetuses recovered

Table 10. Physiological measurements from pressure-loaded fetuses. $n = 6$.

	Baseline	Day 4	Final Day
Mean arterial pressure (mmHg)	46.3 ± 3.1	54.1 ± 9.6	57.4 ± 6.0 *
Heart rate (bpm)	172 ± 26	164 ± 29	139 ± 19
Arterial pH	7.36 ± 0.03	7.36 ± 0.01	7.33 ± 0.05
Arterial PO_2 (mmHg)	19 ± 5	19 ± 4	19 ± 2
Arterial PCO_2 (mmHg)	52.0 ± 3.3	51.1 ± 3.8	50.9 ± 1.1
Arterial O_2 content (ml/100ml)	8.0 ± 1.8	8.1 ± 1.2	7.8 ± 1.7
Hematocrit (%)	35 ± 4	35 ± 3	34 ± 3

** $p < 0.05$ compared with baseline; Mean ± SD.*

well until I attempted to inflate the occluder, at which point they died; therefore, I stopped placing these ventricular transducers. Nevertheless, the other three fetal deaths were probably due to cardiac failure in response to the load.

Fetuses were pressure-loaded by inflation of the occluder for 10 ± 1 days (range 9-10); their mean age at the conclusion of the experiment was 139 ± 1dGA ($n = 6$). At the conclusion of the experiment the hearts were frozen for RNA analysis. The experimental fetuses were compared to twin and historical controls (138 ± 1dGA, $n = 6$).

Aortic blood pressure proximal to the occluder, measured prior to adjustment of the occluder, increased between the baseline day and the final day (Table 10). There was a non-significant trend for heart rate to decline during this period, a normal maturational change. Fetal blood gases and hematocrit were normal over the course of the experiment. There were no differences in body weight, heart weight, or weights of heart components between control and experimental fetuses (Table 11).

Table 11. Weights of pressure-loaded fetuses and controls. Each group $n = 6$.

	Control	Loaded
Body weight (kg)	4.3 ± 0.5	4.2 ± 0.8
Heart weight (g)	27.7 ± 5.5	28.4 ± 6.0
Heart / Body weight ratio (g/kg)	6.5 ± 0.8	6.8 ± 0.9
Component weights (g)		
LV	7.3 ± 1.5	7.4 ± 1.5
RV	8.0 ± 1.7	8.1 ± 2.1
Septum	5.6 ± 0.7	5.8 ± 1.6
Left Atrium	1.9 ± 0.5	2.1 ± 0.5
Right Atrium	1.8 ± 0.7	2.3 ± 0.5

Values displayed as mean ± SD.

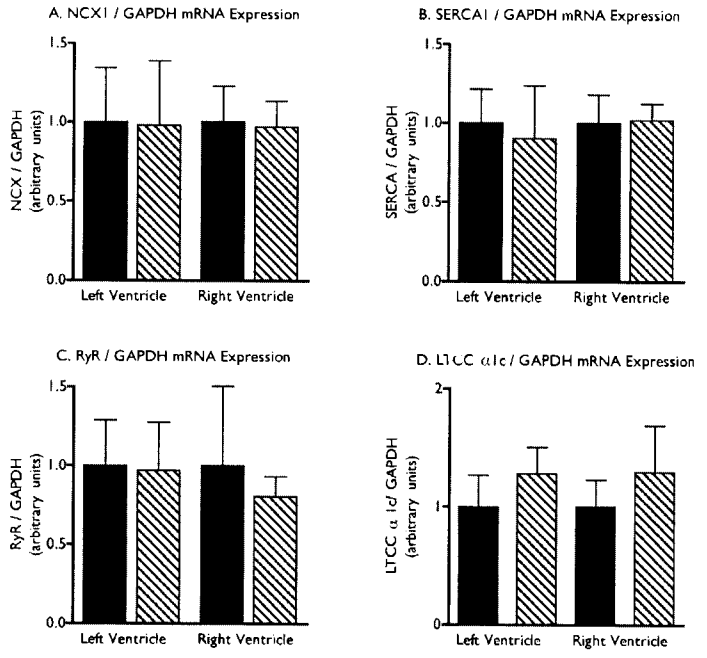

Figure 22. mRNA expression levels in hearts from pressure loaded fetuses. ■ control; ▨ experimental. No significant differences were found. Each group $n = 6$.

I performed northern blot analysis to determine the relative expression levels of mRNA of genes responsible for calcium transport in the hearts of plasma-loaded fetuses. I probed three consecutive sets of duplicate membranes, each of which contained both RV and LV samples of systolic load and control fetuses as well as a standard. The results of the analyses were similar. Expression of SERCA2, NCX1, RyR, and LTCC α1c mRNA was not different between control and loaded fetuses (Figure 22), although there is a trend for LTCC α1c to increase with load.

Increased Volume Load and the Fetal Cardiac Calcium Transport System

I measured the mRNA expression levels of NCX1 and SERCA2 in extracts of volume-loaded fetal hearts. These gene levels were not different in experimental hearts compared to hearts of control fetuses (Figure 23).

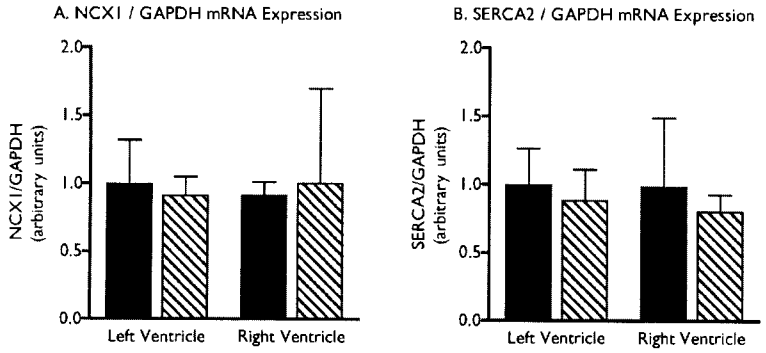

Figure 23. mRNA expression levels in hearts of volume-loaded fetuses. ■ control; ▨ experimental. No significant differences were found (each group n = 5, except RV control n = 4, RV load n = 3).

Sustained Fetal Anemia and Growth of the Fetal Heart

Fetal sheep from 8 twin pregnancies and 2 singleton pregnancies were instrumented in order to produce fetal anemia. A complete data set was collected for 5 twin and 2 singleton pregnancies. Of the unsuccessful preparations, 2 were due to the effects of anemia and 1 was excluded because of a congenital defect. In each twin pair, one fetus was made anemic and the other was used as a non-anemic control. One uninstrumented twin, for which there are no *in vivo* data, is included as a non-anemic control. Of the 2 singletons, 1 was made anemic and 1 was used as non-anemic controls.

The average length of the experimental period was 9 ± 1 full days (range 8-10); the fetuses were 137 ± 1dGA at the conclusion of the experiment. Three ewes displayed signs of premature labor that

Table 12. Hemodynamics, blood gas values and pH in anemic and control fetuses. Anemic group n = 6, control group n = 5.

	Control		Anemic	
	Baseline	Final Day	Baseline	Final Day
Mean Arterial Pressure (mmHg)	45 ± 5	51 ± 6	44 ± 4	41 ± 5 †
Venous Pressure (mmHg)	2.1 ± 0.6	2.3 ± 1.1	2.6 ± 0.9	3.5 ± 2.1
Heart Rate (bpm)	169 ± 11	136 ± 17 *	162 ± 13	174 ± 18 *
pH	7.38 ± 0.03	7.33 ± 0.02	7.38 ± 0.02	7.32 ± 0.06 †
Arterial PCO_2 (mmHg)	51 ± 4	53 ± 2	50 ± 3	53 ± 2
Arterial PO_2 (mmHg)	20 ± 2	18 ± 2	20 ± 3	16 ± 2 †
Arterial O_2 Content (g/100ml)	8.5 ± 2.4	7.2 ± 1.3	8.3 ± 2.0	2.3 ± 0.2 †*
Hematocrit (%)	36 ± 4	38 ± 8	36 ± 4	16 ± 3 †*
AngII (pg/ml)	24.7 ± 17.9	42.0 ± 41.0	16.7 ± 12.7	50.3 ± 76.5
Cortisol (ng/ml)	5.3 ± 2.3	58.6 ± 17.1 *	3.7 ± 1.7	53.9 ± 21.7 *

*† different than control, * different than baseline; Mean ± SD.*

Table 13. Heart and body weights of anemic and control fetuses. Each group n = 6.

	Control	Anemic
Body weight (kg)	4.0 ± 0.5	4.1 ± 0.7
Heart weight (g)	25.4 ± 4.1	35.7 ± 6.4 **
Heart/Body weight ratio (g/kg)	6.4 ± 0.9	8.8 ± 1.1 ****
LV wet / dry weight ratio	8.3 ± 2.7	7.8 ± 2.1

***p <0.01, ****p<0.0001 different than control; Mean ± SD.*

brought the experiment to a conclusion. All fetal hearts were dissociated for myocyte analysis; a section of LV was removed prior to dissociation in 3 hearts from each group for wet-to-dry weight analysis.

During the experimental production of fetal anemia, hematocrit and oxygen content were markedly reduced by daily phlebotomy (Table 12). Arterial pH and P_{O_2} were affected by this treatment, but P_{CO_2} was not altered. Mean venous pressure was not different between groups. Heart rate in the anemic fetuses was increased on the final day compared to baseline. On the final day, the arterial pressure of the anemic animals was lower than control fetuses.

Table 14. Cardiac myocyte in anemic and control fetuses. No differences were significant. Anemic group n = 5, control group n = 6.

	Control	Anemic
Binucleated myocyte length (μm)		
Left ventricle	89.0 ± 5.4	92.2 ± 3.6
Right ventricle	99.0 ± 7.5	103.0 ± 5.3
Binucleated myocyte width (μm)		
Left ventricle	12.8 ± 0.8	13.7 ± 1.0
Right ventricle	15.8 ± 2.1	16.1 ± 2.0
Mononucleated myocyte length (μm)		
Left ventricle	69.9 ± 4.9	71.6 ± 3.2
Right ventricle	74.2 ± 4.3	79.8 ± 2.5
Mononucleated myocyte width (μm)		
Left ventricle	11.4 ± 0.5	11.7 ± 0.9
Right ventricle	13.4 ± 2.1	13.6 ± 1.6
Binucleation (%)		
Left ventricle	56 ± 12	58 ± 4
Right ventricle	54 ± 10	63 ± 8
Cell cycle activity in mononucleated myocytes (%)		
Left ventricle	5.5 ± 3	7.7 ± 4.4
Right ventricle	5.3 ± 1.5	9.3 ± 7.7

Values are reported as mean ± SD.

Circulating cortisol levels on the final day increased from baseline in the control fetuses ($p<0.001$) and in the anemic fetuses ($p<0.001$). The cortisol levels of the two groups were not different from each other at baseline or on the final day. AngII levels were not different between experimental and control fetuses, or between the baseline and final days of the experiment.

The body weights of anemic fetuses were not different than control fetuses. The hearts, however, were increased in weight by 40% (Table 13). The ratio of the wet weight to the dry weight of the LV was not different between the groups (each group $n = 3$). There were no significant changes in myocyte size or binucleation (Table 14). The rate of cell cycle activity in mononucleated myocytes was not significantly different from control, but there was a trend for increased cell cycle activity in the hearts of anemic fetuses.

The Cardiac Calcium Transport System in Myocyte Culture

In order to test the regulation of NCX1 and SERCA2 protein expression in fetal sheep cardiac myocytes in response to a hormonal stimulation, cardiac myocytes were cultured with no drugs (in serum-free media) or with AngII (100nM), ANP (500nM except one experiment 750nM), cortisol

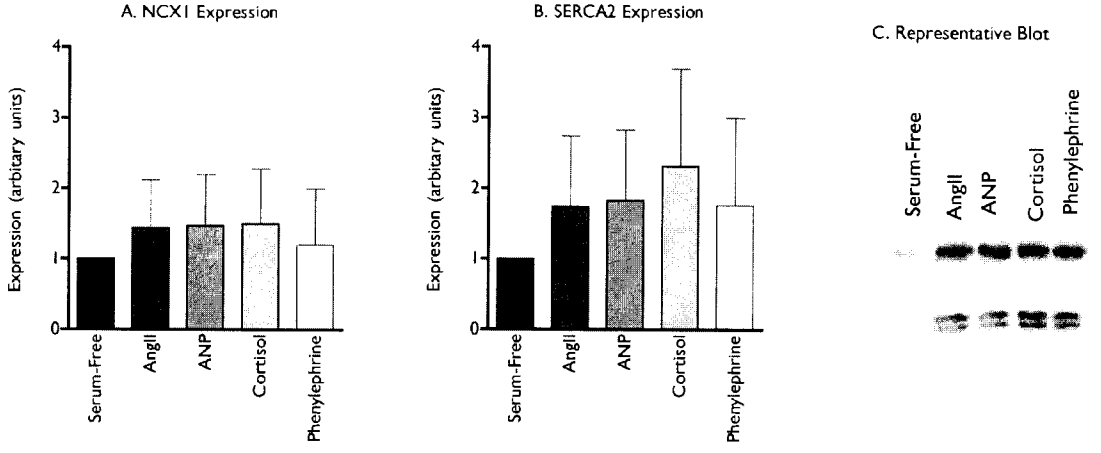

Figure 24. Protein expression levels in cultured cardiac myocytes. A) NCX1, B) SERCA2, and C) a representative blot. SF = serum-free control. Each group $n = 6$.

(138nM) and phenylephrine (98.2μm) for 48 hours. NCX1 and SERCA2 protein levels in these myocytes was compared by immunoblot analysis (Figure 24). When the expression levels of each gene were compared with one-way ANOVA, no differences were found.

CHAPTER 4

Discussion

In order to understand changes in growth that are induced by experimental conditions, it is useful to understand the context of the normal growth occurring in that period.

The purpose of the heart is to constantly maintain forward blood flow through the vascular system to meet tissue demand for nutrients. Fetal somatic growth during mid and late gestation increases the demand for blood flow. I found that growth of the heart was maintained nearly constant relative to body growth during the last third of gestation in sheep. Although the mechanism regulating the constant ratio of heart weight to body weight is unknown, it has also been observed in human fetuses (Mitropoulos *et al.*, 1992). Myocyte proliferation and hypertrophy both contributed to growth of the heart in the last third of gestation.

Cardiac Myocyte Proliferation During the Last Third of Gestation

Cardiac myocyte cell cycle activity over the last third of gestation was highly variable in normal fetuses (Figure 13). Why might this be the case? Little to none of the variability in cell cycle activity during this period was explained by advancing gestational age. The stimulus for cardiac growth during normal growth is unknown, but modulators could include growth factors and growth inhibitors, nutrient levels, and hemodynamic factors. If fetal cardiac growth were periodic rather than constant, this variability would be reflected in the measurement of myocyte cell cycle activity over time. Recent research indicates that post-natal growth may occur intermittently rather than continuously. Long-bone growth occurs intermittently in lambs after birth (Noonan *et al.*, 2004). Fetal sheep display diurnal rhythms in some factors that could regulate cardiac growth, including variations in

heart rate (Dalton *et al.*, 1977) and vasopressin levels (Leake *et al.*, 1986). Also, periodic eating and drinking by the pregnant ewe alters fetal urine osmolality (Mellor & Slater, 1972) and plasma glucose levels (Simonetta *et al.*, 1991). These variable factors may directly or indirectly influence the rate of hyperplastic growth of the fetal heart. If proliferation occurs in intermittant spurts, then single time-point samples of cell cycle activity will be highly variable.

Comparison of cell cycle activities between the ventricles, and between twin fetuses, may give some indication of the source of the variable growth signal. Myocyte cell cycle activities of the LV and RV were similar within fetuses (Figure 25a). Contrarily, it does not seem that rates were consistent between twin fetuses (Figure 25b). Intermittent hyperplastic growth of the fetal heart would be a new finding, and further experimentation would be required to establish that this occurs.

I found that, after birth, the rate of cell cycle activity amongst mononucleated cardiac myocytes decreased in the RV but not the LV (Table 5). Decreased RV myocyte proliferation is also is found in the neonatal mouse (Fernandez *et al.*, 2001). With ventilation of the lungs at birth, pulmonary resistance drops (Reid & Thornburg, 1990; Giraud *et al.*, 1995), thereafter the RV pumps into a

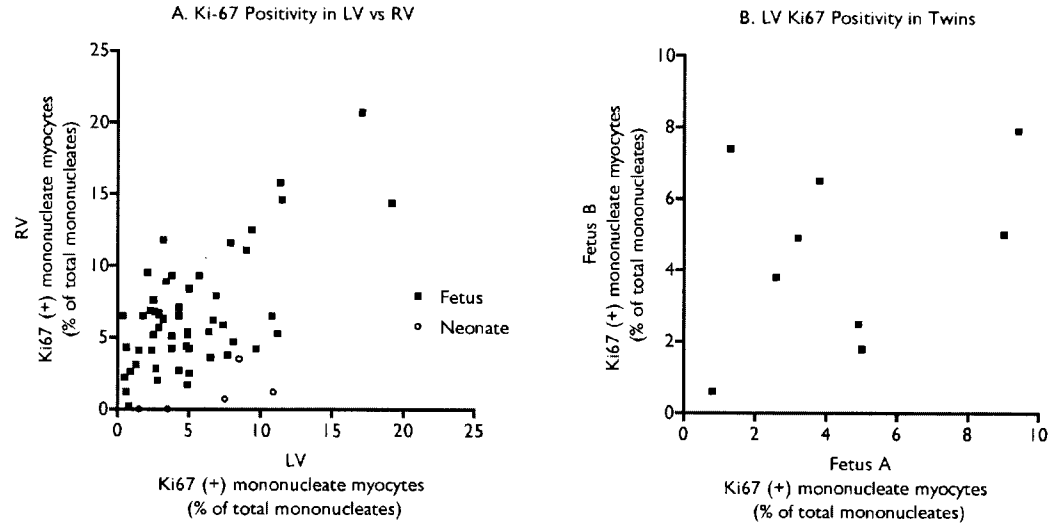

Figure 25. The relationship between Ki-67 positive values in the ventricles and in twin fetuses. A) The percent of Ki-67 positive mononucleated myocytes in the RV is plotted against the RV for fetal (n = 54) and neonatal sheep (n = 5). Correlation of fetal values: r^2 = 0.43, $p<0.001$. B) There is no correlation of cell cycle activity between twin fetuses (n = 9, r^2 =0.12, p=0.3634).

low-resistance circuit. After birth, the RV undergoes a period of apoptosis and remodeling associated with this functional transition (Fernandez *et al.*, 2001). In contrast to the post-natal lamb hearts, I found no Ki-67 positive myocytes in dissociated cells from adult sheep hearts.

It may be that not all myocytes that stained positive for Ki-67 were in the process of proliferating. Mononucleated cells that are becoming binucleated replicate their DNA and progress partially through the cell cycle. These cells do not continue to express Ki-67 protein, otherwise all myocytes in the neonatal and adult hearts that I studied would have stained positive. Instead, I found that a very few myocytes in the fetal hearts were both Ki-67 positive and binucleated with no signs of cytokinesis. Furthermore, Ki-67 positivity correlated with the proportion of myocytes undergoing cytokinesis, a step in proliferative growth (Figure 18). These data suggest that the index of Ki-67 positivity is a good indication of the number of proliferating myocytes.

The process that counters proliferation is apoptosis, the deliberate and controlled self-destruction of a cell. There is some evidence that apoptosis rates in the myocardium are highest during fetal growth, suggesting an important role in maturation of the heart (Table 15). I made some measurements of myocardial apoptosis in the near-term fetal sheep heart and found that the rate was very low, about 0.01% (data not shown). Even when apoptosis was strongly stimulated by cocaine or lipopolysaccharide injection, apoptosis rates were only about 0.1%. Thus, apoptosis is not likely to be a major determinant of myocyte number in the near-term fetal sheep heart.

Cardiac Myocyte Hypertrophy During the Last Third of Gestation

Maturational changes in the appearance and composition of sheep cardiac myocytes have been described, with the best descriptions coming from electron microscope (EM) studies (Sheldon *et al.*, 1976; Brook *et al.*, 1983; Smolich *et al.*, 1989). The changes in appearance of dissociated cardiac myocytes that I observed using a light microscope were similar to the descriptions provided by previous studies. Myocytes from the young fetal heart (~90dGA) typically appeared less dense and were often curved, with tapered ends. When stained with methylene blue, some striations were visible but

Table 15. Myocardial apoptosis during perinatal cardiac growth.

Age	% Apoptotic Myocytes	Species	Citation
Embryonic day 11	4%	mouse	Abdelwahid *et al.*, 1999
Embryonic day 16	0.50%	mouse	Abdelwahid *et al.*, 1999
Embryonic day 21	1.99%	rat	Xiao *et al.*, 2001b
Neonatal day 1	0.1/0.02%	rat RV/LV	Kajstura *et al.*, 1995
Neonatal day 11	0.01/0.005%	rat RV/LV	Kajstura *et al.*, 1995

the cytoplasm was generally pale. EM studies have described these myocytes as having few myofibrils, which are located in the subsarcolemmal space (Figure 26). Near-term fetal cardiac myocytes were generally torpedo shaped, with a more even width. These cells appeared denser, and had darker-staining cytoplasms with more regular striations. By the neonatal period, EM studies have found that sheep cardiac myocytes are packed with contractile apparatus (Figure 26). Adult myocytes had very dark-staining cytoplasms that obscured their nuclei. They were densely packed with contractile apparatus and had squared-off ends.

Changes in myocyte size during the last third of gestation were subtle (Figure 11). The width of binucleated myocytes in the LV and RV increased during that period, although little of the variation in myocyte width was due to increased age. Binucleated myocytes did not increase in length during the last third of gestation. The concept that myocytes can regulate cross-sectional growth independently from longitudinal growth is accepted for adult hearts, although the specific mechanisms that control the type of growth are unknown (Russell *et al.*, 2000). This concept is not established in the fetal heart.

If all else were constant, myocyte cross-sectional growth would lead to wall thickening and diminish the size of the chamber. In my observation, myocytes undergoing cytokinesis were always separating end-to-end, never side-to-side. This type of longitudinal growth may contribute to appropriate scaling of the heart as it grows. In order for the three-dimensional structure of the heart to grow appropriately, some reorganization of myocytes within the myocardium must be required.

Cross-sectional, rather than longitudinal, hypertrophy may necessitate the increased maturation of structures such as t-tubules and SR in order to decrease diffusional distances from sarcolemma to

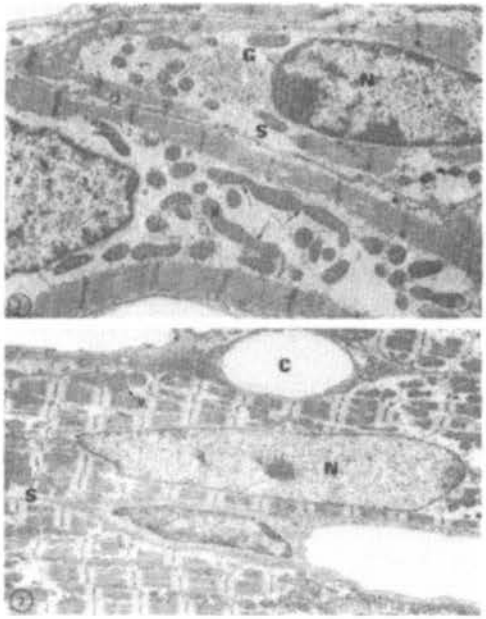

Figure 26. Transmission EM photographs of cardiac myocytes from the 90-day fetal sheep heart (top) and the neonatal sheep heart (bottom). N, nucleus; C, capillary; S, sarcolemma; M, mitochondria; G, Golgi apparatus. (Taken from Sheldon *et al.*, 1976).

contractile protein. Indeed, in the newborn rabbit cardiac myocyte, the greatest change in calcium concentration during excitation-contraction coupling occurs in the sub-sarcolemmal space (Haddock *et al.*, 1999). In immature hearts, abnormally rapid cross-sectional growth of myocytes may outpace the growth of t-tubules and SR, limiting the access of calcium to the center of these cells. For functional contraction, it may be necessary for the myofibrils to be located at the periphery of these myocytes. This may account for the observation that, in the hearts of the pressure-loaded fetal sheep, the sarcomeres were localized next to the plasma membrane (Barbera *et al.*, 2000). If I were to inspect the myocytes of plasma-infused fetuses, or other load models, I may find the same sub-cellular organization.

Cardiac Myocyte Terminal Differentiation During the Last Third of Gestation

DNA synthesis can be induced in adult mouse cardiac myocytes by expression of the proto-oncogene c-myc, but this results in multi-nucleation and polyploidy rather than proliferation (Xiao *et al.*, 2001a). Likewise, binucleated cardiac myocytes in the sheep are thought to represent a population of myocytes that are non-proliferative. I found that binucleated cardiac myocytes were rare in the fetal heart prior to 115dGA, from which point this fraction increased rapidly until birth, thereafter

increasing more slowly. (Figure 13a and b). The percent of myocytes in the myocardium that were binucleated in the neonatal period was about 75-80%. The specific agent responsible for regulation of the rate of binucleation is not understood. The rate at which myocytes become binucleated is not known, because the binucleated fraction is influenced by the rate of myocyte proliferation (Figure 27).

I found that the process of binucleation contributes to heart growth. While myocyte hypertrophy was not substantial over the last third of gestation (Figure 11), the combined average size of mononucleated and binucleated myocytes increased near term (Figure 28). This effect was due to the rapid rate of binucleation following 125dGA, and the change in myocyte size between mononucleated and binucleated cells. As the size of the "average" myocyte increases, the mass of the heart will increase as well.

Maturational Changes of the Cardiac Calcium Transport System

I found that the proteins responsible for calcium fluxes across the sarcolemmal and SR membranes underwent maturational regulation at the level of mRNA and protein expression. At ~95dGA, NCX1 mRNA expression in the heart was about 7-fold higher than the level in the adult (Figure 15a), while steady-state protein expression was about 3.5-fold higher than adult levels (Figure 16a).

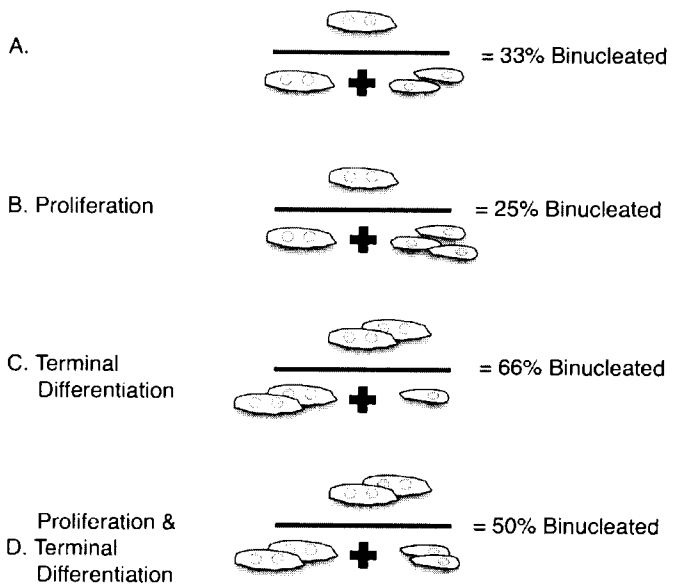

Figure 27. The rates of terminal differentiation and proliferation both influence the fraction of myocytes that are binucleated. In (A), 1 in 3 myocytes are binucleated. If half of the mononucleated myocytes proliferate, as shown in (B), the fraction of myocytes that are binucleated is reduced to 1 in 4. If half of the mononucleated myocytes from (A) terminally differentiate, as shown in (C), the fraction of myocytes that are binucleated is increased to 2 in 3. If half of the mononucleated myocytes from (A) proliferate, and half terminally differentiate, as shown in (D), then 1 in 2 myocytes will be binucleated.

This suggests that there was a change in post-transcriptional regulation of NCX1 between these ages. The mRNA and protein levels of NCX1 in the near-term fetal heart (at an age comparable to the fetuses in the experiments reported here) were lower than in the ~95dGA fetus, and protein levels were higher than in the adult heart.

Expression of SERCA2 mRNA did not change much during the period studied, although there was a transitory peak in the RV of the neonate (Figure 15b). In contrast, levels of SERCA2 protein rose steadily in each period studied (Figure 16b). This suggests that the maturational rise of SERCA2 was due to post-transcriptional regulation. In the rat heart, the rate of transcription of SERCA2 between the fetal and neonatal period is not different, but SERCA2 levels increase because of increased mRNA stability (Ribadeau-Dumas *et al.*, 1999). This increased stability may be due to regulation of mRNA degradation by the 3' untranslated region of the molecule (Misquitta *et al.*, 2002). These mechanisms may be at work in sheep hearts; however, the changed protein levels during maturation

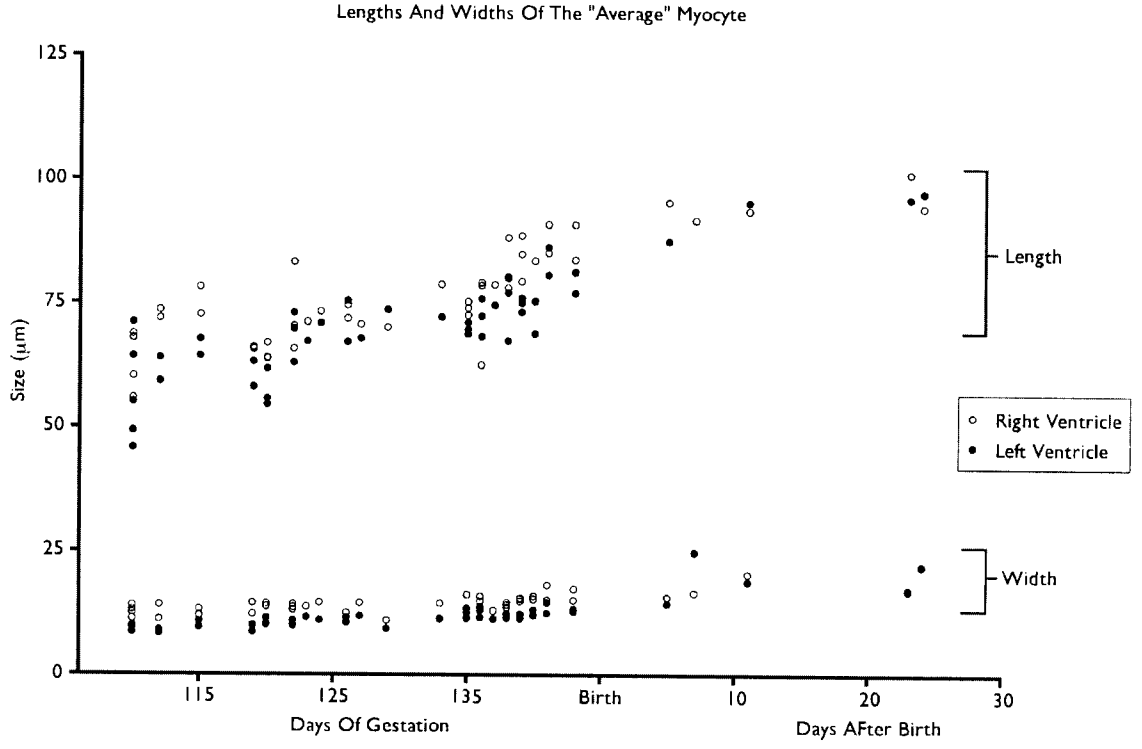

Figure 28. The mean size of myocytes (mononucleated and binucleated together) in the heart. Length and width increased significantly ($p<0.0001$) in the LV (length $r^2=0.63$, width $r^2=0.67$) and the RV (length $r^2=0.56$, width $r^2=0.61$).

in this species did not seem to be due to changed mRNA levels. Altered protein production per mRNA or protein stability are possible points of regulation that may explain the increased protein expression that occurred without altered mRNA levels.

Did sustained arterial and venous hypertension increase fetal cardiac mass by inducing myocyte hypertrophy? Did the heart undergo early terminal differentiation?

Our laboratory has shown that either increased arterial or venous load can stimulate cardiac growth (Barbera *et al.*, 2000; Appendix A), and both were elevated in plasma-infused fetuses. The hearts of plasma-infused fetuses grew 30% larger than controls so that the heart-to-body weight ratio was well above the ratio that is normal during any part of the perinatal period. The rate of increase in cardiac mass was different between the 4- and 8-day infusion groups. If the 4-day group is representative of the 8-day group at 4 days, then I can conclude that experimental hearts grew 10% per day for the first 4 days, but only 4% per day for the second 4 days (assuming the controls grew 3% per day, see Appendix B).

After 8 days of plasma infusion, mean arterial pressure in fetuses was increased by about 50% from baseline, while central venous pressure was increased by about 75%. Pressure changes in this model occur gradually (Giraud *et al.*, 2005), although they tended to plateau during the second half of the loading period because the infusion rates were adjusted conservatively. Increased vascular pressures would have increased ventricular wall stress in these fetuses; both diastolic and systolic wall stress mediate cardiac growth. It is possible that the growth of the fetal hearts in the first 4 days of the infusion period largely normalized the ventricular wall stress, as estimated by the law of Laplace, by reducing the ratio of the ventricular radius to the wall thickness. If this occurred, the stimulus for cardiac growth would have been reduced during the second four days of load. Unfortunately, I do not have the measurements necessary to determine if this occurred.

The pericardium has been found to be a limiting factor in exercise-induced cardiac hypertrophy (Hammond *et al.*, 1992). The increased hypertrophy associated with removal of pericardial con-

straint may be due to elevated wall stress, resulting from increased diastolic filling. Similarly, in adult humans with congenital absence of the pericardium, or following surgical removal of the pericardium, the chamber of the RV enlarges as seen in volume overload (Payvandi & Kerber, 1976). In the fetal sheep, the pericardium limits filling (Morton & Thornburg, 1987; Grant *et al.*, 2001). Although the pericardium does not constrain the heart during normal fetal growth (Morton & Thornburg, 1987), the very rapid growth of the hearts in plasma-infused fetuses may have outpaced the growth of the pericardium. This would have limited diastolic wall stress, and is an alternate explanation for the slow rate of growth that occurred during the second 4 days of load.

Venous pressure is probably responsible for some unknown component of the myocardial hypertrophy in recipient twins of TTTS, as well as fetuses receiving plasma. Agenesis of the ductus venosus in the human fetus suggests a role for venous pressure in fetal cardiac growth. The ductus venosus typically provides resistance between the uterine vein and the inferior vena cava; in the sheep fetus there is a ~1.9mmHg pressure drop across the ductus venosus (Schroder *et al.*, 2003). When it is absent, the "high pressure" umbilical vein drains directly into the internal iliac vein, the inferior vena cava, or the right atrium (Jaeggi *et al.*, 2002). This abnormal preload results in cardiomegaly and chamber dilatation (although it should be noted that some animals, such as the guinea pig, do not have a ductus venosus).

Why did arterial and venous pressure increase in the plasma-infused fetus?

Plasma for chronic infusions was extracted from blood obtained from exsanguinated ewes. The composition and contents of the plasma is somewhat different between adult and fetal sheep, and factors released into the blood during hemorrhage could have had an effect on fetal pressures. The delayed and gradual onset of increased pressure that occurred with infusion makes this unlikely. Furthermore, agents that regulate blood pressure typically have a short lifespan in the circulation, as suited for their dynamic regulation; however, pressures were maintained at high levels for days following cessation of infusion (data not shown). In order to test if the hypertensive effect of plasma

infusion was due to a vasoactive compound in plasma from adult sheep, one fetus received a chronic infusion of fetal plasma. The fetus receiving the infusion of fetal plasma responded the same as other plasma-infused fetuses with regards to its blood pressures and cardiac growth. Although the protein composition of fetal blood was certainly altered by our infusion protocol, it is unlikely that the observed increased fetal pressures were due to the actions of an infused vasoactive compound.

Another possible explanation for the observed hypertension is that plasma-infusion may have increased the blood volume of the fetuses. The balance of water movement between the fetus and the mother is regulated by the hydrostatic and oncotic pressure gradients in the placenta. Large volumes of isotonic saline can be rapidly infused into fetuses and produce only small, transient changes in mean arterial pressure, because the fetus can quickly lose that excess to the maternal circulation (Brace & Moore, 1991). However, infusion of plasma may have increased the oncotic pressure of fetal blood because plasma protein has a high reflection coefficient and is not freely diffusible across the exchange barrier in the placenta. This may have resulted in a small increase in fetal blood volume.

Support for this volume-load hypothesis may be found in the origins of TTTS. An unbalanced sharing of blood between identical twin fetuses results in the development of hypertension in the recipient. These fetuses also develop hyperproteinemia (Weiner & Ludomirski, 1994), as produced in plasma-infused fetal sheep. Increases in intravascular colloids eventually lead to increased interstitial colloids and tissue fluid accumulation. Some plasma-infused fetal sheep were hydropic; hydrops is also a commonly reported feature of the recipient fetuses in TTTS. Clinical studies that follow the outcomes of treatment of TTTS may provide some evidence as to the actual recovery time.

Would correction of intrauterine transfusion result in resolution of symptoms in recipient twins? A study by Dr. Bajoria, who has published extensively on TTTS, followed the outcome of monochorionic twin pregnancies after an intrauterine fetal death (Bajoria *et al.*, 1999b). Intrauterine death of the donor twin (which stops transfusion to the recipient) was associated with spontaneous resolution of polyhydramnios and hydrops in only 6 of 10 recipient fetuses (median age of death 25 weeks, median age at deliver 29.3 weeks). The current treatment of choice for TTTS is laser coagulation

therapy, which stops the inter-twin transfusion *in utero*. One study followed fetuses for 5 days following laser coagulation therapy and found that the pulsatility index of the ductus venosus did not begin to improve until the fifth day following treatment (Gratacos *et al.*, 2002). Even then, the values were well above normal (Tchirikov *et al.*, 1998). These data suggest that resolution of symptoms in recipient twins does not occur immediately following cessation of transfusion. This prolonged period of recovery may be related to the time needed for the fetus to metabolize its excess protein.

The plasma-infusion model in near term fetuses is relevant to understanding the physiology of fetofetal transfusion, although most cases of TTTS are described as occurring in mid second trimester. Acute late-gestation TTTS has been described several times (Shih *et al.*, 1996; Nikkels *et al.*, 2001). However, there are aspects in which the plasma-infused fetus does not resemble the TTTS recipient twin. For example, recipient twins are known to be polycythemic, which is not found in plasma-infused fetal sheep.

Cardiac Myocyte Proliferation in Plasma-Infused Fetuses

Cardiac myocyte cell cycle activity was doubled after both 4 and 8 days of plasma infusion-induced load, compared to control levels (Figure 17). Increased myocyte proliferation is also seen in the hearts of fetal lambs with an arteriovenous fistula (Appendix A), pulmonary artery banding (Barbera *et al.*, 2000) and IGF-I infusion (Sundgren *et al.*, 2003a). In all of these experimental conditions the mass of the heart increased and a measure of myocyte proliferation increased. It seems that the fetal heart responds readily to growth stimuli with proliferation.

The specific stimulus for proliferation is unknown in plasma-infused fetuses. Intracellular signaling pathways could have been activated via mechanotransduction mechanisms, as both arterial and venous pressures were increased in these fetuses. Hypoxemia could have been a stimulus for myocyte proliferation in these fetuses as well. Hypoxemia induces cardiac proliferation in fetal rats (Pietschmann & Bartels, 1985; Clubb *et al.*, 1986). However, this proliferation may not result in increased numbers of myocytes in the heart if terminal differentiation occurs early. Li *et al.* showed

that fetal rats made hypoxic during the second half of gestation had larger myocytes, despite a normal heart and body size (Li *et al.*, 2004). This suggests that the hearts of these rats had fewer myocytes.

Low myocardial oxygen tensions cause accumulation of HIF-1α, which induces expression of VEGF. Cyclic stretch also induces production and release of VEGF from cardiac myocytes (Seko *et al.*, 1999), and both myocyte stretch and VEGF activate the ERK1/2 signaling pathway via focal adhesion kinase (Takahashi *et al.*, 1999; Domingos *et al.*, 2002). Activation by phosphorylation of ERK1/2 is necessary for both proliferative and hypertrophic growth of fetal sheep cardiac myocytes in culture (Sundgren *et al.*, 2003a; Sundgren *et al.*, 2003b). ERK1/2 phosphorylation is elevated after 8 days of plasma infusion in fetal sheep (Figure 19). Thus, hypoxemia and increased vascular pressures may have worked together via the MAPK pathway to stimulate cardiac proliferation in the plasma-loaded fetuses.

A high rate of cardiac myocyte proliferation may be detrimental to cardiac function. It has been shown in mice and newts that each time a myocyte undergoes cytokinesis, the sarcomeres are disassembled (Kaneko *et al.*, 1984; Ahuja *et al.*, 2004). Although the relative contribution of each cardiac myocyte to the contraction of the heart is miniscule, a high rate of proliferation in the myocardium may limit the capacity of the ventricle to eject blood. I found that, in normal fetal hearts only, 1-3% of all cardiac myocytes were in the cell cycle, but after 4 days of plasma infusion, 5-8% of all myocytes were in the cell cycle. This may have affected the mechanics of the cardiac pump. After 8 days of infusion, despite the high levels of cell cycle activity amongst mononucleated cardiac myocytes, the cell cycle activity amongst all myocytes had decreased to 1-2%, due to changes in the fraction of binucleated myocytes.

Doubling the rate of cardiac myocyte proliferation in the final days of prenatal life almost certainly results in increased myocyte numbers in the heart at birth. For example, banding the pulmonary artery of the fetal sheep increased the number of myocytes in the fetal myocardium (Barbera *et al.*, 2000). Nevertheless, increased terminal differentiation occurred prematurely in the plasma-infused

fetuses, which may ultimately limit the number of myocytes in the post-mitotic heart.

Cardiac Myocyte Hypertrophy in Plasma-Infused Fetuses

The hypertrophic response of cardiac myocytes to arterial and venous hypertension caused by plasma infusion occurred in two phases. The initial (4-day) response of the binucleated myocytes was an increase in length. The increased length was maintained in the 8-day group, even as more mononucleated cells became binucleated. Binucleated myocytes were wider than controls only in the 8 day group. Why did longitudinal growth occur early in plasma infusion-induced load, whereas cross-sectional growth was delayed?

The plasma infusion model is different from other fetal sheep models in several ways, including the development of venous hypertension (Table 7). In fact, of all the interventions used in this laboratory, plasma infusion is the only one to increase central venous pressure. Is it possible that the high venous pressure was the cause of the increased myocyte width? This is not in keeping with what is known about myocardial responses to hemodynamic load in the mature heart (Grossman *et al.*, 1975). If the ventricles of the plasma-infused fetuses underwent eccentric hypertrophy during the first 4 days, it is possible that systolic wall stress was increased, which may have stimulated myocyte widening. However, arterial pressure was increased during the first 4 days of load, but the myocytes in this group were not wider then normal. Furthermore, pulmonary arterial pressure was elevated in fetuses with a pulmonary artery occluder, but the myocytes from the hearts of these fetuses also were not wider than controls (Barbera *et al.*, 2000). It is not clear what stimulus lead to increased myocyte widths after 8 days of plasma infusion load.

Cardiac Myocyte Terminal Differentiation in Plasma-Infused Fetuses

Some studies have suggested that there is an intrinsic counter or timer process in cardiac myocytes that determines when they permanently withdraw from proliferative growth (Machida *et al.*, 1997; Burton *et al.*, 1999). The internal counter hypothesis may be supported by my findings in plasma-

infusion hearts. After 4 experimental days, the cell cycle activity was increased, but binucleation was not. By 8 days, binucleation had increased by ~50% (Figure 17). An increase in proliferation early in the load period may have resulted in many cells reaching their maximum number of divisions and becoming binucleated.

One extracellular factor that has been found to modulate terminal differentiation is thyroid hormone (Burton *et al.*, 1999). Physiologically relevant increases in circulating cortisol in the fetus cause thyroid hormone levels to rise (Thomas *et al.*, 1978; Sensky *et al.*, 1994). The period during which cardiac myocyte become binucleated corresponds approximately to pre-partum rise in cortisol and thyroid hormone, although binucleation may begin prior to the rise in cortisol. Furthermore, fetal hypoxemia can increase cortisol levels, or accelerate maturation of the hypothalamic-pituitary axis (Gardner *et al.*, 2004; Roelfsema *et al.*, 2005). Cortisol is linked with other perinatal changes, such as lung maturation (Flecknoe *et al.*, 2004) and a slow-down in over-all somatic growth (Fowden *et al.*, 1996). If thyroid hormone acts in the fetal sheep as it does in the rat to "seal" terminal differentiation, a cortisol-induced rise in thyroid hormone via cortisol may explain the increased binucleation I found in hearts of plasma-infused fetuses. I have not yet determined if cortisol levels were increased in plasma-infused fetuses relative to control fetuses.

Fetal arterial pressure increases continuously throughout gestation, and it is not likely that the normal gradual increase in arterial pressure is the trigger that stimulates binucleation in the normally-developing late-term fetus. However, increased binucleation is a common response to hemodynamic overload in our studies, including volume overload (Appendix A) and pressure overload (Barbera *et al.*, 2000). Excessive mechanical stretch or stress on late-gestation fetal cardiac myocytes may not directly stimulate binucleation in these models. Binucleation was not increased after 4 days of plasma infusion-induced hypertension. However, increased proliferation in all of these models may have resulted in myocytes reaching the end of their (hypothetical) proliferation counter, and then terminally differentiating and becoming binucleated.

As during normal cardiac growth, in fetal hearts subjected to increased hemodynamic load, terminal

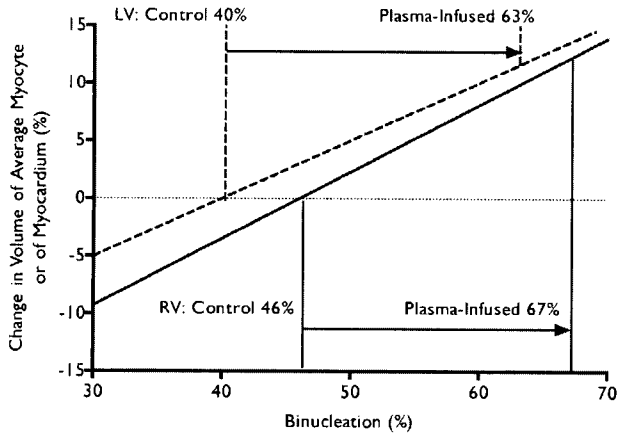

Figure 29. Average myocyte volume based on myocyte sizes of control hearts. The average myocyte volume can be increased in this model by increasing the rate of binucleation from the levels found in normal fetuses to the levels found after 8 days of plasma infusion. The mean myocyte sizes were calculated from the controls of the 8-day plasma infusion group using a cylindrical myocyte model.

differentiation contributed to increased cardiac mass simply because binucleated myocytes are larger than mononucleated myocytes. I used the lengths and widths of the mononucleated and binucleated myocytes from control hearts to calculate the volume of the "average" myocyte as a function of percent binucleation (see Appendix B). I assumed for this mathematical model that the number of myocytes and sizes of mononucleated and binucleated myocytes heart were constant. If all the (smaller) mononucleated myocytes were changed to (larger) binucleated myocytes, the average myocyte volume would increase. This change in the volume of the "average" myocyte would result in a proportional change in myocardial volume. Thus, the mass of the heart could change substantially at 138 days simply by the increase in binucleation seen after 8 days of plasma infusion (Figure 29).

Chronic plasma infusion in fetal sheep caused substantial cardiac hypertrophy, as hypothesized. Cardiac growth occurred by both myocyte enlargement and, unexpectedly, proliferation (Figure 30). The binucleated myocytes were elongated after 4 days of hemodynamic loading, but they only

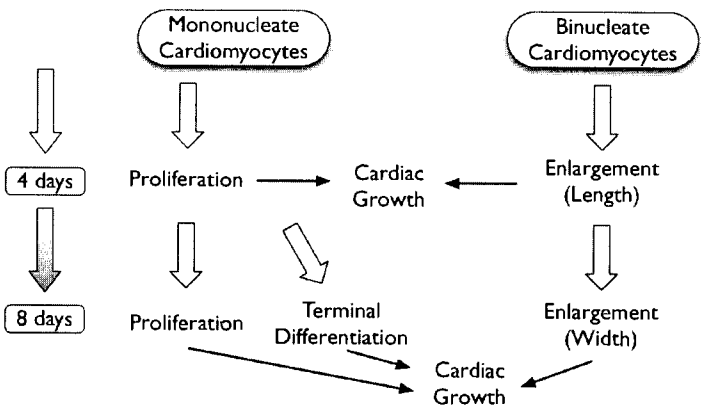

Figure 30. Growth responses of fetal cardiac myocytes to plasma-infusion. Proliferative growth occurred during both the first and second experimental periods. Accelerated myocyte elongation occurred only during the first 4 days of plasma infusion. Myocyte cross-sectional growth and increased terminal differentiation occurred only during the second 4 days of plasma infusion.

increased in width in the 8-day group. Terminal differentiation of the myocytes was also only seen in the 8-day infusion group.

Did combined arterial and venous hypertension lead to the down-regulation of SERCA2, RyR and calsequestrin and the up-regulation of NCX1 and LTCC?

I demonstrated that the myocytes of the fetal sheep heart are capable of remodeling substantially over a 4 or 8-day period in response to plasma infusion. Increased cell cycle activity, binucleation and hypertrophy of these hearts all indicate that intracellular signaling pathways were activated, genes were transcribed, and proteins were translated in response to the hemodynamic load. Nevertheless, the expression of the genes that regulate the calcium of excitation-contraction coupling were remarkably stable under these circumstances. It is notable that the calcium transport system of the fetal heart is well protected or insensitive to increased hemodynamic load.

The only changes that occurred in the expression levels of the genes studied were found in the RV. Due to the geometry of the ventricles, the wall stress of the fetal RV is greater than the LV. This may mean that the RV is more sensitive to the effects of sustained arterial and venous hypertension due it its geometry.

No changes in SERCA2 or NCX1 protein levels were found with AngII, ANP, cortisol or phenylephrine treatments in cultured cardiac myocytes, supporting the conclusion that fetal cardiac myocytes are relatively resistant to alteration of expression levels of these genes. These compounds have been shown to be associated with changes in expression of the cardiac calcium transport proteins in other species. In cultured adult rat cardiac myocytes, 24 hours of 10μM phenylephrine induced a two-fold increase in NCX1 protein (Reinecke *et al.*, 1997). AngII decreases expression of SERCA2 and NCX1 in rat cardiac myocyte cultures (Ju *et al.*, 1996; Hashida *et al.*, 1999). Cortisol has been shown to regulate NCX1 in immortalized rat aortic myocytes (Smith & Smith, 1994), although its effect on cardiac muscle has not been investigated. More detailed experiments of protein expression in cultured fetal sheep cardiac myocytes may help determine how the calcium transport system is

regulated in immature sheep hearts.

Cardiac mRNA expression levels of NCX1, PLN, and the α1c subunit of LTCC were all found to decrease in the RV of the plasma-infused fetuses. The decrease in NCX1 was also found in protein levels, although PLN protein levels were not found to decrease. Protein levels of LTCC were not studied. Taken together, these changes suggest an increased reliance on intracellular calcium. The direction of the change in NCX1 was contrary to that predicted by my hypothesis, although of greater surprise was the modesty of the changes in the face of such substantial cardiac growth.

Did increased fetal arterial pressure lead to down-regulation of SERCA2 and up-regulation of NCX1?

Postductal aortic occluders were placed in fetal sheep in order to impose an arterial pressure load on both ventricles of the growing heart. Arterial pressure proximal to the occluder was increased ~24% in fetuses (Table 10), but cardiac mass did not increase (Table 11). Steady state mRNA expression of

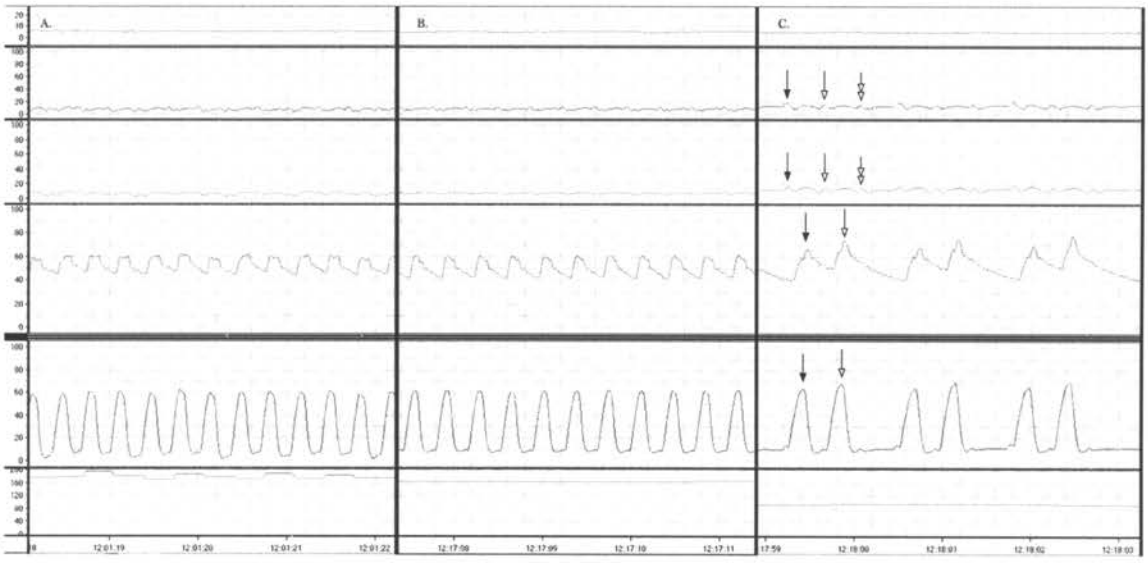

Figure 31. Fetal pressures while inflating the postductal occluder. The top strip is the reference amniotic pressure, the second is the right atrial pressure, the third is the left atrial pressure, the fourth is arterial pressure proximal to the occluder, the fifth is the left ventricular pressure (all pressures are mmHg), and the sixth strip is the heart rate (bpm). Three periods are shown: A) baseline, prior to inflation of the occluder, B) the occluder is partially inflated (to 80% of C), and C) the occluder is more fully inflated. Filled arrow points to a normal atrial contraction that is followed by a ventricular contraction. Open arrow points to a premature atrial contraction that is followed by a ventricular contraction. Double-headed open arrow points to a premature atrial contraction that is not followed by a ventricular contraction.

NCX1 and SERCA2 also failed to change in the hearts of fetuses subjected to 10 days of biventricular pressure load.

Why did the fetal heart not hypertrophy in response to this load? The answer is not known. The compliance of the abdominal aorta modifies the impedance to ventricular output, and application of an occluder can greatly increase impedance (Ioannou *et al.*, 2003). Several fetuses died suddenly as the occluder load was being applied, and it is possible that the myocardium failed under the stress of the load. Under these conditions the normal adaptive responses to load may not be available to the fetal heart. It is possible that the rapid biventricular loading is particularly difficult for the fetal heart to adapt to, and so death is likely to result before ventricular remodeling. If the load had been greater in magnitude, or of longer duration, cardiac hypertrophy may have resulted.

The magnitude of the load was adjusted to avoid killing the fetus. When the occluder was inflated with a high pressure the fetal heart rate dropped substantially (80bpm was not uncommon) and abnormal rhythms emerged (Figure 31). It was my goal to inflate the occluder close to, but below, the pressure at which this occurred. Periodic asystolic events were common in the experimental fetuses. The responses of other fetal organs to the inflation of the aortic occluder is not known. It is likely, however, that occlusion altered the flow of blood to organs distal to the occluder.

It is possible to produce cardiac hypertrophy with a postductal aortic outflow obstruction. Dr. Burrington published a report in 1978 describing the cardiac growth responses to a variety of outflow obstruction models, including postductal aortic banding. Unfortunately his descriptions of the ensuing cardiac hypertrophy are not quantitative and comparison between the models is difficult. I interpret his descriptions to mean that obstruction of the pulmonary artery and preductal aorta produced moderate hypertrophy of the relevant ventricle, while obstruction of the ductus arteriosis and postductal aorta produced mild biventricular hypertrophy. In any case, some amount of hypertrophy was produced by a severe postductal obstruction that was left in place for ~60 days.

The changes in NCX1 and SERCA2 mRNA levels I hypothesized did not occur in response to

increased arterial pressure load. This lack of response is difficult to interpret in light of the lack of a cardiac growth response.

Did increased fetal volume load lead to down-regulation of SERCA2 and up-regulation of NCX1?

Although the total cardiac mass was not increased in fetuses with a surgical carotid to jugular anastamosis, the mass of the RV was increased (Appendix A). This growth was due to increased length of binucleated myocytes, as well as increased cell cycle activity of mononucleated myocytes. The specific stimulus that caused accelerated growth was unclear from the physiological measurements. The amount of blood traveling through the shunt is not productive in terms of tissue perfusion needs, and thus cardiac output ought to increase to provide for tissue perfusion. Venous pressure was not elevated in these fetuses, but perhaps the ventricle is sensitive to changes in venous pressure that cannot be measured by the fluid-filled catheter system used in this laboratory. It is also possible that the kinetic energy of increased venous return had some part in the cardiac growth response. The blood flowing to the heart from the inferior vena cava has a measurable and important kinetic energy component (Anderson *et al.*, 1985), but I did not deliberately measure it with the venous catheters.

Despite the growth of the heart in response to volume overload, neither NCX1 nor SERCA2 mRNA expression was changed in the ventricles these fetuses.

Was increased cardiac growth in fetuses with sustained anemia due in part to cardiac myocyte proliferation and enlargement, and did the hearts of these fetuses undergo early terminal differentiation?

Dr. Davis and his colleagues at OHSU have found that chronic anemia in fetal sheep increases cardiac output by ~50%, and stroke volume by ~30% (Davis & Hohimer, 1991). In my study, cardiac mass increased in the chronically anemic fetal sheep by 40% compared to control fetuses (Table 13). Stroke volume can be increased in the adult heart by changing preload, afterload, contractility, or by growth of the ventricular chamber. Kilby *et al.* concluded that the increase in LV stroke volume

in the anemic sheep fetus is primarily due to decreased afterload, not increased contractility (Kilby *et al.*, 1998). I too found a slight decrease in arterial pressure. However, I also know that chronic anemia caused cardiac remodeling and growth because of the increased cardiac mass observed by myself, and by others.

Although cardiac output, and thus venous return, increased dramatically in chronically anemic fetuses, venous pressure did not increase in my experience (Table 12), or that of Dr. Davis (Davis & Hohimer, 1991; Davis *et al.*, 1996; Davis *et al.*, 1999). However, the fetal ventricle may be sensitive to changes in venous pressure smaller than our system measures (see discussion of the volume-loaded fetuses). Hypoxemia is another possible stimulus of cardiac growth during sustained fetal anemia. HIF-1α and VEGF are upregulated in fetal lambs after chronic anemia (Martin *et al.*, 1998). These factors are proposed to be responsible for the vascular remodeling that is observed in the hearts of chronically anemic fetuses, and are good candidates for modulation of fetal cardiac myocyte growth. Other models of fetal hypoxemia also cause an increase in heart growth relative to body growth (Pietschmann & Bartels, 1985; Clubb *et al.*, 1986; Bae *et al.*, 2003).

We hypothesized that both myocyte hypertrophy and proliferation would occur in the hearts of chronically anemic fetuses. The hearts of anemic fetuses were larger than the hearts of control fetuses, but the myocytes of the anemic fetuses were not larger than those of control fetuses. The fraction of myocytes that were binucleated was also unchanged between the anemic and control fetuses. Although not statistically different, there was a trend for the rate of cell cycle activity to be greater in the hearts of anemic fetuses compared to control fetuses (Table 14).

The greater heart weight of the anemic fetuses was not due to increased water content, as measured by wet-to-dry weight ratio of the LV. It is possible that the hearts grew by myocyte proliferation early in the period of anemia. After 4 days of phlebotomy, the oxygen content of the anemic fetuses was down to 3.5 ±1.3g/100ml (from a normal value of about 8g/100ml). It is possible that this early and rapid decline in the carrying capacity of the blood stimulated cardiac growth early in the experimental period, as was seen in the plasma-infused fetuses.

Some part of the substantial increase in cardiac mass observed in anemic fetuses may have been due to growth of the non-myocyte fraction of the heart. By determining the fraction of the myocardium that is composed of myocyte and non-myocyte fraction, analysis of fixed sections could have been used to address this question. The non-myocyte component of the fetal heart can be changed by hemodynamic load (Barbera *et al.*, 2000). The work of Dr. Davis and his colleagues showed that capillary density is increased in hearts of the anemic fetus (Martin *et al.*, 1998).

Chronic anemia stimulated robust myocardial hypertrophy in fetal sheep, but cardiac hypertrophy is not reported in donor twins with TTTS (Karatza *et al.*, 2002; Raboisson *et al.*, 2004). This may be because the chronic low-volume loss of blood experienced by donor fetuses does not often result in profound anemia (Denbow *et al.*, 1998), probably as a result of increased red cell production due to increased EPO (Bajoria *et al.*, 2001b). The hemodynamics of the donor twin are not well described; most studies have focused on the recipient twin because of their extreme cardiac phenotype. The composition of the myocardium may well be different in these fetuses because growth factors and hemodynamic cues for growth are altered.

I hypothesized that the increased cardiac mass of anemic fetuses was due to hypertrophy and proliferation of the cardiac myocytes. I did not find evidence that either of these had occurred, although I cannot rule out the possibility that proliferation occurred early in the anemic period. Early proliferative growth and an increase in the non-myocyte fraction of the myocardium are possible explanations for the observed increase in cardiac mass.

Why wasn't the cardiac calcium transport system affected by increased fetal hemodynamic load?

It was a surprise to me that the expression levels of calcium transport genes were so little altered by increased fetal hemodynamic load. I hypothesized that the levels of these genes would be regulated as they are in the failing adult heart, toward a more immature pattern. It is difficult to explain why there was only a small change in one gene of those studied. I address five possibilities that may explain this finding: 1) fetuses may be refractory to regulation of the calcium transport system, 2) the

length of the load may have been inadequate, 3) I may not have had the statistical power to detect differences, 4) the intensity of the load may have been inadequate, and 5) sheep may be refractory to regulation of the calcium transport system.

1) An explanation for the modest regulation of the cardiac calcium transport system during increased hemodynamic load in the fetus may be that these genes are uniquely protected from modulation by hemodynamic load in the fetus. Aortic banding-induced hypertrophy of the growing lamb was not associated with cardiac dysfunction, whereas hypertrophy was associated with depressed function in adult sheep (Aoyagi *et al.*, 1992). The functional deficits were the result of decreased SERCA2 and NCX1 expression in the heart, and reduced SR calcium uptake, which occurred only in the adult heart (Aoyagi *et al.*, 2001). These studies indicated that the immature heart is resistant to regulation of the calcium transport genes by hemodynamic load. There are studies with the opposite conclusion, however: that the immature myocardium has an increased sensitivity to regulation of calcium transport genes. Cardiac volume load in infants less than one year of age causes reduced right atrial expression of SERCA2 and PLN mRNA and protein, while this effect was not seen in older pediatric patients (Pavlovic *et al.*, 2005). Similarly, an AT1-dependent down-regulation in SERCA2, NCX1 and RyR mRNA was found in neonatal rat cardiac myocytes, but not adult myocytes (Ju *et al.*, 1996). It is reasonable that there is a difference in how the mature and immature cardiac myocytes regulate the proteins that control intracellular calcium levels. A mechanism for this difference remains to be found.

2) The length of the hemodynamic load may be a critical issue in all three fetal models where I measured expression of the calcium transport system. How could the length of the loading period interact with the expression levels that I measured? Two ways come to mind: 1) the time between the stimulus and the measurement could be too short for a new level of regulation to alter expression levels enough to make a measurable difference, or 2) the ongoing response of the heart to chronic load could have failed to reach some critical point where this system would be affected.

I know that this length of time is adequate for changes in mRNA or protein synthesis/degradation

to alter levels enough to measure differences in tissue levels. Indeed, the loading period was long enough to measure large differences in myocyte growth between the plasma-loaded fetuses and controls. More to the point, however, in other *in vivo* models of increased hemodynamic load in mature animals, changes in the expression of calcium transport genes have been observed within a similar short period (Matsui *et al.*, 1995; Arai *et al.*, 1996). I conclude, therefore, that the stimulation of heart by hemodyamic loading conditions and all associated hormonal changes at the time that the fetuses was killed was not an adequate stimulus to alter levels of these genes.

A question of great interest is whether increased hyperplastic growth, hypertrophic growth and early terminal differentiation are maladaptive. The adaptive (or maladaptive) response of the heart to hemodynamic load is complex. An initial period of adaptive growth and functional modification may be followed by a series of changes that are interpreted as pathophysiological because they hinder the capacity of the heart to perform its vital function. The poor cardiac function observed in some recipient twins of TTTS may be due in part to dysregulation of the cardiac calcium transport system, due to progressive loading through gestation. It may be, therefore, that a longer experimental period was necessary for the fetal hearts to transition from an adaptive to a maladaptive phenotype.

3) Often, many data points are needed to detect small changes in biological systems. It is possible that hemodynamic loading mildly affected the expression of the cardiac calcium transport system, but my groups weren't large enough to detect the differences. The advantages of using fetal sheep as a model are several-fold: as a large mammal they are analogous to humans; sheep do not abort easily, making it possible to perform surgery the fetus while maintaining the pregnancy; and the fetuses are large enough to implant catheters and make long-term *in utero* physiological measurements. A disadvantage of sheep is that they are expensive, and so group sizes must be limited. Consequently, investigators that use the fetal sheep model attempt to maximize the effect of their intervention.

4) As I mentioned earlier, large increases in arterial pressure resulted in fetal death. Similarly, as the plasma infusion progressed, and the fetuses became very hypertensive, they tended to become hypoxic and we were forced to turn the infusion rates down. When a large arteriovenous anastomosis

is created in the fetal chest (not the same protocol for the A-V anastamosis described in Appendix A), allowing a greater flow across the shunt, the fetuses tend to die soon after the shunt was created (Dr. Thornburg's observation). The increased hemodynamic load in all experimental preparations described here was titrated so that a majority of fetuses lived for the full study period. It may be that the level at which the stimulus that regulates expression of the calcium transport system in hemodynamic load was too high relative to the mortality due to the load itself. If this were the case, it may be difficult or impossible to load the fetus enough to produce a change in the expression of the cardiac calcium transport system.

5) A final possibility is that sheep hearts do not respond to increased cardiac load by the regulation of the cardiac calcium system. This can quickly be dismissed- NCX1 was regulated in the RV of the plasma-infused fetuses. Furthermore, in the adult sheep heart, the experimental production of a myocardial infarction produces long-term changes in myocyte calcium transport (Kim *et al.*, 2002). Also in the adult sheep, pressure-overload hypertrophy induced by aortic banding alters regulation of the calcium transport system (Aoyagi *et al.*, 2001). In fetal sheep, SERCA2 levels are diminished after about 30 days of mild pressure load induced by partial occlusion of the preductal transverse aorta (Samson *et al.*, 2000). It is clear that the system for the regulation of the cardiac calcium transport system is intact in sheep.

Summary and Conclusions

The purpose of the heart is to constantly move the blood forward through the vascular system to meet tissue demand for oxygen and other nutrients. Neither the fetus nor the adult can live for any length of time without the proper function of the heart. Appropriate regulation of growth and control of intracellular calcium are both critical to the fetal heart for immediate and future health.

The growth of the normal fetal sheep heart during the last third of gestation is proportional to the growth of the body, even as the variation in fetal weight increases near term. I have shown that dur-

ing the last third of gestation, the fetal sheep heart grows primarily by proliferation of cardiac myocytes although the proportion of proliferative cells decreases rapidly after about 115dGA. Cardiac myocyte enlargement *in utero* is small and, surprisingly, occurs primarily by cross-sectional growth. Myocytes also become larger when they terminally differentiate, enlarging in both in length and in cross-sectional dimensions. Myocyte hypertrophy occurs more rapidly after birth.

I have shown, as others have, that if the hemodynamic load on the fetal heart is increased, it grows such that the relationship between the size of the heart and the size of the body is no longer normal. I investigated how different types of hemodynamic load modify the modes of fetal cardiac myocyte growth. I have shown that plasma infusion caused arterial and venous hypertension and stimulated a doubling of the cell cycle activity of the cardiac myocytes. This proliferative response was maintained even as the proportion of myocytes able to proliferate declined. Myocytes initially responded to this increased hemodynamic load by longitudinal growth, a mode of growth that does not ordinarily occur in fetal myocytes. Myocyte lengthening was followed by cross-sectional growth. Early and late growth responses to increased hemodynamic load are a new finding in the fetal sheep heart. It was surprising to find that fetal hypertension caused similar myocyte growth in the LV and RV.

I have shown that sustained anemia in the near-term fetus increased the mass of the heart to a similar degree as plasma infusion. However, the cardiac myocytes from the anemic fetuses were not larger, nor did the heart contain a greater fraction of binucleated myocytes. Cardiac cell cycle activity at the conclusion of the experimental period was not greater than in control fetuses. It is possible the increased cardiac mass of the anemic fetus is due to transiently increased proliferative growth early in the anemic period. Another possibility is that the non-myocyte fraction of the heart expanded, although not due to tissue edema.

Growth of the heart in the perinatal period is accompanied by maturation of myocyte organelles and the calcium transport system. I have shown, as have others, that the fetus has a much lower ratio of SERCA2 to NCX1 than has the adult. However, neither isolated arterial pressure load nor isolated volume load affected the expression of cardiac NCX1 or SERCA2 mRNA. Combined arterial and

Table 16. A comparison of the fetal sheep models presented in this dissertation.

	Heart/ Body Weight	Arterial Load	Venous Load	Arterial Oxygen	Binucleated Myocytes		Mononucleated Myocytes		Percent Binucleation	Cell Cycle Activity Amongst Mononucleated Myocytes	Ratio: SERCA/ NCX
					Length	Width	Length	Width			
Advancing Age (last third of gestation)	↔				↔	↑	↔	↑	↑	↔	↑
Advancing Age (pre- to post-natal)	↔				↑	↑	↑	↑	↑	↓	↑
Plasma Infusion (4 days)	↑	↑	↑	↓	↑	↔	↑	↔	↔	↑	↔
Plasma Infusion (8 days)	↑	↑	↑	↓	↑	↑	↑	↑	↑	↑	↔
Anemia (9 days)	↑	↓	↔	↓	↔	↔	↔	↔	↔	↔	
Biventricular Aortic Occluder (10 days)	↔	↑		↔							↔
Arterio-venous Fistula (7 days)	↔	↔	↑	↔	↑	↔	↔	↔	↑	↑	↔

venous hypertension, which substantially increased the size of the fetal heart, caused a small decrease in RV NCX1, PLN and LTCC α1c expression. It was surprising to find that increased hemodynamic loads were ineffectual as stimuli to alter cardiac calcium transport system expression levels.

In summary, I have shown that the growth of the fetal sheep heart was modified by increased hemodynamic load (Table 16). Arterial and venous hypertension caused cardiac hypertrophy and induced myocyte enlargement and proliferation, as well as increased terminal differentiation. Fetal anemia also caused cardiac hypertrophy, although the myocytes of these hearts were not found to be enlarged, have increased cell cycle activity, or have altered binucleation. Few changes were found in the cardiac expression levels of proteins integral to control of excitation-contraction calcium when fetuses were subjected to increased hemodynamic load. From this, I conclude that the fetal sheep heart is responsive to hemodynamic load as a regulator of myocardial growth, which may be an important adaptive mechanism, whereas the relative insensitivity to regulation of the calcium transport system by hemodynamic load may be protective in the fetal heart.

References

Abdelwahid E, Pelliniemi LJ, Niinikoski H, Simell O, Tuominen J, Rahkonen O & Jokinen E. (1999). Apoptosis in the pattern formation of the ventricular wall during mouse heart organogenesis. *Anatomical Record* **256**, 208-217.

Abramoff MD, Magelhaes PJ & Ram SJ. (2004). Image Processing with ImageJ. *Biophotonics International* **11**, 36-42.

Adler CP & Costabel U. (1975). Cell number in human heart in atrophy, hypertrophy, and under the influence of cytostatics. *Recent Advances in Studies on Cardiac Structure and Metabolism* **6**, 343-355.

Agata N, Tanaka H & Shigenobu K. (1994). Inotropic effects of ryanodine and nicardipine on fetal, neonatal and adult guinea-pig myocardium. *European Journal of Pharmacology* **260**, 47-55.

Ahuja P, Perriard E, Perriard JC & Ehler E. (2004). Sequential myofibrillar breakdown accompanies mitotic division of mammalian cardiomyocytes. *Journal of Cell Science* **117**, 3295-3306.

Al-Merani SA, Brooks DP, Chapman BJ & Munday KA. (1978). The half-lives of angiotensin II, angiotensin II-amide, angiotensin III, Sar1-Ala8-angiotensin II and renin in the circulatory system of the rat. *Journal of Physiology* **278**, 471-490.

Altschul SF, Gish W, Miller W, Myers EW & Lipman DJ. (1990). Basic local alignment search tool. *Journal of Molecular Biology* **215**, 403-410.

Anderson DF, Bissonnette JM, Faber JJ & Thornburg KL. (1981). Central shunt flows and pressures in the mature fetal lamb. *American Journal of Physiology* **241**, H60-66.

Anderson DF, Faber JJ, Morton MJ, Parks CM, Pinson CW & Thornburg KL. (1985). Flow through the foramen ovale of the fetal and new-born lamb. *Journal of Physiology* **365**, 29-40.

Aoyagi T, Fujii AM, Flanagan MF, Arnold L, Mirsky I & Izumo S. (2001). Maturation-dependent differences in regulation of sarcoplasmic reticulum Ca(2+) ATPase in sheep myocardium in response to pressure overload: a possible mechanism for maturation-dependent systolic and diastolic dysfunction. *Pediatric Research* **50**, 246-253.

Aoyagi T, Mirsky I, Flanagan MF, Currier JJ, Colan SD & Fujii AM. (1992). Myocardial function in immature and mature sheep with pressure-overload hypertrophy. *American Journal of Physiology* **262**, H1036-1048.

Arai M, Suzuki T & Nagai R. (1996). Sarcoplasmic reticulum genes are upregulated in mild cardiac hypertrophy but downregulated in severe cardiac hypertrophy induced by pressure overload. *Journal of Molecular and Cellular Cardiology* **28**, 1583-1590.

Assayag P, D CH, Marty I, de Leiris J, Lompre AM, Boucher F, Valere PE, Lortet S, Swynghedauw B & Besse S. (1998). Effects of sustained low-flow ischemia on myocardial function and calcium-regulating proteins in adult and senescent rat hearts. *Cardiovascular Research* **38**, 169-180.

Austin A, Fagan DG & Mayhew TM. (1995). A stereological method for estimating the total number of ventricular myocyte nuclei in fetal and postnatal hearts. *Journal of Anatomy* 187, 641-647.

AVMA Panel on Euthanasia. American Veterinary Medical Association. (2001). 2000 Report of the AVMA Panel on Euthanasia. *Journal of the American Veterinary Medical Association* 218, 669-696.

Baartscheer A, Schumacher CA, Belterman CN, Coronel R & Fiolet JW. (2003). [Na+]i and the driving force of the Na+/Ca2+-exchanger in heart failure. *Cardiovascular Research* 57, 986-995.

Bae S, Xiao Y, Li G, Casiano CA & Zhang L. (2003). Effect of maternal chronic hypoxic exposure during gestation on apoptosis in fetal rat heart. *American Journal of Physiology* 285, H983-990.

Bajoria R. (1998). Vascular anatomy of monochorionic placenta in relation to discordant growth and amniotic fluid volume. *Human Reproduction* 13, 2933-2940.

Bajoria R, Hancock M, Ward S, D'Souza SW & Sooranna SR. (2000). Discordant amino acid profiles in monochorionic twins with twin-twin transfusion syndrome. *Pediatric Research* 48, 821-828.

Bajoria R, Sullivan M & Fisk NM. (1999a). Endothelin concentrations in monochorionic twins with severe twin-twin transfusion syndrome. *Human Reproduction* 14, 1614-1618.

Bajoria R, Ward S & Chatterjee R. (2003). Brain natriuretic peptide and endothelin-1 in the pathogenesis of polyhydramnios-oligohydramnios in monochorionic twins. *American Journal of Obstetrics and Gynecology* 189, 189-194.

Bajoria R, Ward S & Sooranna SR. (2001a). Atrial natriuretic peptide mediated polyuria: pathogenesis of polyhydramnios in the recipient twin of twin-twin transfusion syndrome. *Placenta* 22, 716-724.

Bajoria R, Ward S & Sooranna SR. (2001b). Erythropoietin in monochorionic twin pregnancies in relation to twin--twin transfusion syndrome. *Human Reproduction* 16, 574-580.

Bajoria R, Ward S & Sooranna SR. (2004). Influence of vasopressin in the pathogenesis of oligohydramnios-polyhydramnios in monochorionic twins. *European Journal of Obstetrics, Gynecology, and Reproductive Biology* 113, 49-55.

Bajoria R, Wee LY, Anwar S & Ward S. (1999b). Outcome of twin pregnancies complicated by single intrauterine death in relation to vascular anatomy of the monochorionic placenta. *Human Reproduction* 14, 2124-2130.

Bajoria R, Wigglesworth J & Fisk NM. (1995). Angioarchitecture of monochorionic placentas in relation to the twin-twin transfusion syndrome. *American Journal of Obstetrics and Gynecology* 172, 856-863.

Ball AJ & Levine F. (2005). Telomere-independent cellular senescence in human fetal cardiomyocytes. *Aging Cell* 4, 21-30.

Barbera A, Giraud GD, Reller MD, Maylie J, Morton MJ & Thornburg KL. (2000). Right ventricular systolic pressure load alters myocyte maturation in fetal sheep. *American Journal of Physiology* 279, R1157-1164.

Barcroft J. (1946). *Researches on pre-natal life.* Blackwell, Oxford.

Barker DJP. (2001). *Fetal origins of cardiovascular and lung disease.* M. Dekker, New York.

Barrea C, Alkazaleh F, Ryan G, McCrindle BW, Roberts A, Bigras JL, Barrett J, Seaward GP, Smallhorn JF & Hornberger LK. (2005). Prenatal cardiovascular manifestations in the twin-to-twin transfusion syndrome recipients and the impact of therapeutic amnioreduction. *American Journal of Obstetrics and Gynecology* **192**, 892-902.

Bassani JW, Qi M, Samarel AM & Bers DM. (1994). Contractile arrest increases sarcoplasmic reticulum calcium uptake and SERCA2 gene expression in cultured neonatal rat heart cells. *Circulation Research* 74, 991-997.

Beltrami CA, Di Loreto C, Finato N, Rocco M, Artico D, Cigola E, Gambert SR, Olivetti G, Kajstura J & Anversa P. (1997). Proliferating cell nuclear antigen (PCNA), DNA synthesis and mitosis in myocytes following cardiac transplantation in man. *Journal of Molecular and Cellular Cardiology* **29**, 2789-2802.

Benson DA, Karsch-Mizrachi I, Lipman DJ, Ostell J & Wheeler DL. (2004). GenBank: update. *Nucleic Acids Research* **32 Database issue**, D23-26.

Bers DM. (2002). Cardiac excitation-contraction coupling. *Nature* 415, 198-205.

Blumenthal I. (2004). Periventricular leucomalacia: a review. *European Journal of Pediatrics* **163**, 435-442.

Boerth SR & Artman M. (1996). Thyroid hormone regulates Na(+)-Ca2+ exchanger expression during postnatal maturation and in adult rabbit ventricular myocardium. *Cardiovascular Research* 31 Spec No, E145-152.

Book CB, Sun X & Ng YC. (1997). Developmental changes in regulation of the Na+, K(+)-ATPase alpha 3 isoform by thyroid hormone in ferret heart. *Biochimica et Biophysica Acta* **1358**, 172-180.

Botting R & Vane JR. (1989). Vasoactive mediators derived from the endothelium. *Archives des Maladies du Coeur et des Vaisseaux* **82 Spec No 4**, 11-14.

Brace RA & Moore TR. (1991). Transplacental, amniotic, urinary, and fetal fluid dynamics during very-large-volume fetal intravenous infusions. *American Journal of Obstetrics and Gynecology* **164**, 907-916.

Brillantes AM, Bezprozvannaya S & Marks AR. (1994). Developmental and tissue-specific regulation of rabbit skeletal and cardiac muscle calcium channels involved in excitation-contraction coupling. *Circulation Research* 75, 503-510.

Brodsky WY, Arefyeva AM & Uryvaeva IV. (1980). Mitotic polyploidization of mouse heart myocytes during the first postnatal week. *Cell Proliferation* **210**, 133-144.

Brook WH, Connell S, Cannata J, Maloney JE & Walker AM. (1983). Ultrastructure of the myocardium during development from early fetal life to adult life in sheep. *Journal of Anatomy* **137**, 729-741.

Bruno S & Darzynkiewicz Z. (1992). Cell cycle dependent expression and stability of the nuclear protein detected by Ki-67 antibody in HL-60 cells. *Cell Proliferation* 25, 31-40.

Burrell JH, Boyn AM, Kumarasamy V, Hsieh A, Head SI & Lumbers ER. (2003). Growth and maturation of cardiac myocytes in fetal sheep in the second half of gestation. *Anatomical Record* 274, 952-961.

Burrington JD. (1978). Response to experimental coarctation of the aorta and pulmonic stenosis in the fetal lamb. *Journal of Thoracic and Cardiovascular Surgery* 75, 819-826.

Burton PB, Raff MC, Kerr P, Yacoub MH & Barton PJ. (1999). An intrinsic timer that controls cell-cycle withdrawal in cultured cardiac myocytes. *Developmental Biology* 216, 659-670.

Cadre BM, Qi M, Eble DM, Shannon TR, Bers DM & Samarel AM. (1998). Cyclic stretch down-regulates calcium transporter gene expression in neonatal rat ventricular myocytes. *Journal of Molecular and Cellular Cardiology* 30, 2247-2259.

Cheung YF, Taylor MJ, Fisk NM, Redington AN & Gardiner HM. (2000). Fetal origins of reduced arterial distensibility in the donor twin in twin-twin transfusion syndrome. *Lancet* 355, 1157-1158.

Chi NC & Karliner JS. (2004). Molecular determinants of responses to myocardial ischemia/reperfusion injury: focus on hypoxia-inducible and heat shock factors. *Cardiovascular Research* 61, 437-447.

Christensen AM, Daouk GH, Norling LL, Catlin EA & Ingelfinger JR. (1999). Postnatal transient renal insufficiency in the feto-fetal transfusion syndrome. *Pediatric Nephrology* 13, 117-120.

Cincotta RB, Gray PH, Phythian G, Rogers YM & Chan FY. (2000). Long term outcome of twin-twin transfusion syndrome. *Archives of Disease in Childhood: Fetal and Neonatal Edition* 83, F171-176.

Clubb FJ, Jr. & Bishop SP. (1984). Formation of binucleated myocardial cells in the neonatal rat. An index for growth hypertrophy. *Laboratory Investigation* 50, 571-577.

Clubb FJ, Jr., Penney DG, Baylerian MS & Bishop SP. (1986). Cardiomegaly due to myocyte hyperplasia in perinatal rats exposed to 200 ppm carbon monoxide. *Journal of Molecular and Cellular Cardiology* 18, 477-486.

Cooper Gt. (1997). Basic determinants of myocardial hypertrophy: a review of molecular mechanisms. *Annual Review of Medicine* 48, 13-23.

Creazzo TL, Burch J & Godt RE. (2004). Calcium buffering and excitation-contraction coupling in developing avian myocardium. *Biophysical Journal* 86, 966-977.

Dalton KJ, Dawes GS & Patrick JE. (1977). Diurnal, respiratory, and other rhythms of fetal heart rate in lambs. *American Journal of Obstetrics and Gynecology* 127, 414-424.

Davis LE & Hohimer AR. (1991). Hemodynamics and organ blood flow in fetal sheep subjected to chronic anemia. *American Journal of Physiology* **261**, R1542-1548.

Davis LE, Hohimer AR & Brace RA. (1996). Changes in left thoracic duct lymph flow during progressive anemia in the ovine fetus. *American Journal of Obstetrics and Gynecology* 174, 1469-1476.

Davis LE, Hohimer AR & Morton MJ. (1999). Myocardial blood flow and coronary reserve in chronically anemic fetal lambs. *American Journal of Physiology* 277, R306-313.

Denbow M, Fogliani R, Kyle P, Letsky E, Nicolini U & Fisk N. (1998). Haematological indices at fetal blood sampling in monochorionic pregnancies complicated by feto-fetal transfusion syndrome. *Prenatal Diagnosis* 18, 941-946.

Denbow ML, Cox P, Taylor M, Hammal DM & Fisk NM. (2000). Placental angioarchitecture in monochorionic twin pregnancies: relationship to fetal growth, fetofetal transfusion syndrome, and pregnancy outcome. *American Journal of Obstetrics and Gynecology* **182**, 417-426.

Diaz ME, Graham HK, O'Neill S C, Trafford AW & Eisner DA. (2005). The control of sarcoplasmic reticulum Ca content in cardiac muscle. *Cell Calcium* **38**, 391-396.

Domingos PP, Fonseca PM, Nadruz W, Jr. & Franchini KG. (2002). Load-induced focal adhesion kinase activation in the myocardium: role of stretch and contractile activity. *American Journal of Physiology* **282**, H556-564.

Drew JH, Guaran RL, Cichello M & Hobbs JB. (1997). Neonatal whole blood hyperviscosity: the important factor influencing later neurologic function is the viscosity and not the polycythemia. *Clinical Hemorheology and Microcirculation* 17, 67-72.

Fernandez E, Siddiquee Z & Shohet RV. (2001). Apoptosis and proliferation in the neonatal murine heart. *Developmental Dynamics* **221**, 302-310.

Fesslova V, Villa L, Nava S, Mosca F & Nicolini U. (1998). Fetal and neonatal echocardiographic findings in twin-twin transfusion syndrome. *American Journal of Obstetrics and Gynecology* **179**, 1056-1062.

Fishman NH, Hof RB, Rudolph AM & Heymann MA. (1978). Models of congenital heart disease in fetal lambs. *Circulation* **58**, 354-364.

Fisk NM & Galea P. (2004). Twin-twin transfusion--as good as it gets? *New England Journal of Medicine* **351**, 182-184.

Flecknoe SJ, Boland RE, Wallace MJ, Harding R & Hooper SB. (2004). Regulation of alveolar epithelial cell phenotypes in fetal sheep: roles of cortisol and lung expansion. *American Journal of Physiology* **287**, L1207-1214.

Flink IL, Oana S, Maitra N, Bahl JJ & Morkin E. (1998). Changes in E2F complexes containing retinoblastoma protein family members and increased cyclin-dependent kinase inhibitor activities during terminal differentiation of cardiomyocytes. *Journal of Molecular and Cellular Cardiology* **30**, 563-578.

Forsgren S & Thornell LE. (1981). The development of Purkinje fibres and ordinary myocytes in the bovine fetal heart. An ultrastructural study. *Anatomy and Embryology* **162**, 127-136.

Fouron JC, Chemtob S, Chartrand C, Russo P, Haswani P, Sonesson SE, Skoll A, Teyssier G & Castor S. (2001). Generation of reactive O2 species in the myocardium of newborn lambs following intrauterine increase in right ventricular pressure. *Pediatric Cardiology* **22**, 143-146.

Fowden AL, Szemere J, Hughes P, Gilmour RS & Forhead AJ. (1996). The effects of cortisol on the growth rate of the sheep fetus during late gestation. *Journal of Endocrinology* **151**, 97-105.

Frank JS, Mottino G, Reid D, Molday RS & Philipson KD. (1992). Distribution of the Na(+)-Ca2+ exchange protein in mammalian cardiac myocytes: an immunofluorescence and immunocolloidal gold-labeling study. *The Journal of Cell Biology* **117**, 337-345.

Gardiner HM. (2001). Early changes in vascular dynamics in relation to twin-twin transfusion syndrome. *Twin Research* **4**, 371-377.

Gardiner HM, Taylor MJ, Karatza A, Vanderheyden T, Huber A, Greenwald SE, Fisk NM & Hecher K. (2003). Twin-twin transfusion syndrome: the influence of intrauterine laser photocoagulation on arterial distensibility in childhood. *Circulation* **107**, 1906-1911.

Gardner DS, Jamall E, Fletcher AJ, Fowden AL & Giussani DA. (2004). Adrenocortical responsiveness is blunted in twin relative to singleton ovine fetuses. *Journal of Physiology* **557**, 1021-1032.

Gerdes J, Lemke H, Baisch H, Wacker HH, Schwab U & Stein H. (1984). Cell cycle analysis of a cell proliferation-associated human nuclear antigen defined by the monoclonal antibody Ki-67. *Journal of Immunology* **133**, 1710-1715.

Gergs U, Boknik P, Buchwalow I, Fabritz L, Matus M, Justus I, Hanske G, Schmitz W & Neumann J. (2004). Overexpression of the catalytic subunit of protein phosphatase 2A impairs cardiac function. *Journal of Biological Chemistry* **279**, 40827-40834.

Giraud GD, Faber JJ, Jonker S, Davis L & Anderson DF. (2005). Intravascular infusions of plasma into fetal sheep cause arterial and venous hypertension. *Journal of Applied Physiology* **99**, 884-889.

Giraud GD, Morton MJ, Reid DL, Reller MD & Thornburg KL. (1995). Effects of ductus arteriosus occlusion on pulmonary artery pressure during in utero ventilation in fetal sheep. *Experimental Physiology* **80**, 129-139.

Goldenthal MJ & Marin-Garcia J. (2004). Mitochondrial signaling pathways: a receiver/integrator organelle. *Molecular and Cellular Biochemistry* **262**, 1-16.

Grant DA, Fauchere JC, Eede KJ, Tyberg JV & Walker AM. (2001). Left ventricular stroke volume in the fetal sheep is limited by extracardiac constraint and arterial pressure. *Journal of Physiology* **535**, 231-239.

Gratacos E, Van Schoubroeck D, Carreras E, Devlieger R, Roma E, Cabero L & Deprest J. (2002). Impact of laser coagulation in severe twin-twin transfusion syndrome on fetal Doppler indices and venous blood flow volume. *Ultrasound in Obstetrics and Gynecology* **20**, 125-130.

Grossman W, Jones D & McLaurin LP. (1975). Wall stress and patterns of hypertrophy in the human left ventricle. *Journal of Clinical Investigation* **56**, 56-64.

Haase H, Pfitzmaier B, McEnery MW & Morano I. (2000). Expression of Ca(2+) channel subunits during cardiac ontogeny in mice and rats: identification of fetal alpha(1C) and beta subunit isoforms. *Journal of Cellular Biochemistry* **76**, 695-703.

Haddock PS, Coetzee WA, Cho E, Porter L, Katoh H, Bers DM, Jafri MS & Artman M. (1999). Subcellular [Ca2+]i gradients during excitation-contraction coupling in newborn rabbit ventricular myocytes. *Circulation Research* **85**, 415-427.

Hammond HK, White FC, Bhargava V & Shabetai R. (1992). Heart size and maximal cardiac output are limited by the pericardium. *American Journal of Physiology* **263**, H1675-1681.

Hanson GL, Schilling WP & Michael LH. (1993). Sodium-potassium pump and sodium-calcium exchange in adult and neonatal canine cardiac sarcolemma. *American Journal of Physiology* **264**, H320-326.

Hashida H, Hamada M & Hiwada K. (1999). Serial changes in sarcoplasmic reticulum gene expression in volume-overloaded cardiac hypertrophy in the rat: effect of an angiotensin II receptor antagonist. *Clinical Science* **96**, 387-395.

Herberg U, Gross W, Bartmann P, Banek CS, Hecher K & Breuer J. (2005). Long-term cardiac follow-up of severe twin-to-twin transfusion syndrome after intrauterine laser coagulation. *Heart*. 6 April epub ahead of print.

Hoerter J, Mazet F & Vassort G. (1981). Perinatal growth of the rabbit cardiac cell: possible implications for the mechanism of relaxation. *Journal of Molecular and Cellular Cardiology* **13**, 725-740.

Huber A, Diehl W, Zikulnig L, Held KR, Bregenzer T, Hackeloer BJ & Hecher K. (2004). Amniotic fluid and maternal blood characteristics in severe mid-trimester twin-twin transfusion syndrome. *Fetal Diagnosis and Therapy* **19**, 504-509.

Hudecova S, Stefanik P, Macejova D, Brtko J & Krizanova O. (2004). Retinoic acid increased expression of the Na+/Ca2+ exchanger in the heart and brain. *General Physiology & Biophysics* **23**, 417-422.

Huttenbach Y, Ostrowski ML, Thaller D & Kim HS. (2001). Cell proliferation in the growing human heart: MIB-1 immunostaining in preterm and term infants at autopsy. *Cardiovascular Pathology* **10**, 119-123.

Hyodo HM, Unno N, Masuda H, Watanabe T, Kozuma S & Taketani Y. (2003). Myocardial hypertrophy of the recipient twins in twin-to-twin transfusion syndrome and cerebral palsy. *International Journal of Gynaecology and Obstetrics* **80**, 29-34.

Institute of Laboratory Animal Resources (U.S.). Committee on Pain and Distress in Laboratory Animals. (1992). *Recognition and alleviation of pain and distress in laboratory animals.* National Academy Press, Washington, D.C.

Ioannou CV, Stergiopulos N, Katsamouris AN, Startchik I, Kalangos A, Licker MJ, Westerhof N & Morel DR. (2003). Hemodynamics induced after acute reduction of proximal thoracic aorta compliance. *European Journal of Vascular and Endovascular Surgery* **26**, 195-204.

Ishii K, Chmait RH, Martinez JM, Nakata M & Quintero RA. (2004). Ultrasound assessment of venous blood flow before and after laser therapy: approach to understanding the pathophysiology of twin-twin transfusion syndrome. *Ultrasound in Obstetrics and Gynecology* **24**, 164-168.

Jackson T, Allard MF, Sreenan CM, Doss LK, Bishop SP & Swain JL. (1990). The c-myc proto-oncogene regulates cardiac development in transgenic mice. *Molecular and Cellular Biochemistry* **10**, 3709-3716.

Jaeggi ET, Fouron JC, Hornberger LK, Proulx F, Oberhansli I, Yoo SJ & Fermont L. (2002). Agenesis of the ductus venosus that is associated with extrahepatic umbilical vein drainage: prenatal features and clinical outcome. *American Journal of Obstetrics and Gynecology* **187**, 1031-1037.

Jorgensen AO & Bashir R. (1984). Temporal appearance and distribution of the Ca2+ + Mg2+ ATPase of the sarcoplasmic reticulum in developing chick myocardium as determined by immunofluorescence labeling. *Developmental Biology* **106**, 156-165.

Ju H, Scammel-La Fleur T & Dixon IM. (1996). Altered mRNA abundance of calcium transport genes in cardiac myocytes induced by angiotensin II. *Journal of Molecular and Cellular Cardiology* **28**, 1119-1128.

Kajstura J, Mansukhani M, Cheng W, Reiss K, Krajewski S, Reed JC, Quaini F, Sonnenblick EH & Anversa P. (1995). Programmed cell death and expression of the protooncogene bcl-2 in myocytes during postnatal maturation of the heart. *Experimental Cell Research* **219**, 110-121.

Kaneko H, Okamoto M & Goshima K. (1984). Structural change of myofibrils during mitosis of newt embryonic myocardial cells in culture. *Experimental Cell Research* **153**, 483-498.

Kang MJ & Koh GY. (1997). Differential and dramatic changes of cyclin-dependent kinase activities in cardiomyocytes during the neonatal period. *Journal of Molecular and Cellular Cardiology* **29**, 1767-1777.

Karatza AA, Wolfenden JL, Taylor MJ, Wee L, Fisk NM & Gardiner HM. (2002). Influence of twin-twin transfusion syndrome on fetal cardiovascular structure and function: prospective case-control study of 136 monochorionic twin pregnancies. *Heart* **88**, 271-277.

Katanosaka Y, Iwata Y, Kobayashi Y, Shibasaki F, Wakabayashi S & Shigekawa M. (2005). Calcineurin inhibits Na+/Ca2+ exchange in phenylephrine-treated hypertrophic cardiomyocytes. *Journal of Biological Chemistry* **280**, 5764-5772.

Kato Y, Masumiya H, Agata N, Tanaka H & Shigenobu K. (1996). Developmental changes in action potential and membrane currents in fetal, neonatal and adult guinea-pig ventricular myocytes. *Journal of Molecular and Cellular Cardiology* **28**, 1515-1522.

Katsube Y, Yokoshiki H, Nguyen L, Yamamoto M & Sperelakis N. (1998). L-type Ca2+ currents in ventricular myocytes from neonatal and adult rats. *Canadian Journal of Physiology and Pharmacology* 76, 873-881.

Kilby MD, Platt C, Whittle MJ, Oxley J & Lindop GB. (2001). Renin gene expression in fetal kidneys of pregnancies complicated by twin-twin transfusion syndrome. *Pediatric and Developmental Pathology* 4, 175-179.

Kilby MD, Szwarc R, Benson LN & Morrow RJ. (1998). Left ventricular hemodynamics in anemic fetal lambs. *Journal of Perinatal Medicine* **26**, 5-12.

Kim YK, Kim SJ, Kramer CM, Yatani A, Takagi G, Mankad S, Szigeti GP, Singh D, Bishop SP, Shannon RP, Vatner DE & Vatner SF. (2002). Altered excitation-contraction coupling in myocytes from remodeled myocardium after chronic myocardial infarction. *Journal of Molecular and Cellular Cardiology* 34, 63-73.

Kiserud T. (1997). In a different vein: the ductus venosus could yield much valuable information. *Ultrasound in Obstetrics and Gynecology* 9, 369-372.

Kumar R & Joyner RW. (2003). Expression of protein phosphatases during postnatal development of rabbit heart. *Molecular and Cellular Biochemistry* 245, 91-98.

Lammerding J, Kamm RD & Lee RT. (2004). Mechanotransduction in cardiac myocytes. *Annals of the New York Academy of Sciences* **1015**, 53-70.

Leake RD, Stegner H, Ross MG, Ervin MG, Oddie TH & Fisher DA. (1986). Diurnal variations in plasma arginine vasotocin (AVT) concentrations in the ovine fetus. *Life Sciences* **38**, 1485-1490.

Legato MJ. (1979a). Cellular mechanisms of normal growth in the mammalian heart. I. Qualitative and quantitative features of ventricular architecture in the dog from birth to five months of age. *Circulation Research* 44, 250-262.

Legato MJ. (1979b). Cellular mechanisms of normal growth in the mammalian heart. II. A quantitative and qualitative comparison between the right and left ventricular myocytes in the dog from birth to five months of age. *Circulation Research* 44, 263-279.

Lewartowski B & Wolska BM. (1993). The effect of thapsigargin on sarcoplasmic reticulum Ca2+ content and contractions in single myocytes of guinea-pig heart. *Journal of Molecular and Cellular Cardiology* **25**, 23-29.

Li F, Wang X, Capasso JM & Gerdes AM. (1996). Rapid transition of cardiac myocytes from hyperplasia to hypertrophy during postnatal development. *Journal of Molecular and Cellular Cardiology* **28**, 1737-1746.

Li G, Bae S & Zhang L. (2004). Effect of prenatal hypoxia on heat stress-mediated cardioprotection in adult rat heart. *American Journal of Physiology* **286**, H1712-1719.

Linask KK, Han MD, Artman M & Ludwig CA. (2001). Sodium-calcium exchanger (NCX-1) and calcium modulation: NCX protein expression patterns and regularion of early heart development. *Developmental Dynamics* 221, 249-264.

Liu L, O'Hara DS, Cala SE, Poornima I, Hines RN & Marsh JD. (2000). Developmental regulation of the L-type calcium channel alpha1C subunit expression in heart. *Molecular and Cellular Biochemistry* 205, 101-109.

Lumbers ER, Boyce AC, Joulianos G, Kumarasamy V, Barner E, Segar JL & Burrell JH. (2005). Effects of cortisol on cardiac myocytes and on expression of cardiac genes in fetal sheep. *American Journal of Physiology* **288**, R567-574.

Luss I, Boknik P, Jones LR, Kirchhefer U, Knapp J, Linck B, Luss H, Meissner A, Muller FU, Schmitz W, Vahlensieck U & Neumann J. (1999). Expression of cardiac calcium regulatory proteins in atrium v ventricle in different species. *Journal of Molecular & Cellular Cardiology* **31**, 1299-1314.

Lutfi S, Allen VM, Fahey J, O'Connell CM & Vincer MJ. (2004). Twin-twin transfusion syndrome: a population-based study. *Obstetrics and Gynecology* **104**, 1289-1297.

Machida N, Brissie N, Sreenan C & Bishop SP. (1997). Inhibition of cardiac myocyte division in c-myc transgenic mice. *Journal of Molecular and Cellular Cardiology* **29**, 1895-1902.

Machin G, Still K & Lalani T. (1996). Correlations of placental vascular anatomy and clinical outcomes in 69 monochorionic twin pregnancies. *American Journal of Medical Genetics* **61**, 229-236.

MacLellan WR & Schneider MD. (2000). Genetic dissection of cardiac growth control pathways. *Annual Review of Physiology* **62**, 289-319.

Magyar CE, Wang J, Azuma KK & McDonough AA. (1995). Reciprocal regulation of cardiac Na-K-ATPase and Na/Ca exchanger: hypertension, thyroid hormone, development. *American Journal of Physiology* **269**, C675-682.

Mahieu-Caputo D, Dommergues M, Delezoide AL, Lacoste M, Cai Y, Narcy F, Jolly D, Gonzales M, Dumez Y & Gubler MC. (2000). Twin-to-twin transfusion syndrome. Role of the fetal renin-angiotensin system. *American Journal of Pathology* **156**, 629-636.

Mahony L & Jones LR. (1986). Developmental changes in cardiac sarcoplasmic reticulum in sheep. *Journal of Biological Chemistry* **261**, 15257-15265.

Martin C, Yu AY, Jiang BH, Davis L, Kimberly D, Hohimer AR & Semenza GL. (1998). Cardiac hypertrophy in chronically anemic fetal sheep: Increased vascularization is associated with increased myocardial expression of vascular endothelial growth factor and hypoxia-inducible factor 1. *American Journal of Obstetrics and Gynecology* **178**, 527-534.

Matsui H, MacLennan DH, Alpert NR & Periasamy M. (1995). Sarcoplasmic reticulum gene expression in pressure overload-induced cardiac hypertrophy in rabbit. *American Journal of Physiology* **268**, C252-258.

Maylie JG. (1982). Excitation-contraction coupling in neonatal and adult myocardium of cat. *American Journal of Physiology* 242, H834-843.

McTiernan CF, Frye CS, Lemster BH, Kinder EA, Ogletree-Hughes ML, Moravec CS & Feldman AM. (1999). The human phospholamban gene: structure and expression. *Journal of Molecular and Cellular Cardiology* 31, 679-692.

Meissner G. (2004). Molecular regulation of cardiac ryanodine receptor ion channel. *Cell Calcium* 35, 621-628.

Mellor DJ & Slater JS. (1972). Daily changes in foetal urine and relationships with amniotic and allantoic fluid and maternal plasma during the last two months of pregnancy in conscious, unstressed ewes with chronically implanted catheters. *Journal of Physiology* 227, 503-525.

Michalak M. (1987). Sarcoplasmic reticulum membrane and heart development. *Canadian Journal of Cardiology* 3, 251-260.

Miller CD, Richard JL, Hembrough FB, Osweiler GD & Cox DF. (1990). In vitro effects of cyclopiazonic acid mycotoxin on turkey papillary muscles. *American Journal of Veterinary Research* 51, 836-838.

Misquitta CM, Mack DP & Grover AK. (1999). Sarco/endoplasmic reticulum Ca2+ (SERCA)-pumps: link to heart beats and calcium waves. *Cell Calcium* 25, 277-290.

Misquitta CM, Mwanjewe J, Nie L & Grover AK. (2002). Sarcoplasmic reticulum Ca(2+) pump mRNA stability in cardiac and smooth muscle: role of the 3'-untranslated region. *American Journal of Physiology* 283, C560-568.

Mitropoulos G, Scurry J & Cussen L. (1992). Organ weight/bodyweight ratios: growth rates of fetal organs in the latter half of pregnancy with a simple method for calculating mean organ weights. *Journal of Paediatrics and Child Health* 28, 236-239.

Moreira de Sa RA, Salomon LJ, Takahashi Y, Yamamoto M & Ville Y. (2005). Analysis of Fetal Growth After Laser Therapy in Twin-to-Twin Transfusion Syndrome. *Journal of Ultrasound in Medicine* 24, 1213-1219.

Moriscot AS, Sayen MR, Hartong R, Wu P & Dillmann WH. (1997). Transcription of the rat sarcoplasmic reticulum Ca2+ adenosine triphosphatase gene is increased by 3,5,3'-triiodothyronine receptor isoform-specific interactions with the myocyte-specific enhancer factor-2a. *Endocrinology* 138, 26-32.

Morton MJ & Thornburg KL. (1987). The pericardium and cardiac transmural filling pressure in the fetal sheep. *Journal of Developmental Physiology* 9, 159-168.

Nakanishi T & Jarmakani JM. (1984). Developmental changes in myocardial mechanical function and subcellular organelles. *American Journal of Physiology* 246, H615-625.

Nakanishi T, Okuda H, Kamata K, Abe K, Sekiguchi M & Takao A. (1987). Development of myocardial contractile system in the fetal rabbit. *Pediatric Research* 22, 201-207.

Nayler WG & Fassold E. (1977). Calcium accumulating and ATPase activity of cardiac sarcoplasmic reticulum before and after birth. *Cardiovascular Research* **11**, 231-237.

Micholas SB & Philipson KD. (1999). Cardiac expression of the Na(+)/Ca(2+) exchanger NCX1 is GATA factor dependent. *American Journal of Physiology* 277, H324-330.

Nikkels PG, van Gemert MJ & Briet JW. (2001). Late onset of discordant growth in a monochorionic twin pregnancy: vascular anastomoses determine fetal growth pattern and not placental sharing. *Fetal Diagnosis and Therapy* **16**, 23-25.

Noonan KJ, Farnum CE, Leiferman EM, Lampl M, Markel MD & Wilsman NJ. (2004). Growing pains: are they due to increased growth during recumbency as documented in a lamb model? *Journal of Pediatric Orthopedics* 24, 726-731.

Page E & Buecker JL. (1981). Development of dyadic junctional complexes between sarcoplasmic reticulum and plasmalemma in rabbit left ventricular myocardial cells. Morphometric analysis. *Circulation Research* **48**, 519-522.

Park KW, Goo JH, Chung HS, Kim H, Kim DH & Park WJ. (1998). Cloning of the genes encoding mouse cardiac and skeletal calsequestrins: expression pattern during embryogenesis. *Gene* 217, 25-30.

Pavlovic M, Schaller A, Pfammatter JP, Carrel T, Berdat P & Gallati S. (2005). Age-dependent suppression of SERCA2a mRNA in pediatric atrial myocardium. *Biochemical and Biophysical Research Communications* **326**, 344-348.

Payvandi MN & Kerber RE. (1976). Echocardiography in congenital and acquired absence of the pericardium. An echocardiographic mimic of right ventricular volume overload. *Circulation* 53, 86-92.

Pedra SR, Smallhorn JF, Ryan G, Chitayat D, Taylor GP, Khan R, Abdolell M & Hornberger LK. (2002). Fetal cardiomyopathies: pathogenic mechanisms, hemodynamic findings, and clinical outcome. *Circulation* **106**, 585-591.

Pegg W & Michalak M. (1987). Differentiation of sarcoplasmic reticulum during cardiac myogenesis. *American Journal of Physiology* **252**, H22-31.

Philipson KD, Longoni S & Ward R. (1988). Purification of the cardiac Na+-Ca2+ exchange protein. *Biochimica et Biophysica Acta* **945**, 298-306.

Philipson KD, Nicoll DA, Ottolia M, Quednau BD, Reuter H, John S & Qiu Z. (2002). The Na+/Ca2+ exchange molecule: an overview. *Annals of the New York Academy of Sciences* **976**, 1-10.

Pietschmann M & Bartels H. (1985). Cellular hyperplasia and hypertrophy, capillary proliferation and myoglobin concentration in the heart of newborn and adult rats at high altitude. *Respiration Physiology* **59**, 347-360.

Pinson CW, Morton MJ & Thornburg KL. (1987). An anatomic basis for fetal right ventricular dominance and arterial pressure sensitivity. *Journal of Developmental Physiology* **9**, 253-269.

Plank DM, Yatani A, Ritsu H, Witt S, Glascock B, Lalli MJ, Periasamy M, Fiset C, Benkusky N, Valdivia HH & Sussman MA. (2003). Calcium dynamics in the failing heart: restoration by beta-adrenergic receptor blockade. *American Journal of Physiology* **285**, H305-315.

Poolman RA & Brooks G. (1998). Expressions and activities of cell cycle regulatory molecules during the transition from myocyte hyperplasia to hypertrophy. *Journal of Molecular and Cellular Cardiology* **30**, 2121-2135.

Qu Y, Ghatpande A, el-Sherif N & Boutjdir M. (2000). Gene expression of Na+/Ca2+ exchanger during development in human heart. *Cardiovascular Research* **45**, 866-873.

Quintero RA, Morales WJ, Allen MH, Bornick PW, Johnson PK & Kruger M. (1999). Staging of twin-twin transfusion syndrome. *Journal of Perinatology* **19**, 550-555.

Raboisson MJ, Fouron JC, Lamoureux J, Leduc L, Grignon A, Proulx F & Gamache S. (2004). Early intertwin differences in myocardial performance during the twin-to-twin transfusion syndrome. *Circulation* **110**, 3043-3048.

Rasband WS. (2005). ImageJ. National Institutes of Health, Bethesda.

Reed TD, Babu GJ, Ji Y, Zilberman A, Ver Heyen M, Wuytack F & Periasamy M. (2000). The expression of SR calcium transport ATPase and the Na(+)/Ca(2+)Exchanger are antithetically regulated during mouse cardiac development and in Hypo/hyperthyroidism. *Journal of Molecular and Cellular Cardiology* **32**, 453-464.

Reeves JT, Daoud FS & Gentry M. (1972). Growth of the fetal calf and its arterial pressure, blood gases, and hematologic data. *Journal of Applied Physiology* **32**, 240-244.

Reid DL & Thornburg KL. (1990). Pulmonary pressure-flow relationships in the fetal lamb during in utero ventilation. *Journal of Applied Physiology* **69**, 1630-1636.

Reinecke H, Vetter R & Drexler H. (1997). Effects of alpha-adrenergic stimulation on the sarcolemmal Na+/Ca(2+)-exchanger in adult rat ventricular cardiocytes. *Cardiovascular Research* **36**, 216-222.

Ribadeau-Dumas A, Brady M, Boateng SY, Schwartz K & Boheler KR. (1999). Sarco(endo)plasmic reticulum Ca(2+)-ATPase (SERCA2) gene products are regulated post-transcriptionally during rat cardiac development. *Cardiovascular Research* **43**, 426-436.

Roelfsema V, Gunn AJ, Fraser M, Quaedackers JS & Bennet L. (2005). Cortisol and ACTH responses to severe asphyxia in preterm fetal sheep. *Experimental Physiology* **90**, 545-555.

Rohrer D & Dillmann WH. (1988). Thyroid hormone markedly increases the mRNA coding for sarcoplasmic reticulum Ca2+-ATPase in the rat heart. *Journal of Biological Chemistry* **263**, 6941-6944.

Rohrer DK, Hartong R & Dillmann WH. (1991). Influence of thyroid hormone and retinoic acid on slow sarcoplasmic reticulum Ca2+ ATPase and myosin heavy chain alpha gene expression in cardiac myocytes. Delineation of cis-active DNA elements that confer responsiveness to thyroid hormone but not to retinoic acid. *Journal of Biological Chemistry* **266**, 8638-8646.

Rosenfeld CR, Gresores A, Roy TA & Magness RR. (1995) Comparison of ANG II in fetal and pregnant sheep: metabolic clearance and vascular sensitivity. *American Journal of Physiology* **268**, E237-247.

Rottbauer W, Baker K, Wo ZG, Mohideen MA, Cantiello HF & Fishman MC. (2001). Growth and function of the embryonic heart depend upon the cardiac-specific L-type calcium channel alpha1 subunit. *Developmental Cell* 1, 265-275.

Rudolph AM, Roman C & Gournay V. (1999). Perinatal myocardial DNA and protein changes in the lamb: effect of cortisol in the fetus. *Pediatric Research* **46**, 141-146.

Rudolph R. (2001). *Congenital Diseases of the Heart: Clinical-Physiological Considerations.* Futura Publishing Company.

Russell B, Motlagh D & Ashley WW. (2000). Form follows function: how muscle shape is regulated by work. *Journal of Applied Physiology* **88**, 1127-1132.

Saiki Y, Konig A, Waddell J & Rebeyka IM. (1997). Hemodynamic alteration by fetal surgery accelerates myocyte proliferation in fetal guinea pig hearts. *Surgery* **122**, 412-419.

Samson F, Bonnet N, Heimburger M, Rucker-Martin C, Levitsky DO, Mazmanian GM, Mercadier JJ & Serraf A. (2000). Left ventricular alterations in a model of fetal left ventricular overload. *Pediatric Research* **48**, 43-49.

Santiago-Garcia J, Mas-Oliva J, Saavedra D & Zarain-Herzberg A. (1996). Analysis of mRNA expression and cloning of a novel plasma membrane Ca(2+)-ATPase splice variant in human heart. *Molecular and Cellular Biochemistry* **155**, 173-182.

Sawada K & Kawamura K. (1991). Architecture of myocardial cells in human cardiac ventricles with concentric and eccentric hypertrophy as demonstrated by quantitative scanning electron microscopy. *Heart Vessels* **6**, 129-142.

Schoen FJ, Lawrie GM & Titus JL. (1984). Left ventricular cellular hypertrophy in pressure- and volume-overload valvular heart disease. *Human Pathology* **15**, 860-865.

Schroder HJ, Tchirikov M & Rybakowski C. (2003). Pressure pulses and flow velocities in central veins of the anesthetized sheep fetus. *American Journal of Physiology* **284**, H1205-1211.

Segar JL, Dalshaug GB, Bedell KA, Smith OM & Scholz TD. (2001). Angiotensin II in cardiac pressure-overload hypertrophy in fetal sheep. *American Journal of Physiology* **281**, R2037-2047.

Segar JL, Scholz TD, Bedell KA, Smith OM, Huss DJ & Guillery EN. (1997). Angiotensin AT1 receptor blockade fails to attenuate pressure-overload cardiac hypertrophy in fetal sheep. *American Journal of Physiology* 273, R1501-1508.

Seko Y, Takahashi N, Shibuya M & Yazaki Y. (1999). Pulsatile stretch stimulates vascular endothelial growth factor (VEGF) secretion by cultured rat cardiac myocytes. *Biochemical and Biophysical Research Communications* 254, 462-465.

Senat MV, Deprest J, Boulvain M, Paupe A, Winer N & Ville Y. (2004). Endoscopic laser surgery versus serial amnioreduction for severe twin-to-twin transfusion syndrome. *New England Journal of Medicine* 351, 136-144.

Sensky PL, Roy CH, Barnes RJ & Heath MF. (1994). Changes in fetal thyroid hormone levels in adrenalectomized fetal sheep following continuous cortisol infusion 72 h before delivery. *Journal of Endocrinology* 140, 79-83.

Seth M, Sumbilla C, Mullen SP, Lewis D, Klein MG, Hussain A, Soboloff J, Gill DL & Inesi G. (2004). Sarco(endo)plasmic reticulum Ca2+ ATPase (SERCA) gene silencing and remodeling of the Ca2+ signaling mechanism in cardiac myocytes. *Proceedings of the National Academy of Science U S A* 101, 16683-16688.

Shannon TR, Pogwizd SM & Bers DM. (2003). Elevated sarcoplasmic reticulum Ca2+ leak in intact ventricular myocytes from rabbits in heart failure. *Circulation Research* 93, 592-594.

Sheldon CA, Friedman WF & Sybers HD. (1976). Scanning electron microscopy of fetal and neonatal lamb cardiac cells. *Journal of Molecular & Cellular Cardiology* 8, 853-862.

Shenoy R, Klein I & Ojamaa K. (2001). Differential regulation of SR calcium transporters by thyroid hormone in rat atria and ventricles. *American Journal of Physiology* 281, H1690-1696.

Sheridan DJ, Cullen MJ & Tynan MJ. (1979). Qualitative and quantitative observations on ultrastructural changes during postnatal development in the cat myocardium. *Journal of Molecular and Cellular Cardiology* 11, 1173-1181.

Shiba R, Yanagisawa M, Miyauchi T, Ishii Y, Kimura S, Uchiyama Y, Masaki T & Goto K. (1989). Elimination of intravenously injected endothelin-1 from the circulation of the rat. *Journal of Cardiovascular Pharmacology* 13 Suppl 5, S98-102.

Shih JC, Shyu MK, Hsieh MH, Yang JH, Huang SF, Lin GJ & Hsieh FJ. (1996). Agenesis of the ductus venosus in a case of monochorionic twins which mimics twin-twin transfusion syndrome. *Prenatal Diagnosis* 16, 243-246.

Simonetta G, Walker DW & McMillen IC. (1991). Effect of feeding on the diurnal rhythm of plasma cortisol and adrenocorticotrophic hormone concentrations in the pregnant ewe and sheep fetus. *Experimental Physiology* 76, 219-229.

Simpson LL, Marx GR, Elkadry EA & D'Alton ME. (1998). Cardiac dysfunction in twin-twin transfusion syndrome: a prospective, longitudinal study. *Obstetrics and Gynecology* 92, 557-562.

Singh RB, Chohan PK, Dhalla NS & Netticadan T. (2004a). The sarcoplasmic reticulum proteins are targets for calpain action in the ischemic-reperfused heart. *Journal of Molecular and Cellular Cardiology* **37**, 101-110.

Singh RB, Dandekar SP, Elimban V, Gupta SK & Dhalla NS. (2004b). Role of proteases in the pathophysiology of cardiac disease. *Mol Cell Biochem* **263**, 241-256.

Sjaastad I, Wasserstrom JA & Sejersted OM. (2003). Heart failure -- a challenge to our current concepts of excitation-contraction coupling. *Journal of Physiology* **546**, 33-47.

Slodzinski MK & Blaustein MP. (1998). Na+/Ca2+ exchange in neonatal rat heart cells: antisense inhibition and protein half-life. *American Journal of Physiology* **275**, C459-467.

Smith HE & Page E. (1977). Ultrastructural changes in rabbit heart mitochondria during the perinatal period. Neonatal transition to aerobic metabolism. *Developmental Biology* **57**, 109-117.

Smith L & Smith JB. (1994). Regulation of sodium-calcium exchanger by glucocorticoids and growth factors in vascular smooth muscle. *Journal of Biological Chemistry* **269**, 27527-27531.

Smolich JJ, Walker AM, Campbell GR & Adamson TM. (1989). Left and right ventricular myocardial morphometry in fetal, neonatal, and adult sheep. *American Journal of Physiology* **257**, H1-9.

Soonpaa MH & Field LJ. (1998). Survey of studies examining mammalian cardiomyocyte DNA synthesis. *Circulation Research* **83**, 15-26.

Soonpaa MH, Kim KK, Pajak L, Franklin M & Field LJ. (1996). Cardiomyocyte DNA synthesis and binucleation during murine development. *American Journal of Physiology* **271**, H2183-2189.

Striessnig J. (1999). Pharmacology, structure and function of cardiac L-type Ca(2+) channels. *Cellular Physiology and Biochemistry* **9**, 242-269.

Sundgren NC, Giraud GD, Schultz JM, Lasarev MR, Stork PJ & Thornburg KL. (2003a). Extracellular signal-regulated kinase and phosphoinositol-3 kinase mediate IGF-1 induced proliferation of fetal sheep cardiomyocytes. *American Journal of Physiology* **285**, R1481-1489.

Sundgren NC, Giraud GD, Stork PJ, Maylie JG & Thornburg KL. (2003b). Angiotensin II stimulates hyperplasia but not hypertrophy in immature ovine cardiomyocytes. *Journal of Physiology* **548**, 881-891.

Takahashi N, Seko Y, Noiri E, Tobe K, Kadowaki T, Sabe H & Yazaki Y. (1999). Vascular endothelial growth factor induces activation and subcellular translocation of focal adhesion kinase (p125FAK) in cultured rat cardiac myocytes. *Circulation Research* **84**, 1194-1202.

Tamamori-Adachi M, Ito H, Sumrejkanchanakij P, Adachi S, Hiroe M, Shimizu M, Kawauchi J, Sunamori M, Marumo F, Kitajima S & Ikeda MA. (2003). Critical role of cyclin D1 nuclear import in cardiomyocyte proliferation. *Circulation Research* **92**, e12-19.

Taylor MJ, Govender L, Jolly M, Wee L & Fisk NM. (2002). Validation of the Quintero staging system for twin-twin transfusion syndrome. *Obstetrics and Gynecology* **100**, 1257-1265.

Tchirikov M, Kertschanska S & Schroder HJ. (2001). Obstruction of ductus venosus stimulates cell proliferation in organs of fetal sheep. *Placenta* **22**, 24-31.

Tchirikov M, Rybakowski C, Huneke B & Schroder HJ. (1998). Blood flow through the ductus venosus in singleton and multifetal pregnancies and in fetuses with intrauterine growth retardation. *American Journal of Obstetrics and Gynecology* **178**, 943-949.

Temsah RM, Kawabata K, Chapman D & Dhalla NS. (2001). Modulation of cardiac sarcoplasmic reticulum gene expression by lack of oxygen and glucose. *FASEB Journal* **15**, 2515-2517.

Terracciano CM & MacLeod KT. (1997). Effects of lactate on the relative contribution of Ca2+ extrusion mechanisms to relaxation in guinea-pig ventricular myocytes. *Journal of Physiology* **500** (**Pt 3**), 557-570.

Thomas AL, Krane EJ & Nathanielsz PW. (1978). Changes in the fetal thyroid axis after induction of premature parturition by low dose continuous intravascular cortisol infusion to the fetal sheep at 130 days of gestation. *Endocrinology* **103**, 17-23.

Thornburg KL & Morton MJ. (1983). Filling and arterial pressures as determinants of RV stroke volume in the sheep fetus. *American Journal of Physiology* **244**, H656-663.

Trudinger BJ & Giles WB. (1989). Clinical and pathologic correlations of umbilical and uterine artery waveforms. *Clinical Obstetrics and Gynecology* **32**, 669-678.

Underwood MA, Gilbert WM & Sherman MP. (2005). Amniotic fluid: not just fetal urine anymore. *Journal of Perinatology* **25**, 341-348.

van den Wijngaard JP, Umur A, Krediet RT, Ross MG & van Gemert MJ. (2005). Modeling a hydropic recipient twin in twin-twin transfusion syndrome. *American Journal of Physiology* **288**, R799-814.

van Tuyl M, Blommaart PE, de Boer PA, Wert SE, Ruijter JM, Islam S, Schnitzer J, Ellison AR, Tibboel D, Moorman AF & Lamers WH. (2004). Prenatal exposure to thyroid hormone is necessary for normal postnatal development of murine heart and lungs. *Developmental Biology* **272**, 104-117.

Vetter R, Studer R, Reinecke H, Kolar F, Ostadalova I & Drexler H. (1995). Reciprocal changes in the postnatal expression of the sarcolemmal Na+-Ca(2+)-exchanger and SERCA2 in rat heart. *Journal of Molecular and Cellular Cardiology* **27**, 1689-1701.

Vivino M. (2005). NIH Image Engineering (Scientific and image processing technical notes related to NIH Image).

Wang Y, Ahmad N, Wani MA & Ashraf M. (2004). Hepatocyte growth factor prevents ventricular remodeling and dysfunction in mice via Akt pathway and angiogenesis. *Journal of Molecular and Cellular Cardiology* 37, 1041-1052.

Wee LY & Fisk NM. (2002). The twin-twin transfusion syndrome. *Seminars in Neonatology* 7, 187-202.

Weiner CP & Ludomirski A. (1994). Diagnosis, pathophysiology, and treatment of chronic twin-to-twin transfusion syndrome. *Fetal Diagnosis and Therapy* **9**, 283-290.

Wheeler DL, Church DM, Edgar R, Federhen S, Helmberg W, Madden TL, Pontius JU, Schuler GD, Schriml LM, Sequeira E, Suzek TO, Tatusova TA & Wagner L. (2004). Database resources of the National Center for Biotechnology Information: update. *Nucleic Acids Research* 32 **Database issue**, D35-40.

Wibo M, Feron O, Zheng L, Maleki M, Kolar F & Godfraind T. (1998). Thyroid status and postnatal changes in subsarcolemmal distribution and isoform expression of rat cardiac dihydropyridine receptors. *Cardiovascular Research* 37, 151-159.

Wibo M, Kilar F, Zheng L & Godfraind T. (1995). Influence of thyroid status on postnatal maturation of calcium channels, beta-adrenoceptors and cation transport ATPases in rat ventricular tissue. *Journal of Molecular and Cellular Cardiology* 27, 1731-1743.

Wier WG & Balke CW. (1999). Ca(2+) release mechanisms, Ca(2+) sparks, and local control of excitation-contraction coupling in normal heart muscle. *Circulation Research* **85**, 770-776.

Wlodek ME, Challis JR & Patrick J. (1988). Urethral and urachal urine output to the amniotic and allantoic sacs in fetal sheep. *Journal of Developmental Physiology* **10**, 309-319.

Xiao G, Mao S, Baumgarten G, Serrano J, Jordan MC, Roos KP, Fishbein MC & MacLellan WR. (2001a). Inducible activation of c-Myc in adult myocardium in vivo provokes cardiac myocyte hypertrophy and reactivation of DNA synthesis. *Circulation Research* **89**, 1122-1129.

Xiao Y, Xiao D, He J & Zhang L. (2001b). Maternal cocaine administration during pregnancy induces apoptosis in fetal rat heart. *Journal of Cardiovascular Pharmacology* 37, 639-648.

Xu A & Narayanan N. (1999). Ca2+/calmodulin-dependent phosphorylation of the Ca2+-ATPase, uncoupled from phospholamban, stimulates Ca2+-pumping in native cardiac sarcoplasmic reticulum. *Biochemical and Biophysical Research Communications* **258**, 66-72.

Yano M, Ikeda Y & Matsuzaki M. (2005). Altered intracellular Ca2+ handling in heart failure. *Journal of Clinical Investigation* **115**, 556-564.

Yasumura Y, Takemura K, Sakamoto A, Kitakaze M & Miyatake K. (2003). Changes in myocardial gene expression associated with beta-blocker therapy in patients with chronic heart failure. *Journal of Cardiac Failure* **9**, 469-474.

APPENDIX A

Fetal Cardiac Volume Load by Arteriovenous Fistula

Introduction

Preload modulates growth of the heart. The purpose of the experiment described here was to determine the mode of growth of the myocardium, whether by myocyte hypertrophy or proliferation. Some fetal hearts from these experiments were banked in a -80°C freezer. I used these hearts to test if increased volume load regulates cardiac gene expression in the fetus (as described in the main body of the thesis). The experiments described below were carried out by Drs. Thornburg, Karamlou and Giraud.

Materials and Methods

Animals were obtained and treated humanely as detailed in the main body of the thesis. The ewes were divided into a sham-control group (n = 9) and a volume load group (n = 9). At an average of 127dGA (range 126-133dGA) sterile surgery was performed on ewes. Anesthesia was induced and surgery initiated as described in the main body of the thesis. The superior portion of the fetus was delivered through a hysterotomy. The left chest was opened at the 4th intercostal space and the pericardium overlying the right atrium and pulmonary artery was incised. The pulmonary artery was then dissected free. A V5 (0.86mm internal diameter) polyvinyl catheter was placed in the proximal pulmonary artery just beyond the pulmonic valve. A Doppler ultrasonic flow probe (Transonics Systems, Inc., Ithaca, NY) was then placed around the main pulmonary artery distal to the pulmonary artery catheter. A V5 polyvinyl catheter was placed in the right atrium. The free edges of the pericardium were loosely approximated. The fetal chest was closed in anatomical layers. The right neck was then opened. The carotid artery and internal jugular vein were dissected free and isolated atraumatically using vessel loops. Occasionally occuring branches in the area of the anastomosis were ligated. The carotid artery and internal jugular vein were opened longitudinally, and flushed with heparinized saline to remove all blood. Hemodynamic measurements were obtained in all fetuses using the methods described below before and after opening of the A-V fistula. The same measurements were made in the sham-control fetuses. A 1.5 cm side-to side anastomosis was then fashioned using continuous 7-0 proline (Ethicon)

suture. The clamps were then sequentially removed (vein, proximal artery, distal artery), and any bleeding was controlled with thrombin-soaked gelfoam or direct suture. The carotid artery and jugular vein just distal to the anastomosis were then ligated with 2-0 silk. A widely patent anastomosis was confirmed by the presence of a palpable thrill prior to closing the neck incision. In the sham-operated animals, identical chest instrumentation and neck dissection were performed. The carotid artery and the internal jugular vein were ligated, and no fistula was created. The pressure transducers were zeroed to the right atrial level by direct inspection. Surgery was concluded as described in the main body of the thesis.

Experimental Protocol: Hemodynamic measurements were obtained in all animals during the initial surgical procedure, as well as on postoperative days 4 and 7. Fetal blood samples were obtained at the initial surgical procedure, and on days four and seven. After study on day 7, the ewe and fetus were euthanized and postmortem carried out as described in the main body of the thesis. The hearts were either dissociated for isolation of cardiomyocytes (5 A-V fistula and 5 sham-control fetuses) or dissected into its component parts (4 A-V fistula and 4 sham-control fetuses). These components were weighed, and frozen for further study. The fetuses were dissected to confirm catheter position and fistula patency.

Cardiac Myocyte Measurements: Myocyte sizes, binucleation, and Ki-67 levels were measured as described in the main text.

Statistical Analysis: All data are presented as mean ± standard deviation. Statistical analysis was done as described in the main body of the thesis. Variables for the sham-control group were compared to the same day variables for the A-V fistula group.

Results

There were no differences in arterial blood pH, blood gases or hematocrit between sham-operated and A-V fistula fetuses at surgery (Day 0), day 4 or day 7 of the study. Right atrial pressure (RAP), pulmonary artery pressure (PAP) and heart rate were not different between sham-operated and A-V fistula fetuses at days 0, 4 or 7. RV stroke volume became greater in the A-V fistula fetuses than in sham-operated fetuses upon opening of the fistula, and remained elevated until day 7. RV output was greater in A-V fistula fetuses than sham fetuses on days 4 and 7.

There was no difference in the heart or body weights of A-V fistula compared to sham-operated fetuses. Binucleated myocytes from both ventricles of the A-V fistula fetuses were longer than those from the sham-operated fetuses, but myocyte widths were not different. The percent of myocytes that were binucleated was increased in both ventricles of the A-V fistula compared to the sham-operated fetuses. The percentage of mononucleated myocytes that were positive for Ki-67 was increased in both ventricles of A-V fistula compared to sham-operated fetuses (data not shown).

Table 1: Arterial blood gas data for the sham-control group and the A-V fistula group.

	Day 0		Day 4		Day 7	
	Sham	Fistula	Sham	Fistula	Sham	Fistula
pH	7.292 ± 0.053	7.320 ± 0.032	7.359 ± 0.034	7.381 ± 0.026	7.350 ± 0.027	7.352 ± 0.025
PCO_2 (mmHg)	54.7 ± 7.9	49.6 ± 5.2	51.8 ± 3.5	53.2 ± 3.9	52.9 ± 2.9	53.6 ± 4.9
PO_2 (mmHg)	22.4 ± 4.6	22.4 ± 3.1	18.9 ± 3.1	16.9 ± 2.8	17.4 ± 2.4	15.4 ± 3.8
O_2 content (g/100ml)	9.4 ± 2.6	10.9 ± 2.9	7.3 ± 2.3	7.2 ± 1.3	6.5 ± 1.7	6.0 ± 2.3
Hematocrit (%)	40 ± 4	43 ± 5	31 ± 5	36 ± 2	33 ± 4	37 ± 4

Table 2: Hemodynamic parameters. Pre shunt = hemodynamic parameters taken immediately before the A-V fistula was opened. Post shunt = hemodynamic parameters immediately after the shunt was opened or after the carotid artery and jugular vein were tied off for the sham control group. SV = stroke volume; $^{+}$ p = 0.05; $^{\#}$ p = 0.02; * p = 0.01.

	Day 0 pre shunt		Day 0 post shunt		Day 4		Day 7	
	Sham	Fistula	Sham	Fistula	Sham	Fistula	Sham	Fistula
RAP (mmHg)	3.9 ± 1.8	3.2 ± 2.1	3.6 ± 2.0	4.1 ± 2.3	4.1 ± 2.2	3.1 ± 1.9	3.3 ± 1.3	3.9 ± 1.4
PAP (mmHg)	42.7 ± 5.1	44.3 ± 6.8	42.3 ± 6.1	42.2 ± 8.0	46.1 ± 4.1	46.3 ± 3.5	46.5 ± 3.5	47.5 ± 6.4
HR (bpm)	167 ± 29	168 ± 24	166 ± 28	175 ± 20	170 ± 24	166 ± 13	160 ± 9	162 ± 9
RV SV (ml/beat)	2.0 ± 0.8	2.4 ± 0.8	2.0 ± 0.6	2.8 ± 0.9^{+}	4.0 ± 5.6	5.6 ± 1.0*	4.9 ± 1.2	6.4 ± 1.1$^{\#}$

Table 3. Fetal weights of animals allocated for myocyte dissociation.

	Sham-Control	A-V Fistula	p Value
Heart weight (g)	29.3 ± 4.6	32.4 ± 7.9	NS
Body weight (kg)	4.00 ± 0.5	4.2 ± 0.6	NS
Heart to body weight ratio (g/kg)	7.4 ± 0.6	7.7 ± 1.6	NS
RV binucleate myocyte length (μm)	87.6 ± 1.1	99.4 ± 6.2	0.003
LV binucleate myocyte length (μm)	83.4 ± 1.7	92.5 ± 3.5	0.0001
RV binucleate myocyte width (μm)	15.9 ± 2.7	16.3 ± 0.7	NS
LV binucleate myocyte width (μm)	12.7 ± 1.1	13.6 ± 1.1	NS
RV binucleation (%)	40 ± 10	64 ± 5	0.001
LV binucleation (%)	42 ± 10	65 ± 5	0.001

APPENDIX B

Calculations

Wall Stress

Throughout the text I discuss the relationships between ventricular wall thickness, the radius of the chamber, and wall stress. For pressure, p, circumferential radius of curvature, r, and ventricular wall thickness, h, the Law of Laplace describes wall stress, S_w, as proportional to $p \bullet r / (2 \bullet h)$. If the pressure against which the ventricles contract were to be the same, then the systolic wall stress is determined by the morphology of the ventricles. The difference in wall stress between the ventricles is due to the differences in ventricular architecture. The relative S_w for the LV and RV at a given transmural pressure was calculated as $(r_{RV} / 2h_{RV}) / (r_{LV} / 2h_{LV})$.

Table 1. Ventricular morphology and wall stress in normal fetuses.

	r (mm)	h (mm)	$r/(2 \bullet h)$
Right Ventricle	12.8*	3*	2.13
Left Ventricle	10.9*	4.2*	1.30
* from Pinson *et al.*, 1987		RV/LV:	1.64

Heart Growth in Loaded Fetuses

I argue in the discussion that the rate of heart growth in the plasma infused fetuses was accelerated during the first 4 days of infusion, but less so during the second 4 days of infusion. These calculations support my argument.

Assuming a constant growth rate, for growth rate g the heart weight C on day 2 is $C_1 + C_1 g$ and on day 3 is $C_2 + C_2 g$ and so forth, so that the daily growth rate on day x is $C_{x-1} + C_{x-1} g$. Solving for C_{x-1} yields $C_{x-1} = C_x \bullet (1+g)^{-1}$.

Applying this to the weights of the control hearts from the plasma-infusion experiments (mean control heart weight at 134 days of gestation was 24.6g; at 138 days of gestation was 29.1g) and assuming a growth rate of 3% per day, I calculate that on day 130 the control fetuses had an average heart weight of 22.4g. I solved for daily growth rate g assuming that the plasma-loaded fetuses had a similar heart weights as controls at 130 days of gestation, before the experiments began (Table 2).

Table 2. Estimated heart growth in plasma loaded fetuses. Actual measured heart weights are shown in parentheses. Growth rates calculated from an estimated weight of 22.4g at 130 days of gestation (see text). Weights in grams.

Growth between days:	130-134	130-138	134-138
Days of gestational age:			
130	22.4	22.4	
134	(32.7)	29.3	(32.7)
138		(38.2)	(38.2)
Daily growth rate:	9.9%	6.9%	4.0%

The overall growth rate for the full 8 experimental days was 6.9%. The growth rate between 130 and 134 days of gestation was about 10%, and between 134 and 138 days of gestation was 4% (calculated from the difference between the experimental heart weights in the 4 and 8 day groups).

These calculations represent an estimate only of the cardiac growth rates in these experiments. The calculations depend on certain assumptions about normal somatic growth rates. They are used to make a point about the magnitude of growth occuring at different times in the plasma-infused fetal heart.

Myocyte Volume

Length and width of cardiac myocytes are useful measures because the growth of each can be independently regulated. It is sometimes useful to know myocyte volume as well. Myocyte volume can be estimated from width and length by using a cylindrical model, overestimating volume by 15% (Barbera *et al.*, 2000). Volume was calculated from the mean length l and the mean width w as $l \bullet \pi \bullet (w \bullet 0.5)^2$.

Myocyte volume was calculated separately for each control in the 8-day group of the plasma-load experiment. The mean volume of binucleated myocytes in the LV is 10411μm^3 and RV is 17750μm^3, while the mean volume of mononucleated myocytes in the LV is 6390μm^3 and RV is 9908μm^3.

The "average" myocyte size for each ventricle was found from the mean mononucleated volume

v_m, the mean binucleated volume v_b, and the binucleated fraction *bi* as $bi \bullet v_b + (1- bi) \bullet v_m$. The "average" myocyte size was calculated for a binucleated fraction from 0 to 1. On average, the fraction of myocytes that were binucleated in the RV of the controls was 0.46 and in the LV was 0.40. The difference from this volume was plotted for each ventricle. When expressed this way the error introduced by the cylindrical model cancels out (this can be checked by performing the calculations using arbitrary numbers for the myocyte sizes. The calculation will yield the same result for any arbitrary values of myocyte size, or those same numbers multiplied by 1.15 to simulate the error of the cylindrical model).

APPENDIX C

Buffers and Solutions

Solutions for Cardiac Dissociation

10x Tyrodes Stock

81.82g Sodium Chloride (NaCl)

3.73g Potassium Chloride (KCl)

2.0g Magnesium Chloride ($MgCl_2 \cdot 6H_20$)

Filtered water to 1L.

Tyrodes

100ml 10x Tyrodes stock

1.8g Dextrose

2.4g Hepes

Filtered water to 950ml.

Solution pH adjusted to 7.35 with NaOH. Final volume adjusted to 1L with filtered water. Aliquots of 500ml sterile filtered with 0.22µm filter. Final solution is 140mM NaCl, 5mM KCl, 1mM $MgCl_2$, 9mM dextrose, 10mM Hepes.

10x Kraftbrühe (KB) Stock

75.2g Glutamic acid (potassium)

11.2g KCl

20.4g Potassium Phosphate (KH_2PO_4)

1.81g Anhydrous Magnesium Sulphate ($MgSO_4$)

0.5g EGTA

Filtered water to 500ml

Sterile filtered with 0.22µm filter.

KB

100ml 10x KB stock

2.502g Taurine

2.83g Hepes

1.8g Glucose

Filtered water to 950ml

Solution pH adjusted to 7.37 with KOH. Final volume adjusted to 1L with filtered water. Sterile filtered into 500ml aliquots with 0.22µm filter. Final solution is 81mM L-glutamic acid, 30mM KCl, 30mM KH_2PO_4, 20mM taurine, 3mM $MgSO_4$, 0.5mM EGTA, 10mM Hepes, 9mM dexrrose.

Collagenase

160 units/ml Worthington's type II collagenase (Worthington 4176, CLS-2 LS004177)

0.78 units/ml protease type XIV (Sigma P5147-1G)

Made in sterile Tyrodes solution immediately prior to use.

Solutions for Cell Culture

Solutions for cell culture mixed in very well rinsed clean glassware, then sterile filtered and stored at 4°C.

Serum-Free Media Stock

1 bottle (14.9g) MCDB105 (Sigma M6395-10x1L)

149.1mg KCl

15mg Glycine

658g Creatine (5mM)

623mg Taurine (5mM)

322mg L-Carnitine (2mM)

950ml filtered water.

Solution adjusted to pH 7.6 with 1M NaOH and 1M HCl. Volume adjusted to 990ml with filtered water. Aliquots of 247.5ml filtered through 0.22µm filters.

Serum-Free Media

To one aliquot of serum-free media stock is added 2.5ml Insulin-Transferrin-Sodium Selenite Media Supplement (Sigma I1884-1VL) and 250µl Antibiotic/Antimycotic (Sigma A5955-20ML).

Serum Media Stock

As for serum-free media stock, except the initial volume of water is 850ml, the final total volume was 890ml, and the aliquot volumes were 222.5ml.

Serum Media

To one aliquot of serum-free media stock is added 2.5ml Insulin-Transferrin-Sodium Selenite Media Supplement, 250µl Antibiotic/Antimycotic, and 25ml Fetal Bovine Serum.

RIPA Lysis Buffer

100µl RIPA Lysis Buffer 10x (Upstate Cell Signaling Solutions 20-188)

900µl filtered water

Make at least 2 hours prior to use, then add:

1µl 10x CHAPS

1µl Phosphatase Inhibitor Cocktail II (Sigma P-5726)

1µl Phosphatase Inhibitor Cocktail I (Sigma P-2850)

1µl Protease Arrest (Genotech)

Solutions for Western Analysis

RIPA Extraction Buffer

1ml RIPA Lysis Buffer 10x (Upstate Cell Signaling Solutions 20-188)

9ml filtered water

Make at least 2 hours prior to use, then add:

100µl 10x CHAPS

100µl Phosphatase Inhibitor Cocktail II (Sigma P-5726)

100µl Phosphatase Inhibitor Cocktail I (Sigma P-2850)

1 tablet mini-Complete Protease Inhibitor (Roche, Indianapolis, IN)

Final solution is 50mM Tris-HCl, 150mM NaCl, 0.25% deoxycholic acid, 1% NP-40, 10mM EDTA and 0.1% CHAPS with 1x Protease Cocktails I and II and Complete protease inhibitor.

Tris Buffer for Stacking Gel (4x)

6.06g Tris Base

4ml 10% sodium dodecyl sulfate (SDS)

Volume to 100ml with filtered water and pH adjusted to 6.8 with very concentrated (12N) HCl. Final solution is 0.5M Tris with 0.4% SDS.

Tris Buffer for Resolving Gel (4x)

18.17g Tris Base

4ml 10% SDS

Volume to 100ml with filtered water and pH adjusted to 8.8 with HCl. Final solution is 1.5M Tris with 0.4% SDS.

Tris-Glycine Reservoir Running Buffer

24.23g Tris Base

144.23g Glycine

10g SDS

Volume adjusted to 1L with filtered water.

Dilute to 1x with water for use.

Transfer Buffer (10x)

30.3g Tris Base

144g Glycine

Volume adjusted to 1L with filtered water.

For 1x solution dilute with water or mix 50ml 10x transfer buffer, 100ml methanol and 350ml water.

Blotting Buffer (10x "TBS")

12.11g Tris Base

87g NaCl

Bring to 1L and pH to 7.5

Diluted to 1x for use.

TBS-Tween (TBST)

100ml 1x TBS

100µl Tween-20

5% Non-fat Milk Buffer

5g Non-fat Powdered Milk

100ml 1x TBST

Laemmli Buffer (4x)

10ml 0.6M Tris-Hcl pH6.8

2g SDS

10ml Glycerol

Pinch Bromophenol Blue

Aliquoted into 900µl and frozen.

Before use warm to resuspend SDS. Add 100µl β-mercaptoethanol or 3M DTT.

Samples heated to 65°C for 30min (DTT solution) or 100°C for 5-10 min (β-mercaptoethanol solution).

Western Membrane Stripping Buffer

52ml 0.6M Tris-HCl pH6.8

50ml 20% SDS

395ml H_2O

Before use add 600µl B-mercaptoethanol per 100ml.

10% Resolving Gel

16.1ml H_2O

10ml Lower Tris (4x)

13.3ml 30% Acrylamide with 0.8%MBA (BioRad)

20µl TEMED

400µl fresh 10% Ammonium Persulfate (APS)

4% Stacking Gel

6ml H_2O

2.5ml Upper Tris (4x)

1.4ml 30% Acrylamide with 0.8%MBA (BioRad)

20µl TEMED

150µl 10% APS

Solutions for Immunohistochemistry

Phosphate Buffered Saline (PBS)

8g NaCl

0.2g KCl

1.44g Na_2HPO_4

0.24g KH_2PO_4

Volume to 1L with filtered water and pH adjusted to 7.4.

Sodium Citrate Solution

0.589g Sodium Citrate (10mM)

Volume to 200ml with filtered water and pH adjusted to 6.0 with HCl.

Blocking Buffer

100mg bovine serum albumin

10ml PBS

50µl Triton X100

Solutions for Northern Blot Analysis

20x MOPS Buffer

41.8g 3-(N-morpholino) propanesulfonic acid (MOPS)

20ml 0.5M EDTA

26.7ml 3M Sodium Acetate

350ml filtered water

pH adjusted to 7.0 with NaOH or acetic acid, volume adjusted to 500ml. Autoclaved prior to use.

DEPC Water

1ml diethylpyrocarbonate

1 liter filtered water

Autoclaved for 30 minutes.

20x Sodium-Sodium Citrate Buffer (SSC)

175.3g NaCl

88.2g sodium citrate

800ml filtered water

Adjusted pH to 7.0 with 10N NaOH and volume to 1 liter with water.

Wash Buffer 1

100ml 20x SSC

0.5g SDS (0.05% w/v)

Wash Buffer 2

25ml 20x SSC

1g SDS (0.1% w/v)

Solutions for Hematoxylin Staining

Acid Alcohol

2ml HCl

198ml 70% ethanol

Scott's Solution

2g $NaHCO_3$

20g $MgSO_4 \cdot 7H_20$

Water to 1 liter.